DYNAMIC ANALYSIS OF FLOATING QUAY AND CONTAINER SHIP FOR CONTAINER LOADING AND OFFLOADING OPERATION

A Thesis

by

BRAJESH KUMAR

Submitted to the Office of Graduate Studies of
Texas A&M University
in partial fulfillment of the requirements for the degree of

MASTER OF SCIENCE

December 2005

Major Subject: Ocean Engineering

DYNAMIC ANALYSIS OF FLOATING QUAY AND CONTAINER SHIP FOR CONTAINER LOADING AND OFFLOADING OPERATION

A Thesis

by

BRAJESH KUMAR

Submitted to the Office of Graduate Studies of
Texas A&M University
in partial fulfillment of the requirements for the degree of

MASTER OF SCIENCE

Approved by:

Chair of Committee,	Moo-Hyun Kim
Committee Members,	Robert Randall
	Achim Stössel
Head of Department,	David V. Rosowsky

December 2005

Major Subject: Ocean Engineering

ABSTRACT

Dynamic Analysis of Floating Quay and Container Ship

for Container Loading and Offloading Operation. (December 2005)

Brajesh Kumar, B.E., Marine Engineering & Research Institute

Chair of Advisory Committee: Dr. Moo-Hyun Kim

A floating quay container terminal is used for loading or unloading from container ships from both sides of a floating quay. The side-by-side Liquefied Natural Gas (LNG) offloading operation from floating terminals to LNG carriers is very similar to that from super-container ships to floating quay-walls. The hydrodynamic interaction effects among a fixed quay, container ship and floating quay, which are parallel to one another, are investigated. The three body side-by-side arrangement is compared with the individual freely floating body in the absence/presence of the fixed quay to identify the interaction effects. Hydrodynamic coefficients of the interacting bodies are obtained using a three dimensional constant panel method, WAMIT. Using a vessel-lines coupled dynamic analysis computer program WINPOST, the relative motion between floating quay and container ship is simulated in time domain. It is assumed in the present study that the floating quay is positioned by a dolphin mooring system. This analysis provides the relative motion among container ship, fixed and floating quay to ascertain that container loading and offloading can be performed in the severe wave condition without any problem.

Dedicated

to

my father Prabhunath Prasad, mother Kaushalya Devi and aunt Giriza Devi.

ACKNOWLEDGMENTS

I would like to express my sincere gratitude to my committee chair, Dr. M. H. Kim, for his encouragement, guidance and financial support throughout my program of study. I would like to thank Dr. Robert Randall and Dr. Stössel for serving as the advisory committee members and for their guidance and support throughout the course of this research. I highly appreciate Dr. S. Y. Hong and the Korean Ocean Research and Development Institute (KORDI), for special observations and financial support for this project. I would also like to thank Mr. Vinu P. Kuriakose, Mr. Chankyu Yang, Dr. D. H. Lee and Mr. Seung Jae Lee for their valuable input during the course of this project.

Finally, I am indebted to my family and my friends, Amitabh Kumar and Radhakrishna Pillai, for their support and encouragement throughout this work.

NOMENCLATURE

FLQW	Floating Quay Wall
FIQW	Fixed Quay Wall
CS	Container Ship
FLQW+FIQW	Floating Quay in the presence of Fixed Quay
CS+FIQW	Container Ship in the presence of Fixed Quay
FLQW+CS+FIQW	Floating Quay and Container Ship in the presence of Fixed Quay
FF	Freely Floating
SBS	Side by side
deg	Degrees
rad	Radians
m	Meter
g	Acceleration due to gravity
ω	Cyclic frequency
s	Second

TABLE OF CONTENTS

Page

LIST OF FIGURES

Page

Page

Page

Page

Page

LIST OF TABLES

1. INTRODUCTION

1.1 Floating Mobile Quay Wall System

A floating quay container terminal is used for loading to container ships or unloading from container ships from both sides of the floating quay. Recently, a large-volume floating concrete container pier (213m x 30.5m) was installed in the Port of Valdez, Alaska, and the system is successfully being operated all season long without any problem and there already exist many floating bridges and floating factory plants over the world. There are various advantages and disadvantages of the floating quay compared to land based structures. The advantages of using floating quay outweigh the disadvantages as mentioned below.

1.1.1 Advantages of Floating Mobile Quay-Wall System

1. The loading and unloading capabilities can be easily expanded and accelerated.
2. It is minimally influenced by the change of water-level by tide and storm surge. Its position with respect to the water surface is constant for a certain loading condition and thus facilitates ship to come alongside.
3. The containers and structures on a floating quay are protected from seismic shocks since it is inherently base isolated.

This thesis follows the style and format of Ocean Engineering.

4. Not influenced by soil/seafloor condition such as sinkage, liquefaction, deposition, and scouring so it does not suffer from differential settlement due to reclaimed soil consolidation.
5. Minimize the construction cost, no foundation work. Components can be constructed easily at different shipyards before assembling near the harbor and so sea-space can be speedily exploited.
6. Can be easily relocated if the sea space is needed in future or if it is required at a different place along the fixed harbor.
7. Reusability is highly possible.
8. Minimum environmental impact on the flow/water-quality system inside a harbor as these do not damage the marine eco-system or silt-up deep harbors or disrupt the tidal/ocean currents.
9. Applicability to related technologies, such as floating factory plants, floating docks.

1.1.2 Disadvantages of Floating Mobile Quay Wall System

1. Possible non-operability in relatively severe wave condition and survivability in a very severe storm condition, such as a Typhoon.
2. Operational cost related to towing or winching system is very high.
3. Owing to the corrosive sea environment, floating structures have to be provided with a good corrosion protection system.
4. Possible degradation due to corrosion or crack growth (fatigue) requires a proper system for inspection, monitoring, maintenance and repair during use.

The analysis and design of floating structures need to account for some special characteristics (Clauss et al. 1992, Moan 2004 - as provided in Watanabe E., Wang C.M., Utsunomiya T. and Moan T., Very large floating structures: applications, analysis and design, centre for offshore research and engineering, National University of Singapore, core report no. 2004-02.) when compared to land-based structures; Namely, horizontal forces due to waves are in general several times greater than the (non-seismic) horizontal loads on land-based structures and the effect of such loads depends upon how the structure is connected to the seafloor. It is distinguished between a rigid and compliant connection. A rigid connection virtually prevents horizontal motion while a compliant mooring will allow maximum horizontal motion of a floating structure of the order of the wave amplitude.

In a floating structure the static vertical self weight and payloads (total weight of the crew, equipment and containers) are carried by buoyancy. If a floating structure has a compliant mooring system, consisting for instance of catenary chain mooring lines, the horizontal wave forces are balanced by inertia forces. Moreover, if the horizontal size of the structure is larger than the wave length, the resultant horizontal forces will be reduced due to the fact that wave forces on different structural parts will have different phase (direction and size). The forces in the mooring system will then be small relative to the total wave forces. The main purpose of the mooring system is then to prevent drift-off due to steady current and wind forces as well as possible steady and slow-drift wave forces. Sizing of the floating structure and its mooring system depends on its function and the environmental conditions in terms of waves, current and wind. The design will be dominated by peak loading due to survival design wave height, tide, current and wind.

1.2 Data for Research and Layout of the Interacting Bodies

The data have been provided by Korea Ocean Research and Development Institute and are shown in Table 1-1.

Table. 1-1. Dimensions of the interacting bodies

	Length	Breadth	Depth	Draft	KG
Floating Quay -1	480	140	6	2.156	3.0
Floating Quay -2	350	140	6	2.172	3.0
Container Ship-1	400	57.5	17	15	10.571
Container Ship-2	347	42.8	16	14.5	10.219
Container Ship-3	280	35.8	15	13	9.162

1.2.1 Layout of the Interacting Bodies

The WAMIT results will be obtained for floating quay -1 and container ship-2 where the container ship is equidistant from the fixed and the floating quay i.e. 8.6 meters apart from the fixed as well as the floating quay as shown in Figure 1-1(a) and Figure 1-1(b). Here, we are interested in the relative motion of the container ship with respect to floating quay and fixed quay for smooth loading/unloading operation. The hydrodynamic interaction among floating quay, container ship and fixed quay is simulated using WAMIT. In Figure 1-1(a), Waves parallel to the positive X-axis direction have a 0 degrees incident angle, whereas waves parallel to the positive Y-axis have a 90 degrees incidence angle. In Figure 1-1(b), Bodies from left to right represent fixed quay, container ship and floating quay respectively. The water depth is 17m in this case.

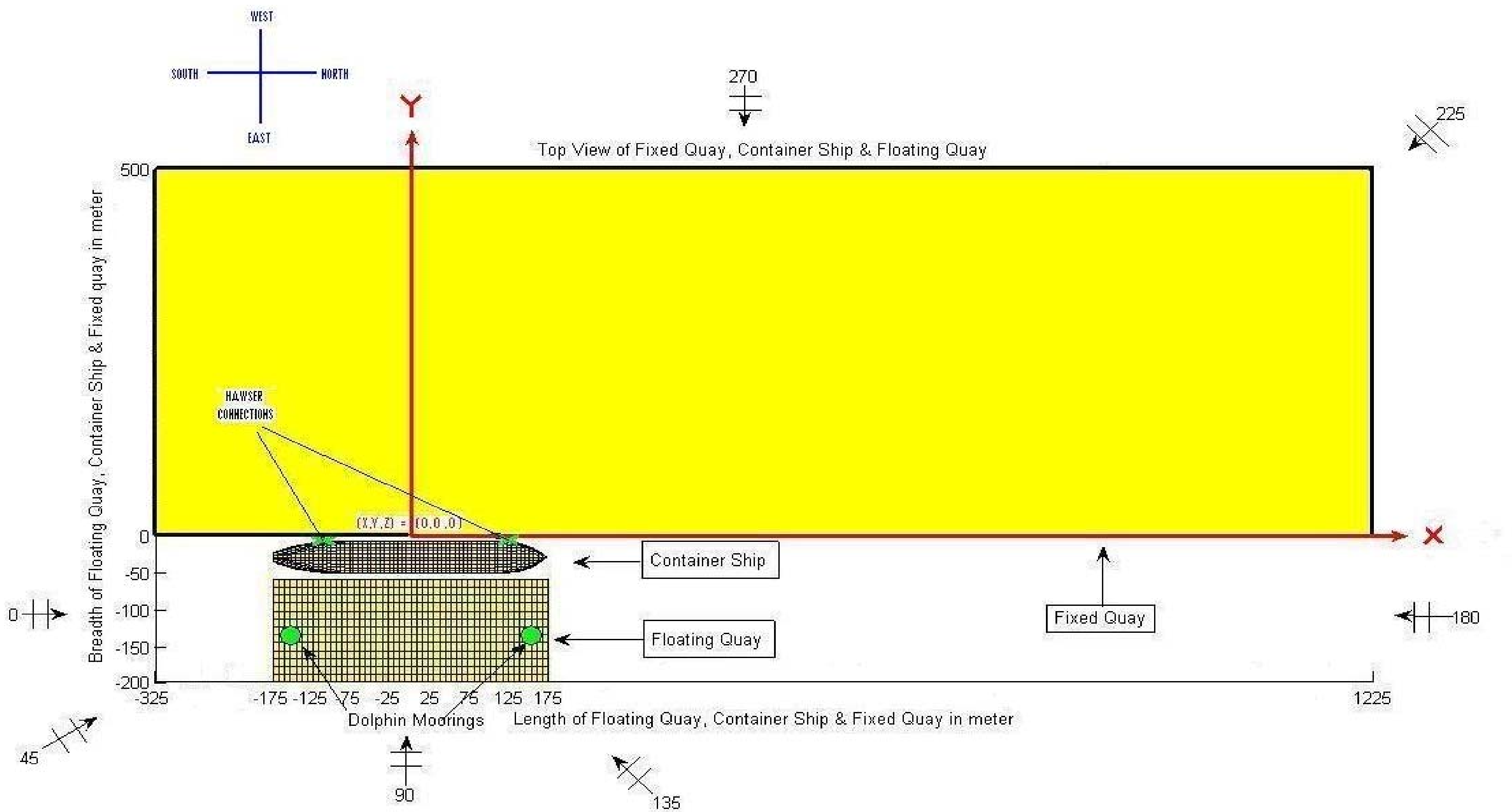

Figure 1-1(a). Plan (X-Y view) of fixed quay, container ship (with hawser connection) and floating quay (with dolphin moorings)

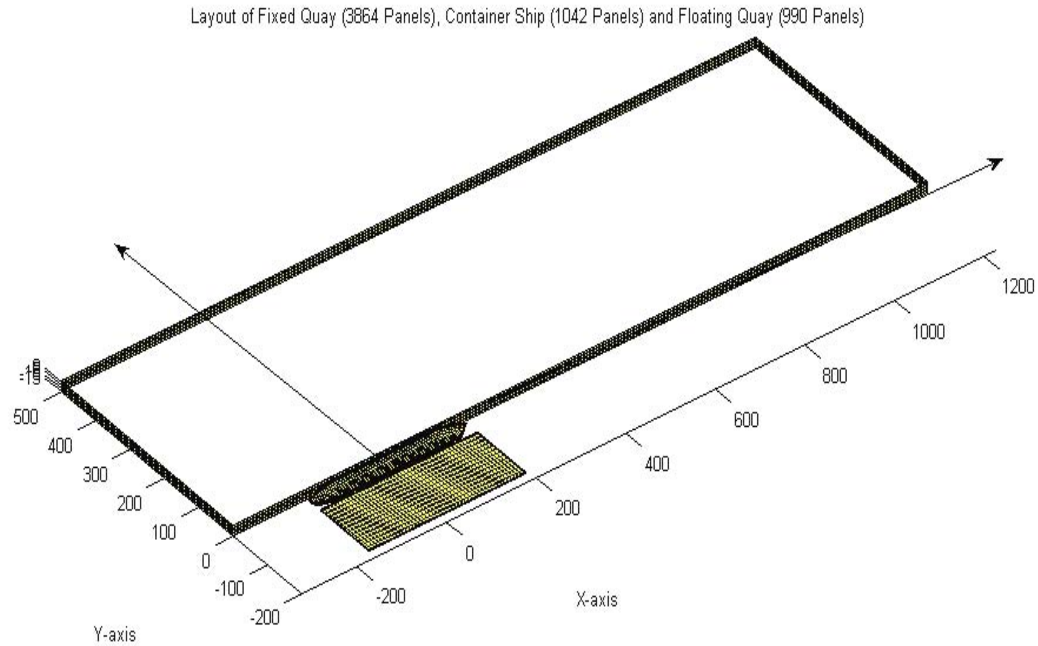

Figure 1-1(b). Panel discretization of fixed quay, container ship and floating quay

As shown in Figure 1-1(a) and Figure 1-1(b), due to close proximity among interacting bodies there is a entrapment of the water waves between two bodies (e.g. container ship and fixed quay or container ship and floating quay) resulting in a standing wave formation when the entrapped length of the water column is approximately equal to one quarter of the incident wave length. The effect of entrapment as well as the effect of the motion of one body on the motion of the other body will be analyzed thoroughly for determining the hydrodynamic motion of the bodies.

1.3 Objectives

This research topic analyzes hydrodynamic interaction effects among a fixed quay wall, container ship and floating quay wall where the container ship is situated in the middle of fixed quay wall and the floating quay wall. Though the size of the floating quay wall is fixed, three different sizes of container ships have been used. As the size of the container ship changes so does the distance between the container ship and floating/fixed quay wall whereas the distance between floating and fixed quay wall is fixed. Coupled analysis is performed to evaluate the tension in the mooring line and the body displacement.

Constant Panel Method based program, WAMIT, is used to determine the hydrodynamic characteristics of the interacting bodies as well as single body and the results of the single body and the multi body are to find out the effects of hydrodynamic interaction of multiple bodies. Hydrodynamic interactions for various angles have been analyzed and the effects of hydrodynamic interaction of multiple bodies compared to single body is seen to be more conspicuous when the incident angle is 90 degrees or 180 degrees .

WAMIT output is used as input to WAMPOST program and the output from WAMPOST as well as WAMIT is used as input to WINPOST program. WINPOST is a finite element program for coupled dynamic analysis. The program performs coupled dynamic analyses both in time domain and frequency domain. In the time domain analysis, various nonlinearities, such as the drag force on the mooring lines, ship's and floating quay's hull, the free surface effects, body motion, and the geometric non-linearity of the mooring system are included in a time marching scheme. WINPOST output provides the results e.g. the displacements and tension in the mooring lines in the time domain. The operational condition in the severe weather is determined by the relative motion among the interacting bodies. So the relative motion, velocity and acceleration of floating quay and container ship in the presence of fixed quay will be estimated to determine the sea state in which offloading operation is possible.

1.3.1 Loads and Load Effects

The following loads must be considered: dead load, hydrostatic pressure (including buoyancy), earth pressure on mooring system such as dolphins, wind load, effects of waves (including swell), effects of dynamic water pressure, effects of water current, effects of tidal change, effects of storm.

1.3.2 Buoyancy, Waves and Current

The buoyancy is computed by the integration of hydrostatic pressure. In the design of very large pontoon floating structures, the change in water level due to tide, tsunami and storm surge may dominate the design loads when the structure is designed with a fixed vertical position relative to the seafloor. The point of action of buoyancy depends on the tide and water level.

1.4 Literature Review

Zhihuang Ran (2000) analyzed coupled dynamic analysis of floating structures in waves and currents. Hamn-Ching Chen and Erick T. Huang (2004) performed time-domain simulation of floating pier/ship interactions and harbor resonance. Kodan(1984) analyzed the hydrodynamic interaction between two parallel slender bodies. Sannasiraj et al.(2000) studied the diffraction-radiation of multiple floating structures in directional waves using Finite Element Method showing that interaction tends to become less in the higher frequency zone. Huijsmans et al. (2001) used the 'lid' technique for suppressing the pumping action in the gap between two closely lying bodies. Multi body analysis using single body hydrodynamics was compared with the lid technique and the Gauss quadrature approach and it showed that multibody hydrodynamics is not free from serious inaccuracies when analyzed with linear diffraction codes. Buchner et al. (2001) analyzed the interaction effects between a LNG Carrier in side-by-side mooring to a LNG FPSO. The conclusion of this analysis says that hydrodynamic cross coupling should not be ignored when interacting bodies are in close to each other. Buchner et al. (2004) studied the hydrodynamic interaction of a LNG Carrier alongside a Gravity Based Structure in shallow water. Inoue et al. (1999) employed momentum approach whereas Huijsmans et al. (2001) used pressure integration technique for wave drift forces. Higher Order Boundary Element Method (HOBEM) was used by Choi and Hong (2002) to study the interaction problem.

2. HYDRODYNAMIC INTERACTION ANALYSIS

2.1 Wave Interactions with Uncoupled Floating Structures in Frequency Domain

In response to incident regular waves of frequency ω**,** the motion of the floating body is $\mathrm{X}_j = \mathrm{Re}\,al\left\{|\mathrm{X}_j| e^{i(\omega t+\zeta_j)}\right\}$, where ζ_j is the phase difference and j =1,2,3,4,5,6 represents surge, sway, heave, roll, pitch and yaw respectively.

For computing X_j, it is required to determine the pressure distribution on the floating body resulting from the wave motion and the body motion so the velocity potential of the flow need to be solved. For a body undergoing small amplitude motions relative to the wave length i.e. $|\mathrm{X}_j| << \lambda$, the velocity potential may be represented as the sum of the incident, scattered and radiated wave components:

$\phi(x,y,z,t) = \phi_I + \phi_S + \phi_R = A\Phi_I + A\Phi_S + \sum_{j=1}^{6}\mathrm{X}_j\Phi_j = A\Phi_D + \sum_{j=1}^{6}\mathrm{X}_j\Phi_j$ where the incident wave potential $\phi_I = A\Phi_I$ corresponds to the potential without the body obstructing the flow. The scattered wave potential $\phi_S = A\Phi_S$ represents the disturbance of the incident waves due to the presence of the body i.e. it corresponds to the wave field that is scattered off the body assuming it is fixed in space. $\phi_D = \phi_I + \phi_S = A\Phi_I + A\Phi_S = A\Phi_D$ represents the wave diffraction which is the combined effects of incident and scattered waves. The radiated wave potentials, $\phi_R = \sum_{j=1}^{6}\mathrm{X}_j\Phi_j$ is the wave field generated by the body motion in all six modes of motion.

When N is the number of bodies then $\phi(x,y,z,t) = A\Phi_D + \sum_{j=1}^{6N} X_j \Phi_j$ where 6N is the total number of degrees of freedom of N rigid bodies.

2.2 Numerical Solution of Scattering and Radiation Potentials

The boundary element method based on Green's functions is preferred over other techniques for solving the hydrodynamic problems for $\Phi_D^{(1)}$ and $\Phi_j^{(1)}$. The boundary element method relies on the fact that the mathematical expression for the Green's functions for diffraction and radiation are known. The Green's function $G(\vec{x} \mid \vec{x}_0)$ is defined to be the potential at any field point $\vec{x}$ due to an oscillating source of unit strength at $\vec{x}_0$.

Green's theorem for two twice differentiable functions f and g is

$$\iiint_{\Omega} (f\nabla^2 g - g\nabla^2 f) d\Omega = \iint_{\partial\Omega} (f \frac{\partial g}{\partial n} - g \frac{\partial f}{\partial n}) dS$$

Where Ω is a closed volume, $d\Omega$ is its boundary and $\vec{n}$ is an outward pointing unit normal to $d\Omega$.

Using the above theorem, the solution to the velocity potential can be given by

$$\Phi(\vec{x}) = \iint_{S_B} \left(\Phi(\vec{x}_0) \frac{\partial G}{\partial n_0} - G \frac{\partial \Phi(\vec{x}_0)}{\partial n_0} \right) dS_0 \quad d\Omega$$

The hydrodynamic interaction analysis theory in the explained above has been understood and written with the help of Dynamics of Offshore Structures, OCEN-676-600, class notes of Dr. Richard Mercier, Texas A&M University.

2.3 Time-Domain Analysis

The equations of conservation of linear and angular momentum are given by

$[M]\{\ddot{X}\}+[K]\{X\}=M_{ij}\ddot{X}_j+K_{ij}X_j=-\rho\iint_{S_B^{(0)}}\frac{\partial\phi^{(1)}}{\partial t}\{n\}dS+\{F\}$ where the first term on the right hand side of the equation represents hydrodynamic force and $\{F\}=\{F_X^{(1)},F_Y^{(1)},F_Z^{(1)},T_X^{(1)},T_Y^{(1)},T_Z^{(1)}\}^T$ are the forces and moments acting on the body. [M] is the mass matrix which contains mass of the floating body as well as added mass due to motion of the body.[K] is hydrostatic stiffness matrix.

$$[M]=\begin{bmatrix} m & 0 & 0 & 0 & mz_{B,g} & -my_{B,g} \\ 0 & m & 0 & -mz_{B,g} & 0 & mx_{B,g} \\ 0 & 0 & m & my_{B,g} & -mx_{B,g} & 0 \\ 0 & -mz_{B,g} & my_{B,g} & (I_{XX}^B) & -I_{YX}^B & -I_{Zx}^B \\ mz_{B,g} & 0 & -mx_{B,g} & -I_{XY}^B & (I_{YY}^B) & -I_{ZY}^B \\ -my_{B,g} & mx_{B,g} & 0 & -I_{XZ}^B & -I_{YZ}^B & (I_{ZZ}^B) \end{bmatrix}$$

Where $M_{44}=I_{11}$, $M_{45}=I_{12}$, $M_{46}=I_{13}$,

$M_{54}=I_{21}$, $M_{55}=I_{22}$, $M_{56}=I_{23}$,

$M_{64}=I_{31}$, $M_{65}=I_{32}$, $M_{66}=I_{33}$.

$I_{XY}^B=I_{YX}^B, I_{XZ}^B=I_{ZX}^B, I_{YZ}^B=I_{ZY}^B$ Here moments of inertia are defined with respect to the origin of the body fixed coordinate system.

$$[K]=\begin{bmatrix} 0 & 0 & 0 & 0 & 0 & 0 \\ 0 & 0 & 0 & 0 & 0 & 0 \\ 0 & 0 & \rho g A^{(0)} & \rho g I_Y^A & -\rho g A_X^A & 0 \\ 0 & 0 & \rho g I_Y^A & \rho g[I_{YY}^A+V^{(0)}z_{B,b}]-mgz_{B,g} & -\rho g I_{XY}^A & -\rho g V^{(0)}x_{B,b}+mgx_{B,g} \\ 0 & 0 & \rho g I_X^A & \rho g I_{YX}^A & \rho g[I_{XX}^A+V^{(0)}z_{B,b}]-mgz_{B,g} & -\rho g V^{(0)}y_{B,b}+mgy_{B,g} \\ 0 & 0 & 0 & 0 & 0 & 0 \end{bmatrix}$$

I_X^A , I_Y^A, I_{XX}^A , I_{YY}^A , $I_{XY}^A = I_{YX}^A$ are the moments of area.

($x_{B,b}$, $y_{B,b}$, $z_{B,b}$) : coordinates of center of buoyancy

$A^{(0)}$: water plane area

$V^{(0)}$: submerged volume

The diagonal terms in the above [M] and [K] matrices represent pure motion (surge, sway, heave, roll, pitch and yaw). In [K] off-diagonal terms are mixed or coupled terms e.g. it can be seen from [K] matrix that heave is coupled with roll and pitch.

2.4 Removal of Irregular Frequency Effects

At irregular frequency, the hydrodynamic response may show a resonant response giving an impression of an interaction effect. So the effects resulting from irregular frequencies should be removed to correctly interpret the interaction effects. WAMIT includes a method for removing the effects of irregular frequencies by discretization of the interior free surface by the user or by the WAMIT program. Constant Panel Method based program, WAMIT was understood from Lee, C.H., 1995. WAMIT theory manual.

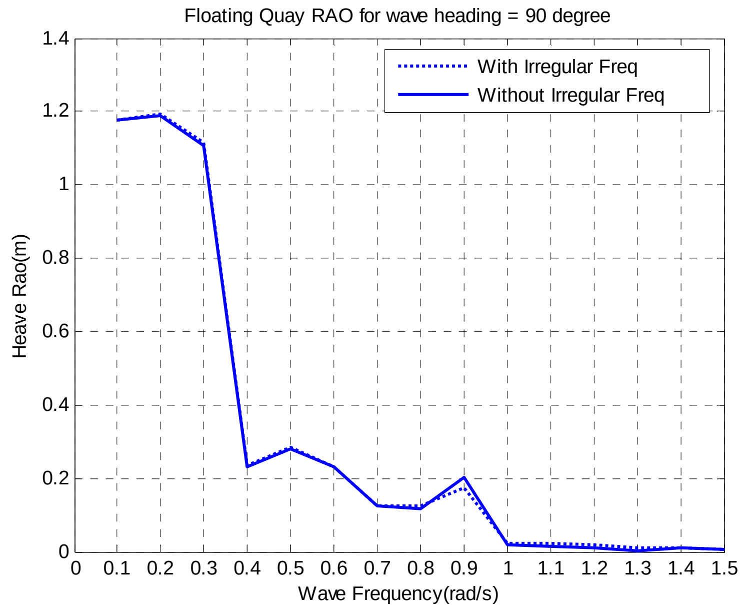

Figure 2-1. Floating quay heave RAO comparison for irregular and regular waves

In Figure 2-1, results obtained with and without irregular frequencies show very similar results in the 0.1:0.1:1.5 rad/s frequency range leading to the conclusion that irregular frequency effects have no bearing on the results at the chosen frequencies.

2.5 Added Mass and Damping Coefficient for "Freely Floating" Container Ship and Floating Quay Wall

Added mass and damping for both floating quay and container ship has been plotted for single, two and three body cases. There is a sharp peak at 0.4 rad/s as a result of hydrodynamic interaction of the floating body with other bodies. The interaction effect also gives rise to negative added mass as shown in Figure 2-2(a). The damping coefficients for the floating quay and container ship also has sharp peaks at 0.4 rad/s due to hydrodynamic interaction effects as shown in Figure 2-2(b).

Our main concern is the motion response at 0, 45 and 90 degrees incident angles as these wave incident angles are the dominant wave angles. Multi-body hydrodynamic interaction is compared to the single body analysis.

The heave, roll and pitch natural frequencies obtained from the hydrostatic stiffness, mass of the body and the added mass for heave, roll and pitch motion is given in Table 2-1.

The first column of Figure 2-2(a) and Figure 2-2(b) corresponds to the floating quay whereas the second column of Figure 2-2(a) and Figure 2-2(b) corresponds to the container ship.

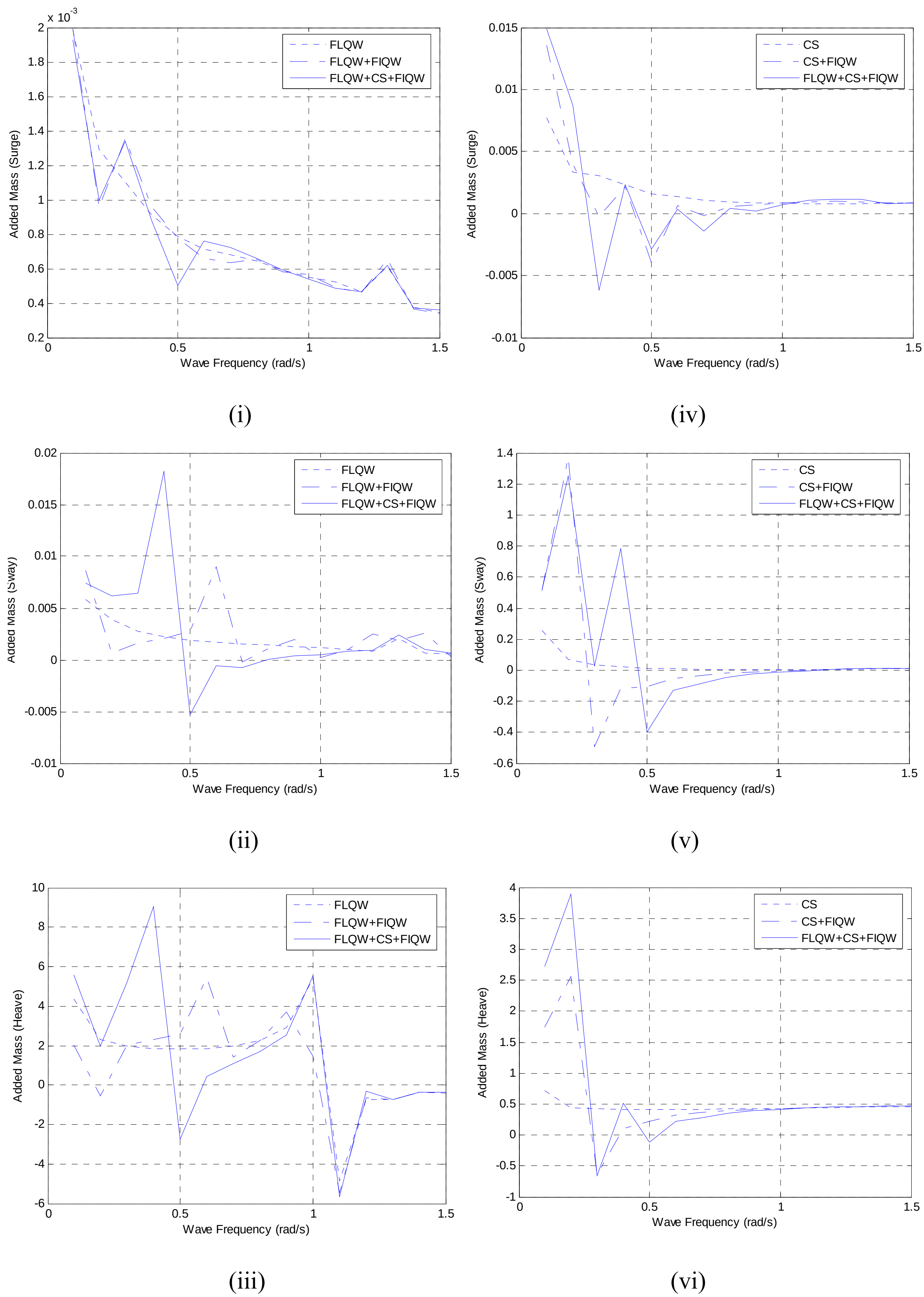

Figure 2-2(a). Added mass coefficients of floating quay and container ship

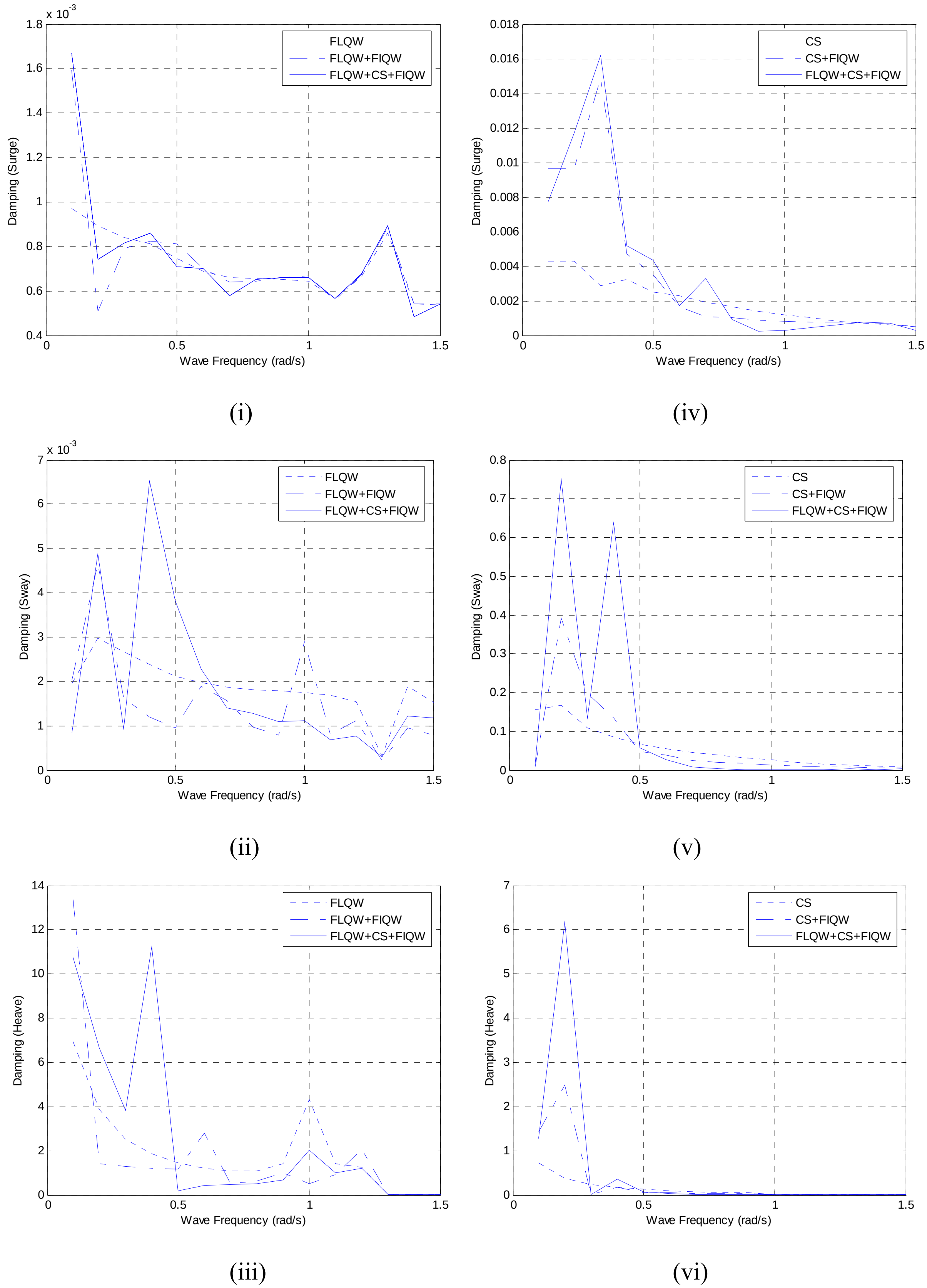

Figure 2-2(b). Damping coefficients of floating quay and container ship

2.6 Uncoupled Analysis in Frequency Domain for “Freely Floating” Container Ship and Floating Quay Wall

The heave, roll and pitch natural frequencies obtained from the hydrostatic stiffness, mass of the body and the added mass for heave, roll and pitch motion is given in Table 2-1.

Table 2-1. Natural frequency of floating quay and container ship

	Floating Quay (rad/s)	Container Ship (rad/s)
Heave	0.2960	0.3143
Roll	0.4540	0.4534
Pitch	0.3471	0.3526

2.6.1 Case 1. Wave Heading = 90 Degrees (beam sea condition) for “Freely Floating” Container Ship and Floating Quay Wall

In this case the incident wave is perpendicular to the floating quay wall i.e. looking to the positive X-direction in the layout, the starboard side of the floating quay is the weather side in this case. Figure 2-3 (i), (v), (vi) shows insignificant surge, pitch and yaw motion RAO in the single body case but there is comparatively significant motion response in the above mentioned degrees of freedom due to interaction effect in multi-body case. Since the three body arrangement is unsymmetrical to the incident waves, the reflected waves are not equally distributed around the floating bodies resulting in surge, pitch and yaw motion RAO in the floating body in multi-body case. The interaction effect in multi-body case also gives rise to sharp peaks at certain frequencies.

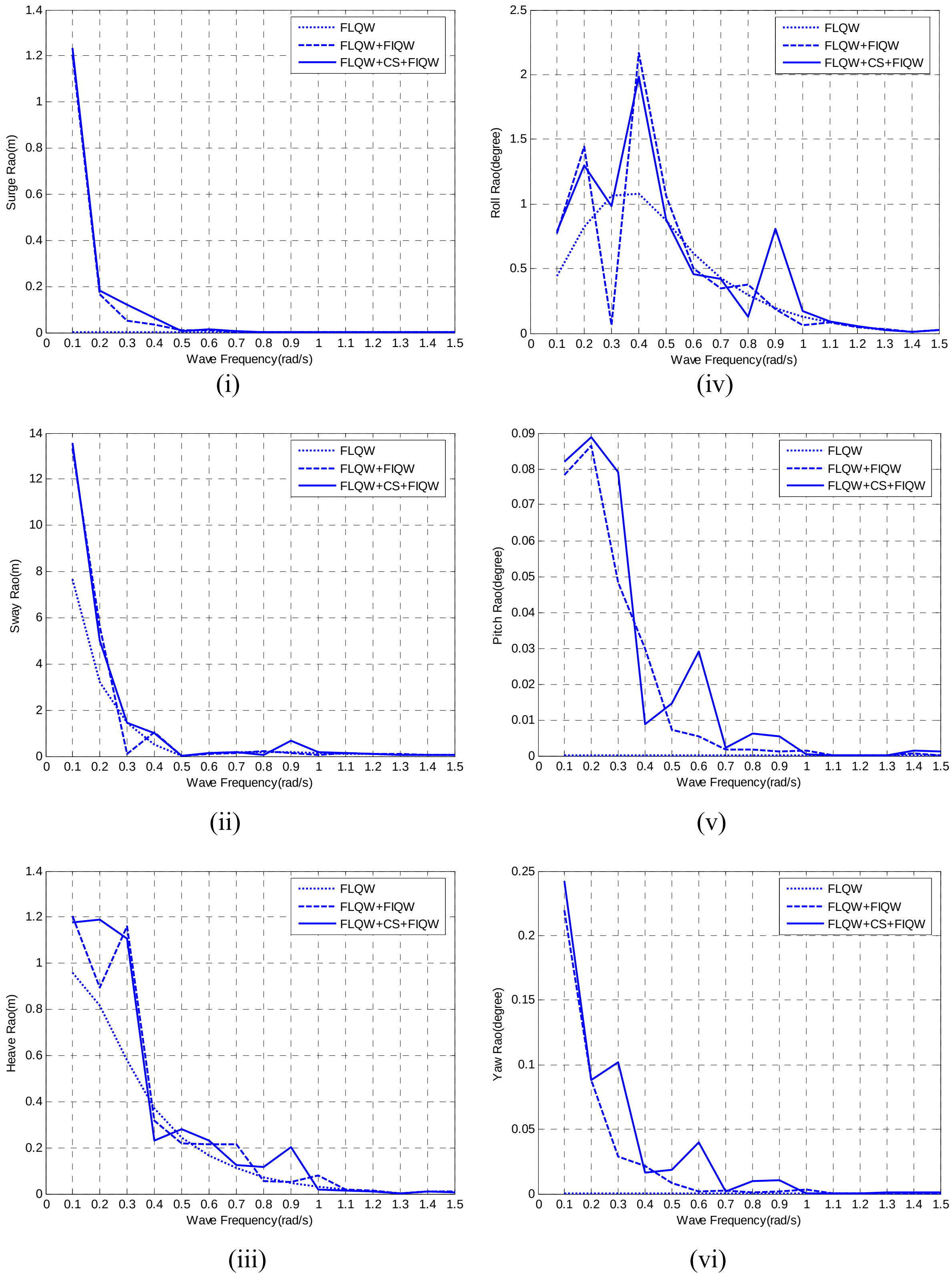

Figure 2-3. Motion response of floating quay for 90 degrees wave heading

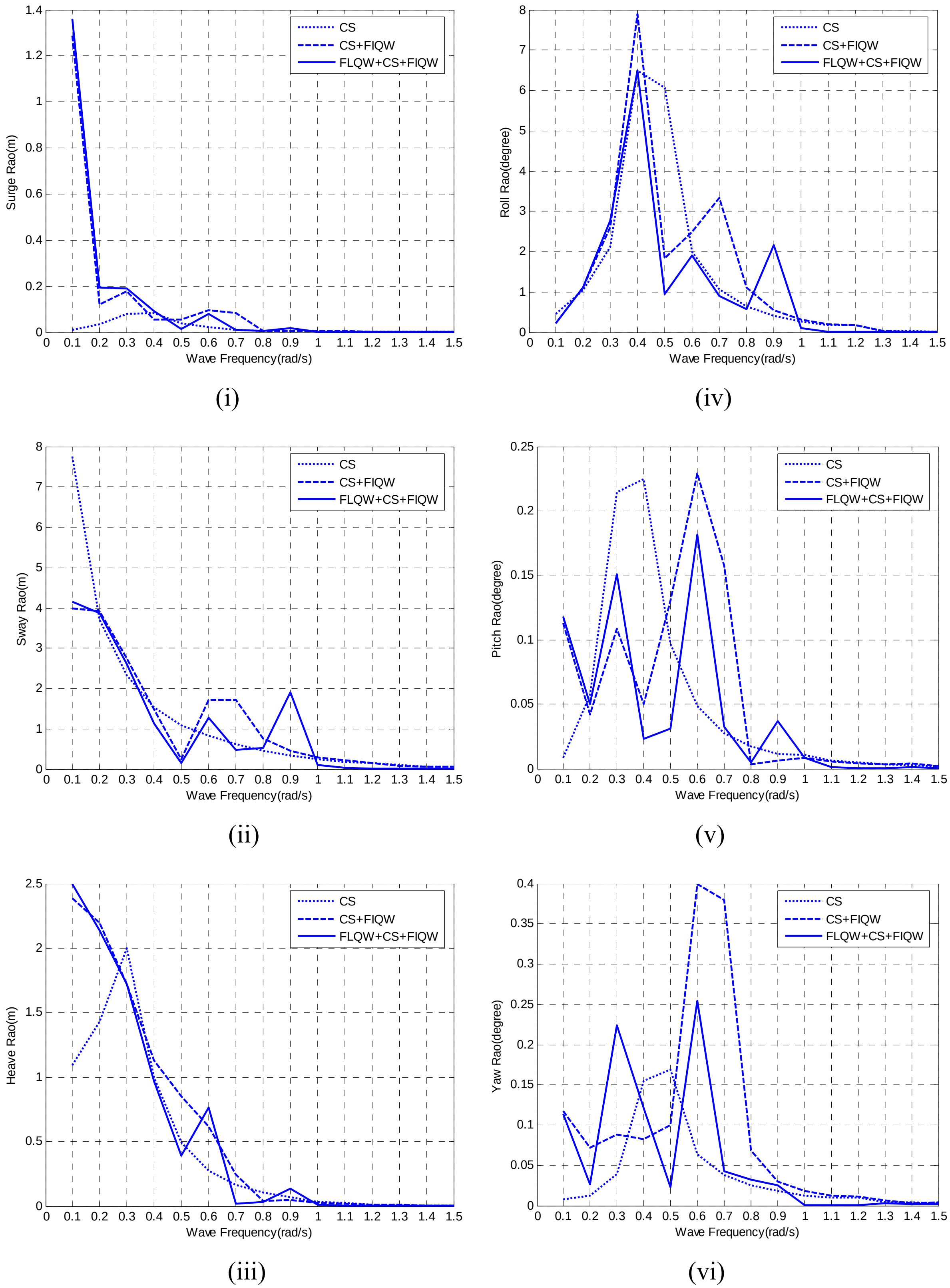

Figure 2-4. Motion response of container ship for 90 degrees wave heading

In Figure 2-4(iii), there is a standing wave formation due to the combination of the incident and reflected waves. When the length of the entrapped water column is about one quarter of the incident wave length then resonance effect takes place. So the heave motion RAO tends to reach 2.0 at very low frequency (long wave). Since container ship is being shielded from the incident waves in multi-body case so sway RAO in Figure 2-4(ii) for multi-body case at low frequency is less than that in single body case.

In Figure 2-5(iii), the relative heave is 3.4m and 2.9m at 0.2 rad/s and 0.3rad/s respectively though it goes even higher between these two frequencies due to the resonance effect. Figure 2-6. and Figure 2-7 illustrate the wave exciting forces on the floating quay and the container ship respectively. The surge excitation force in Figure 2-7(i) can be explained as follows: as the X-Y planer cross-sectional area of the container ship decreases in the negative Z-direction and the asymmetry of the container ship increases further by the shielding effect of the floating quay so the resulting wave excitation force in three body case is more than those in two body and single body case at low frequency range (long wave).

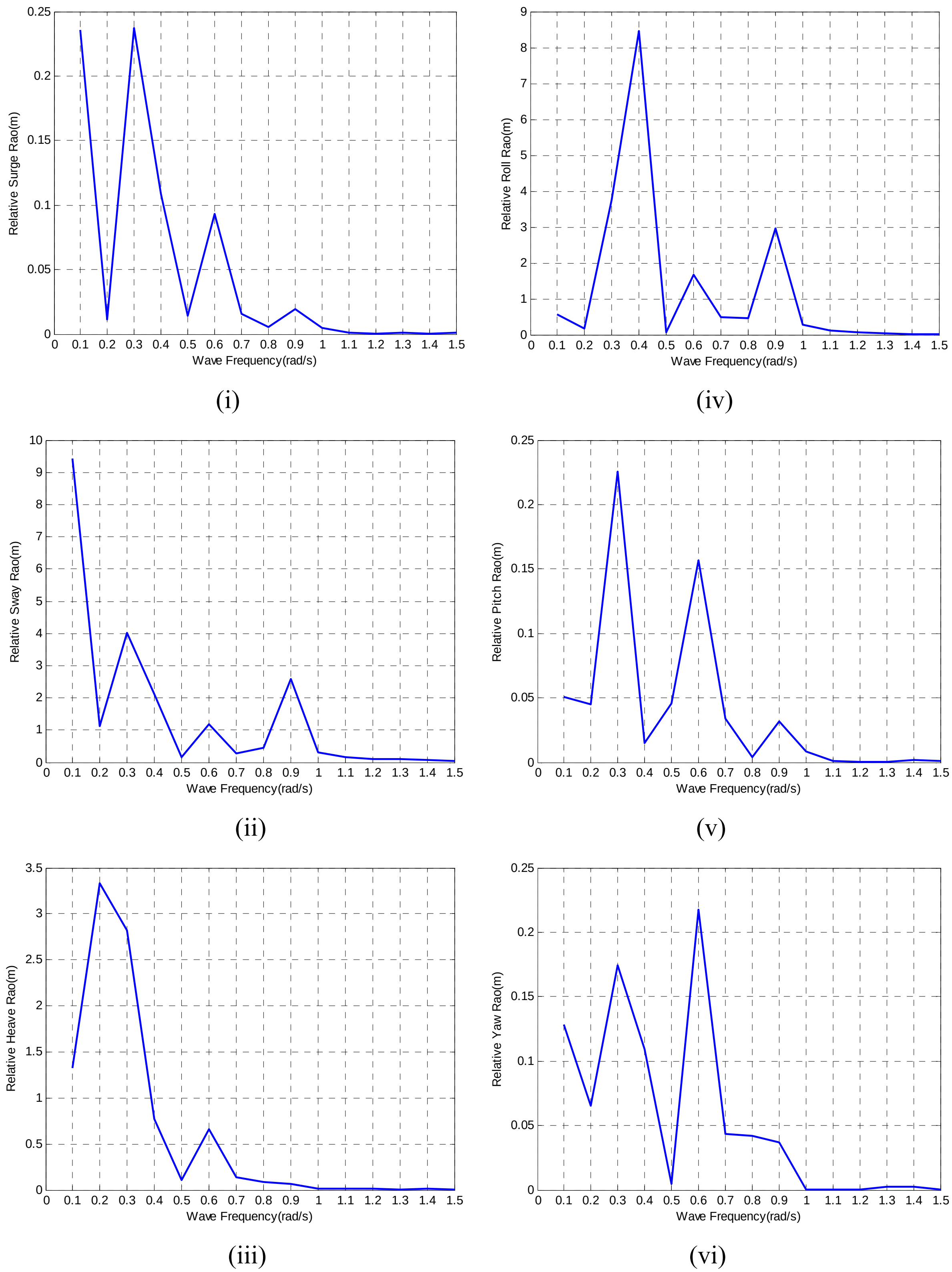

Figure 2-5. Relative motion response for 90 degrees wave heading

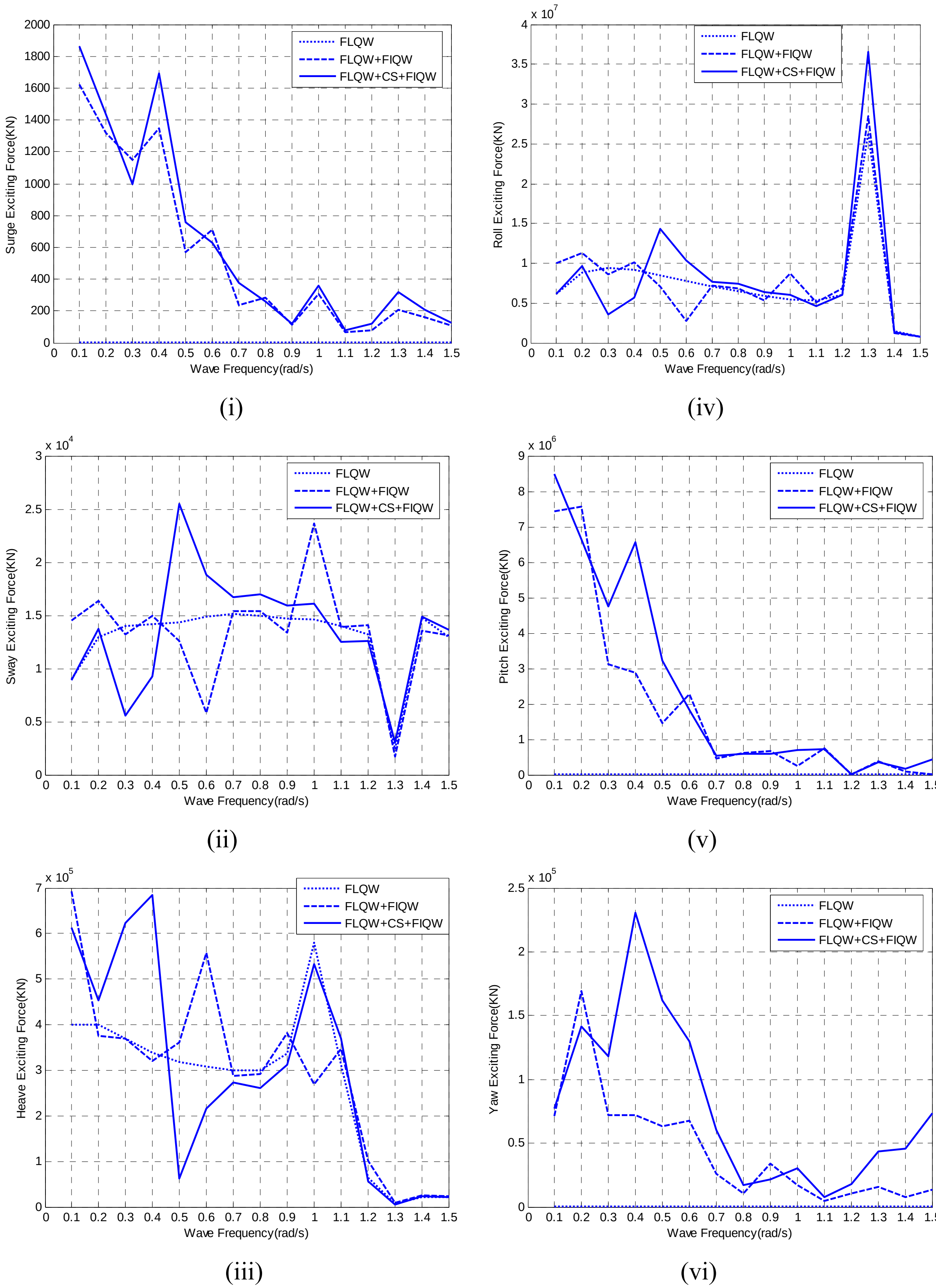

Figure 2-6. Wave exciting force on floating quay for 90 degrees wave heading

At higher frequency (short wave), the diffraction force decreases leading to near convergence of surge wave excitation force in single body, two body and three body cases.

In Figure 2-7[(ii) – (iv)], the wave excitation force in the three body case is less than that in single body case in the 0.5 : 0.1 : 1.5 rad/s frequency range; at 0.4 rad/s, there is a resonant wave exciting force. For container ship, there is a direct wave impact in single body case and two body case whereas the container ship is shielded from direct wave impact in the three body case and this results in the above phenomenon.

In Figure 2-6(iii), the multi-body heave excitation force for the floating quay at low frequency i.e. long wave is more than the single body heave excitation force due to the additional effects of the reflected waves in the multi-body case. In Figure 2-7(iii), the multi-body heave excitation force for the container ship is less than the single body heave excitation force due to the shielding effect.

Figure 2-8(a) and Figure 2-8(b) show mean drift forces acting on the floating quay and the container ship. From Figure 2-8(a) and Figure 2-8(b), it can be seen that the sway drift force at 1.3 rad/s is significantly large trying to make the floating quay and container ship move away from each other. The floating quay moves in the direction opposite to the incident wave i.e. away from the container ship whereas the container ship moves in the direction of the wave i.e. towards fixed quay wall. As the floating quay is symmetrical in the Y-Z plane so the surge drift force for single body is negligibly small.

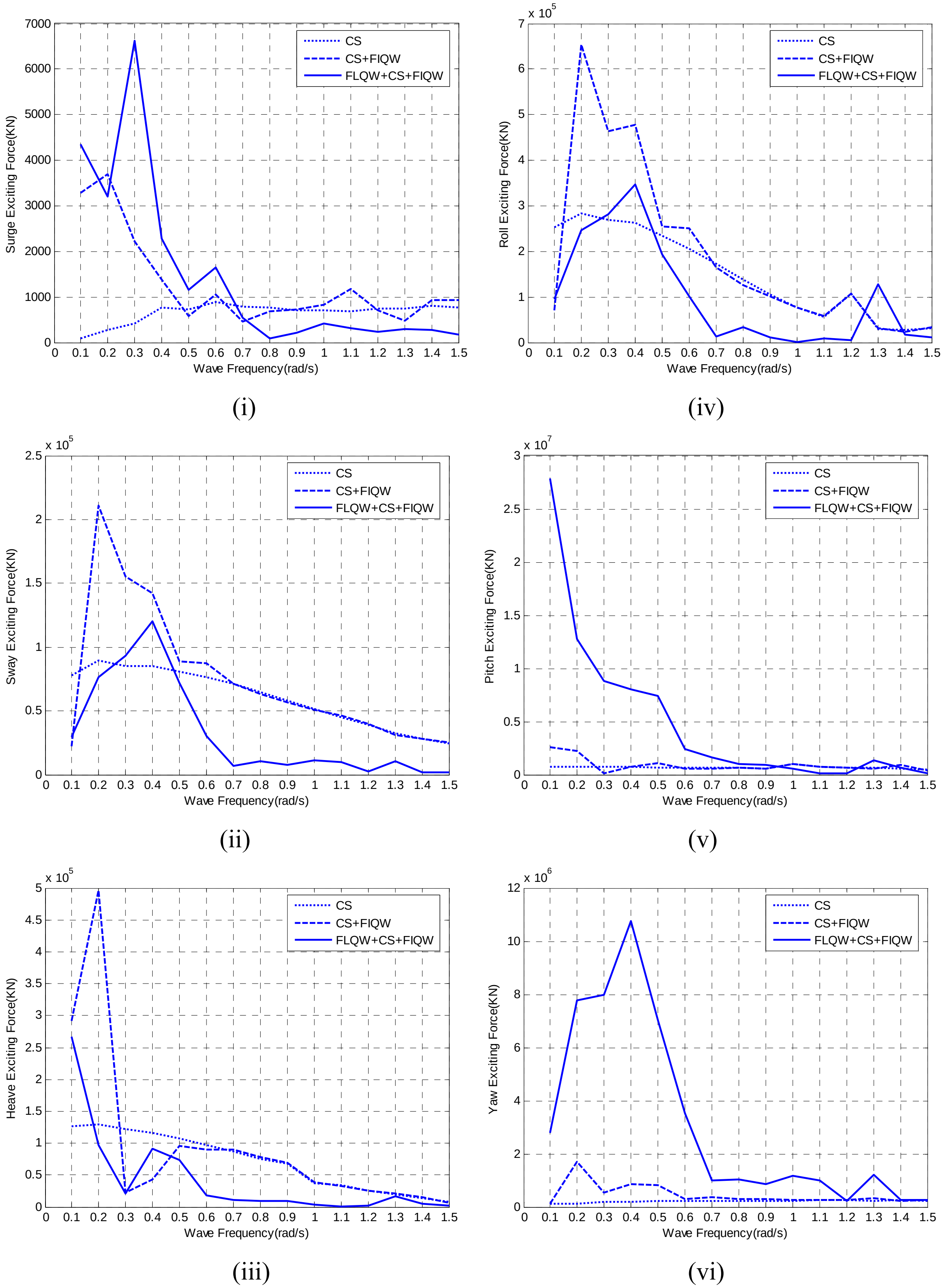

Figure 2-7. Wave exciting force on container ship for 90 degrees wave heading

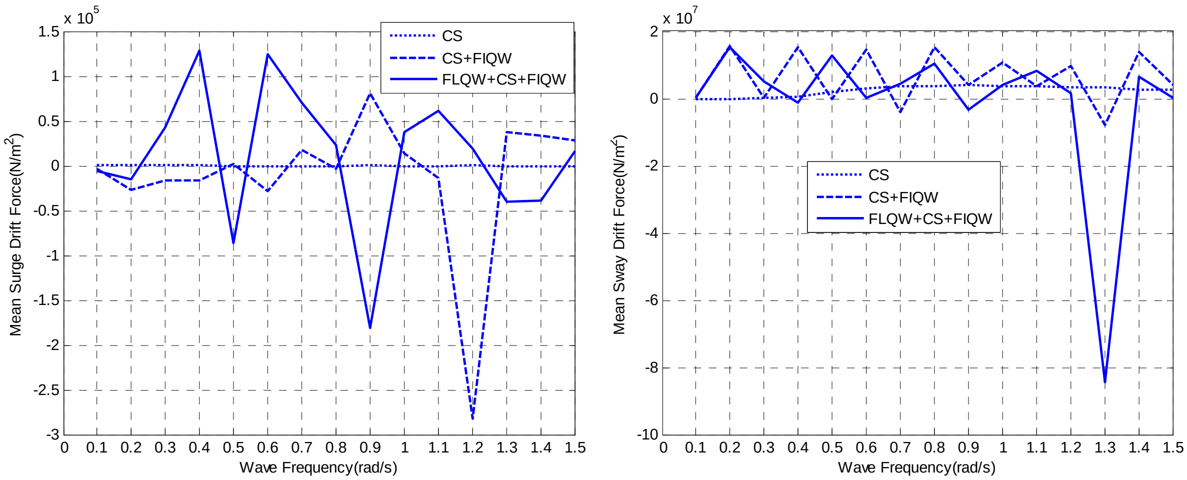

(i) (ii)

Figure 2-8(a). Mean drift force on floating quay for 90 degrees wave heading

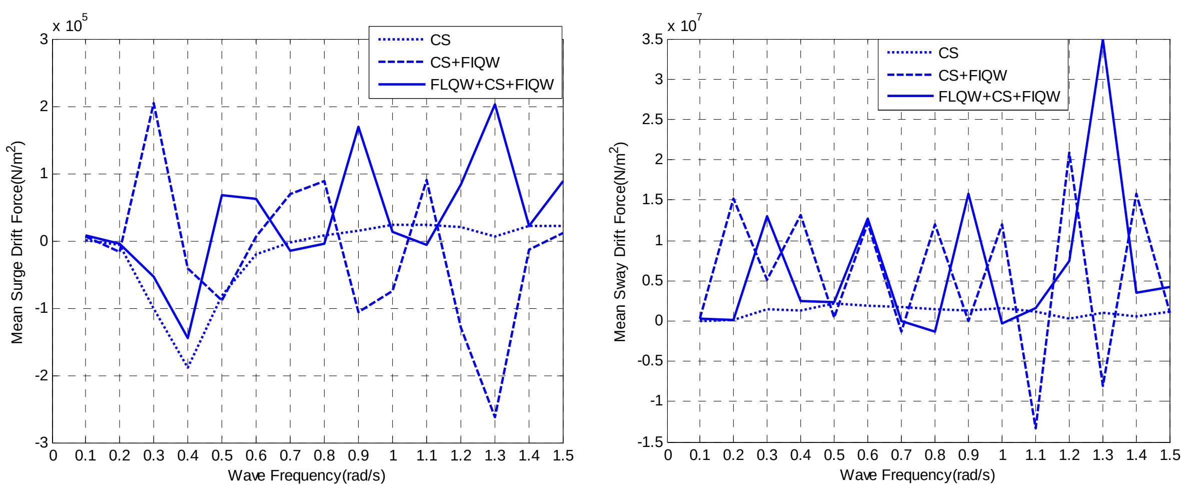

(i) (ii)

Figure 2-8(b). Mean drift force on container ship for 90 degrees wave heading

2.6.1.1 Incident wave = 90 degrees with dolphin and hawser connection

This is the realistic condition in which two dolphins, one on the forward and the other on the aft portion of the floating quay have been attached to restrict surge and sway motion of the floating quay. The hawser connection to the container ship has the same effect of restricting the surge and sway motion though some surge and sway motion of the container ship is allowed compared to that in the case of the floating quay. The motion response of the floating quay and container ship has been illustrated in Figure 2-9(a), Figure 2-9(b) and Figure 2-9(c) with dolphin and hawser connections respectively in the "presence" of fixed quay wall.

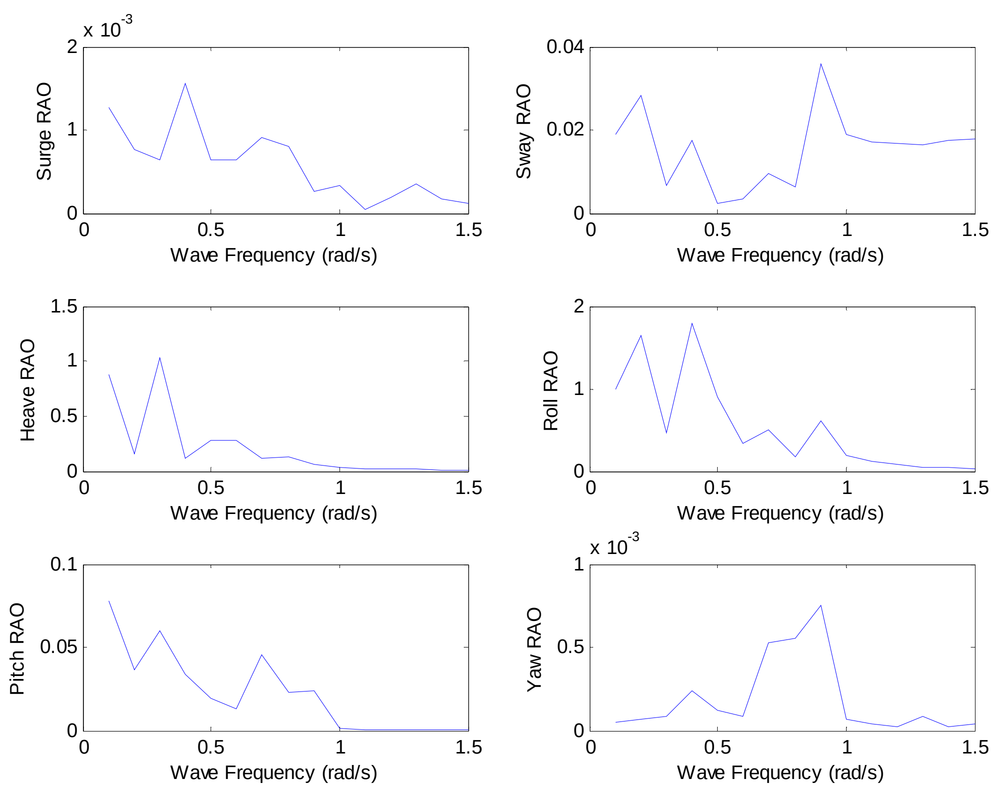

Figure 2-9 (a). Motion response of floating quay for 90 degrees wave heading

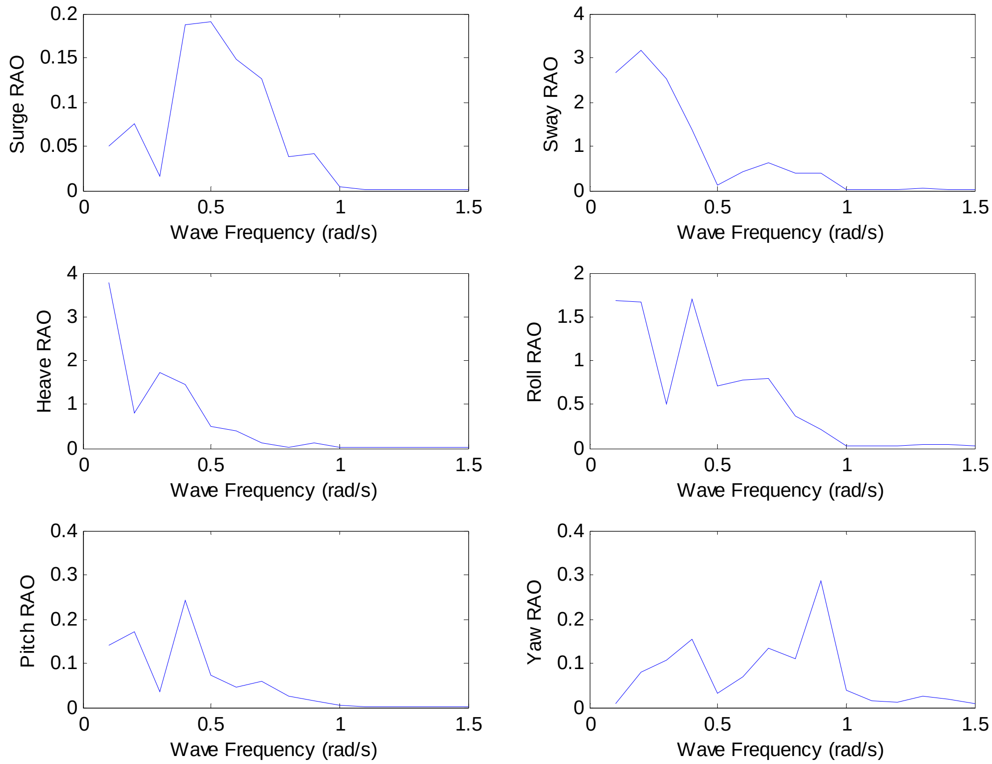

Figure 2-9 (b). Motion response of container ship for 90 degrees wave heading

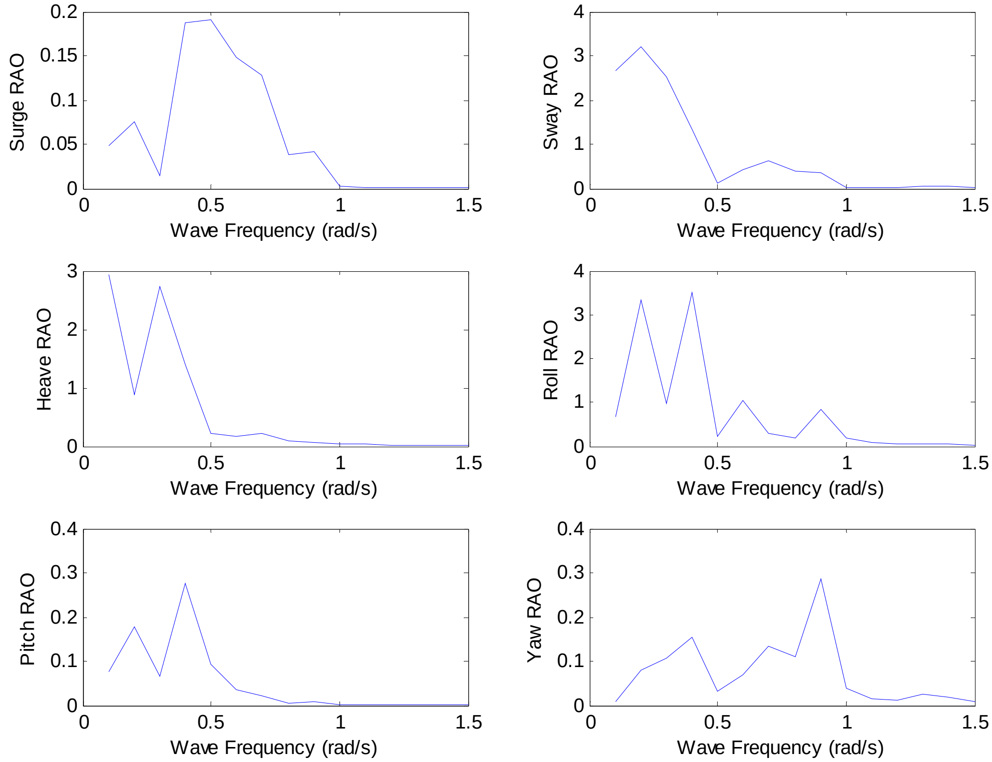

Figure 2-9 (c). Relative motion response of floating quay and container ship with dolphin and hawser connections respectively for 90 degrees wave heading

2.6.2 Case 2. Wave Heading = 45 Degrees i.e. quadrant sea condition for "Freely Floating" Container Ship and Floating Quay Wall

The motion response of single body case and multi-body case in 45 degrees incident wave condition is very similar. In Figure 2-10, multi-body motion response is slightly greater in floating quay case and there is some spiky motion response due to the interaction effects. In Figure 2-11, , multi-body motion response is much greater when there is no shielding effect to the container ship as the motion response without floating quay wall is a combination of direct wave impact and the interaction effect. Figure 2-12 shows the relative motion response for 45 degrees wave heading.

Figure 2-13. and Figure 2-14 illustrate the wave exciting forces on the floating quay and the container ship respectively. In Figure 2-14[(ii) – (iv)], the wave excitation force in the three body case has very sharp peak at 0.2 rad/s in the 0.2 : 0.1 : 1.5 rad/s frequency range. Figure 2-15(a) and Figure 2-15(b) illustrate the mean drift forces on the floating quay and the container ship respectively.

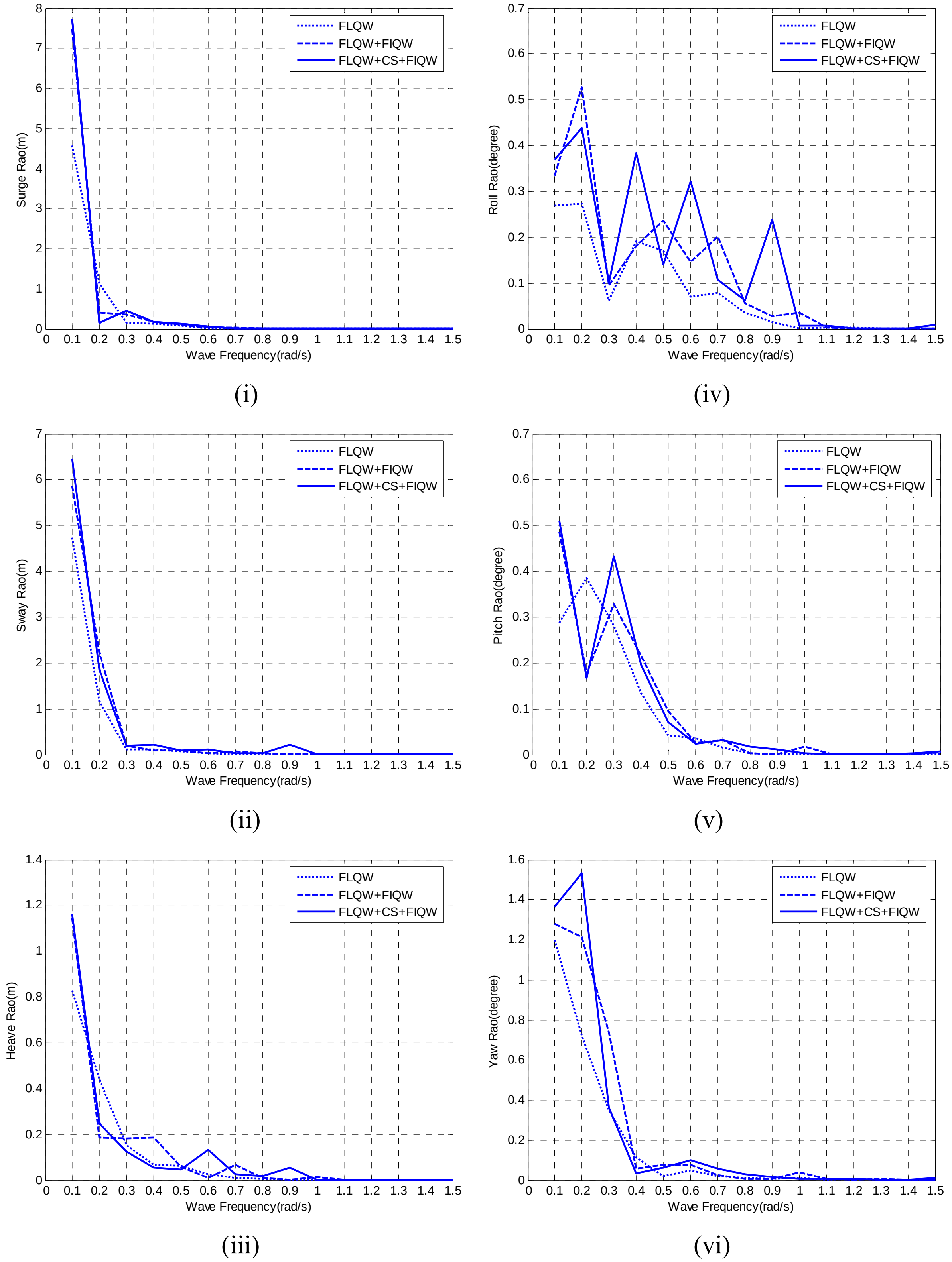

Figure 2-10. Floating quay RAO for 45 degrees wave heading

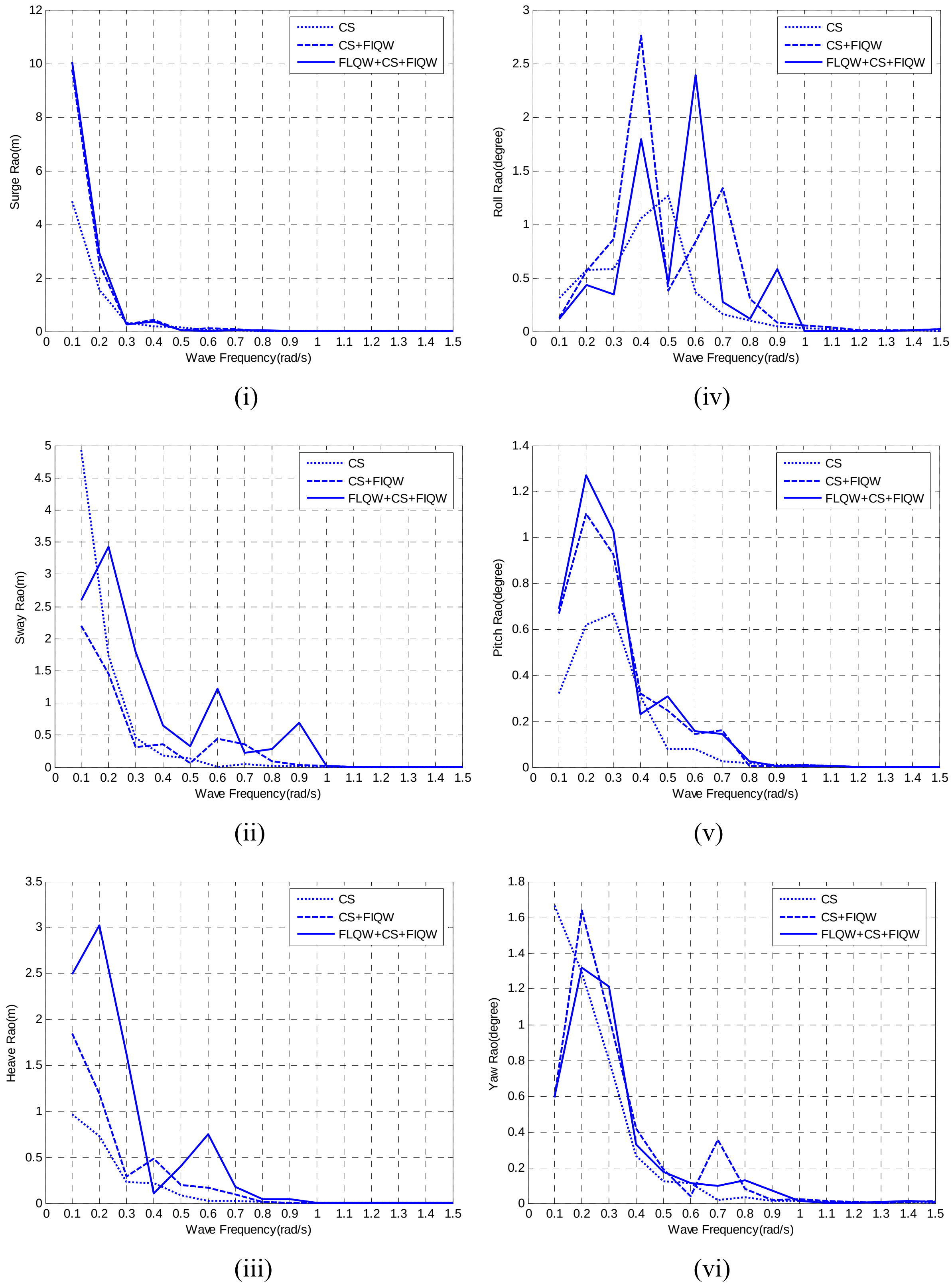

Figure 2-11. Container ship RAO for 45 degrees wave heading

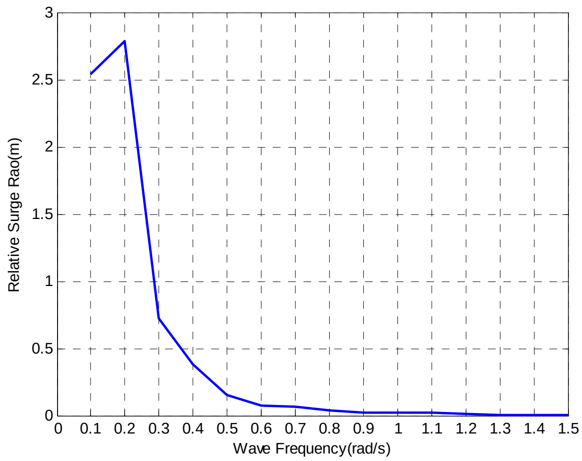

(i)

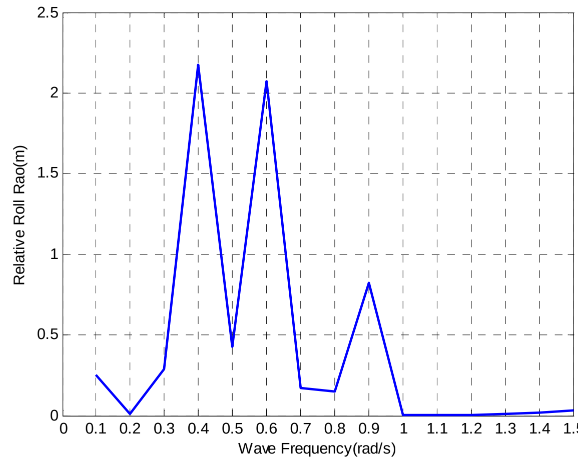

(iv)

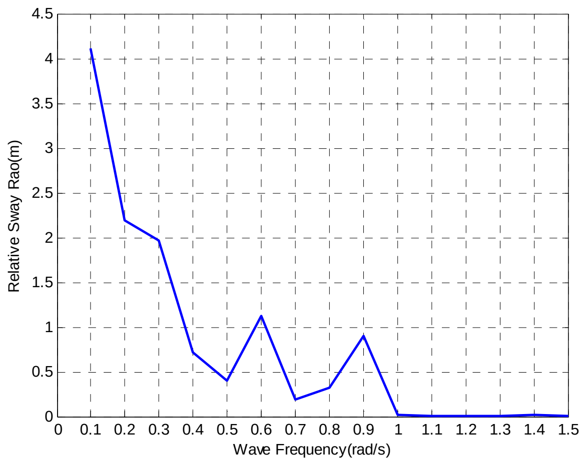

(ii)

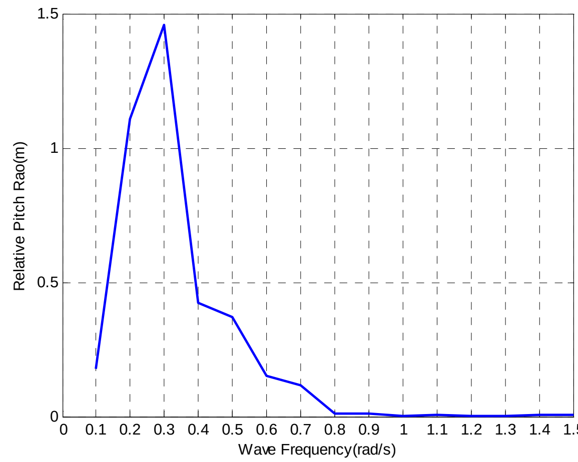

(v)

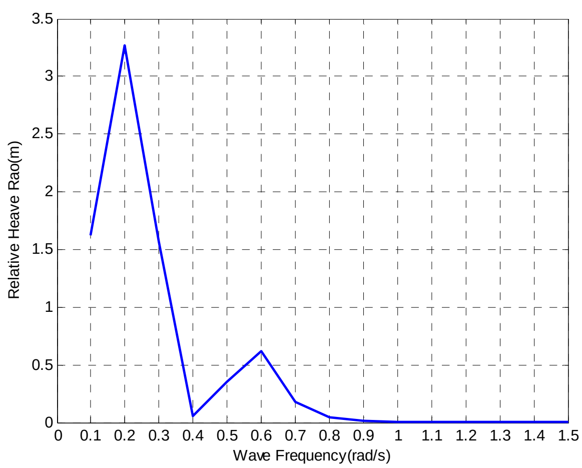

(iii)

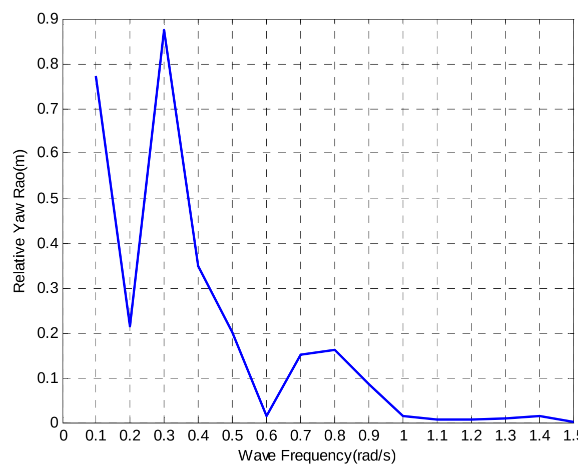

(vi)

Figure 2-12. Relative motion response for 45 degrees wave heading

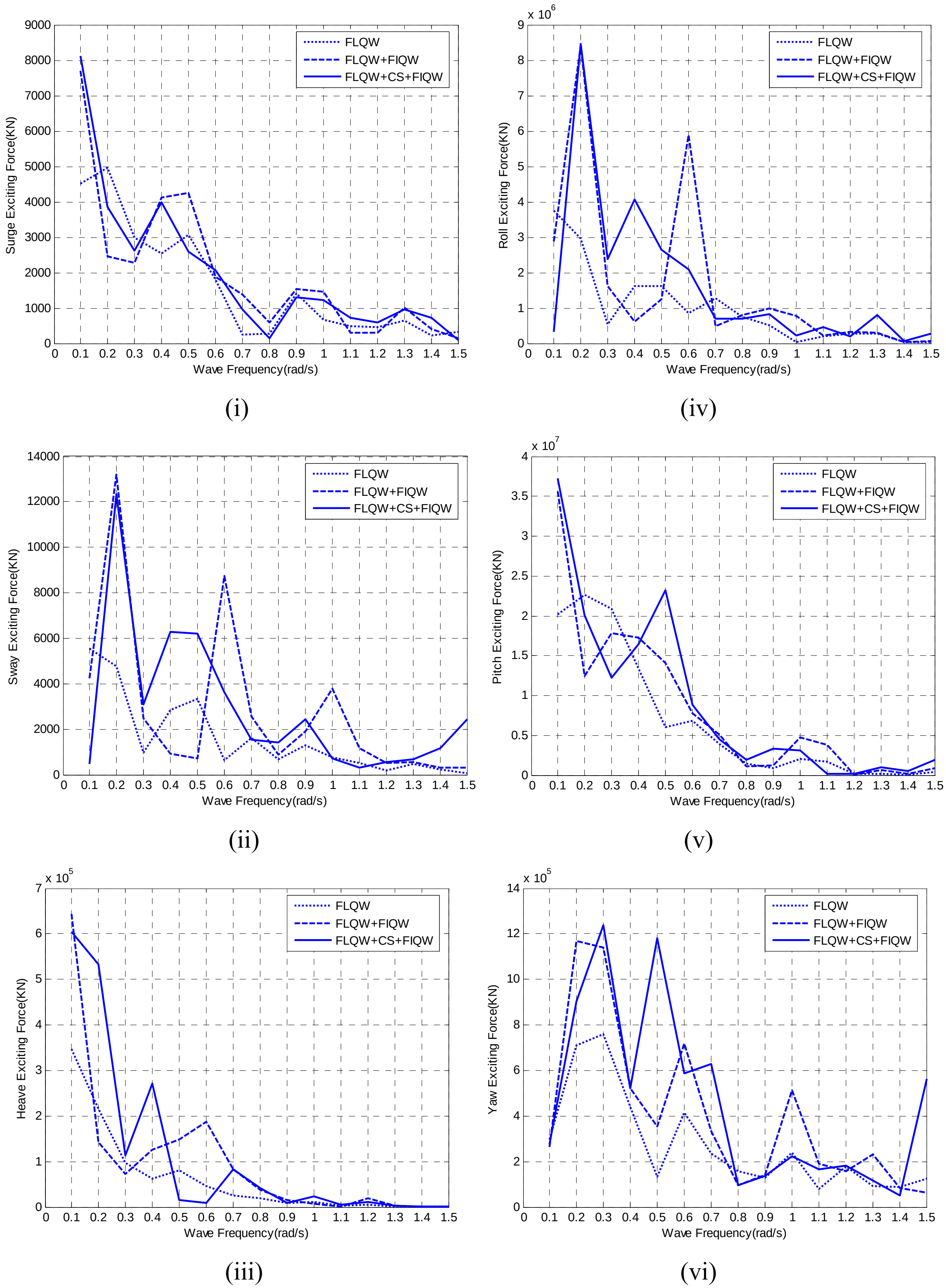

Figure 2-13. Wave exciting force on floating quay for 45 degrees wave heading

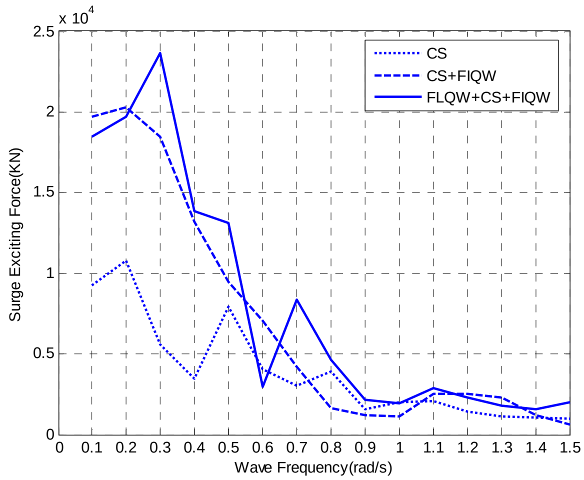

(i)

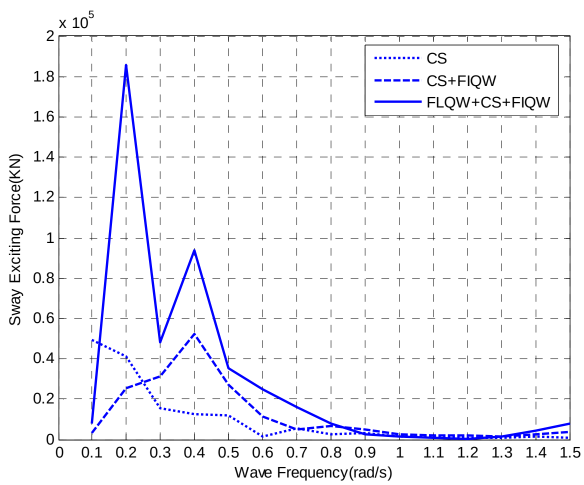

(ii)

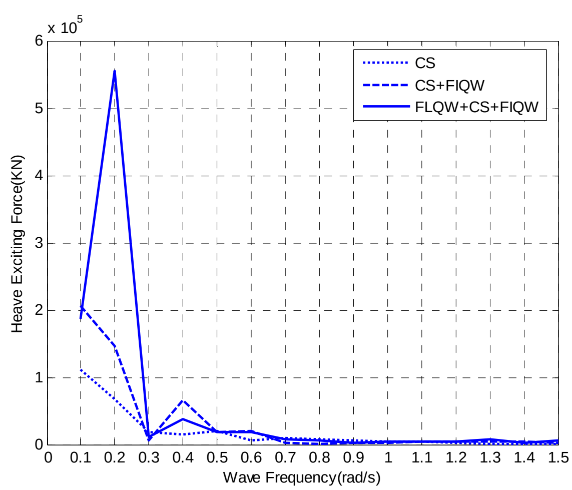

(iii)

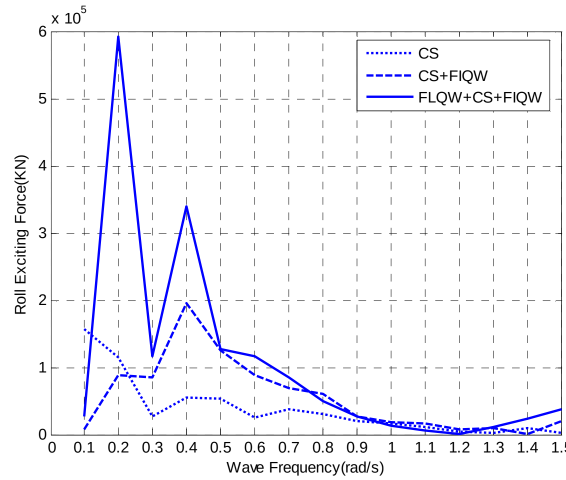

(iv)

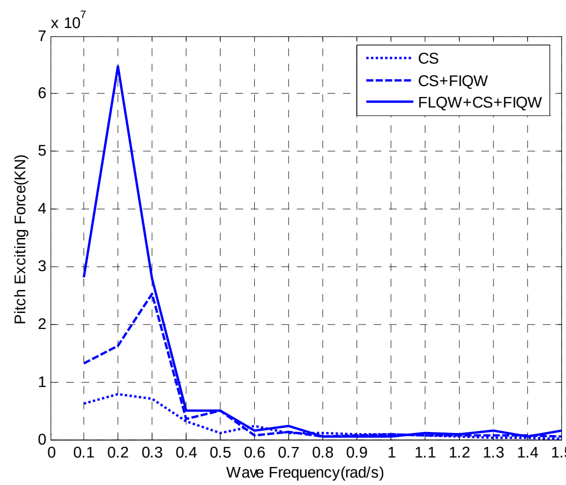

(v)

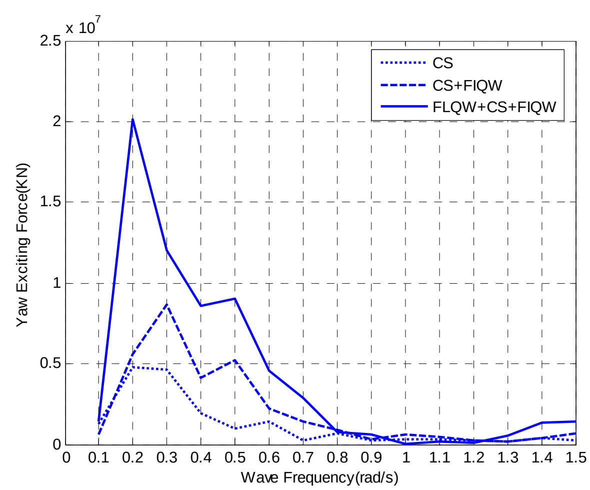

(vi)

Figure 2-14. Wave exciting force on container ship for 45 degrees wave heading

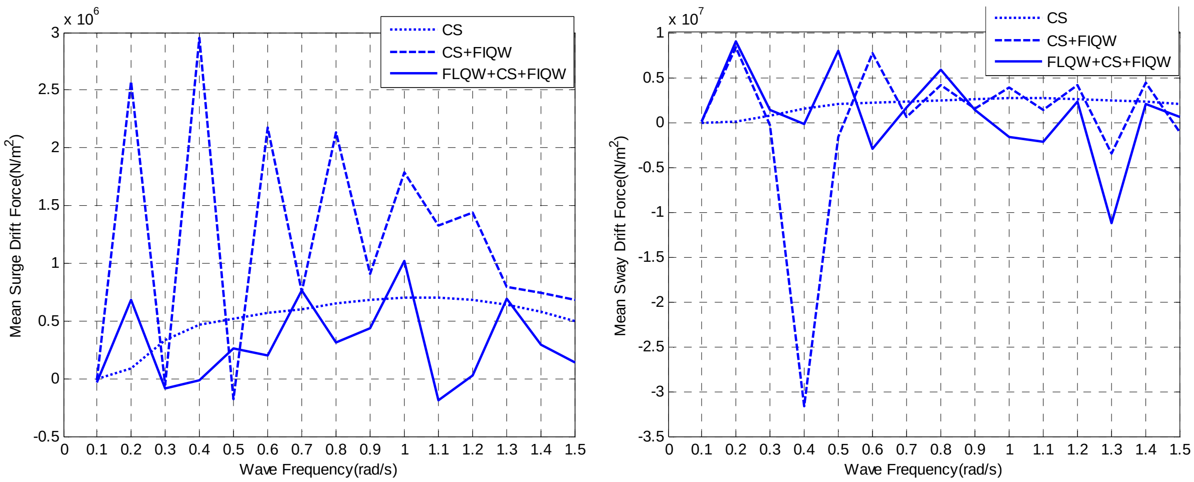

(i) (ii)

Figure 2-15(a). Mean drift force on floating quay for 45 degrees wave heading

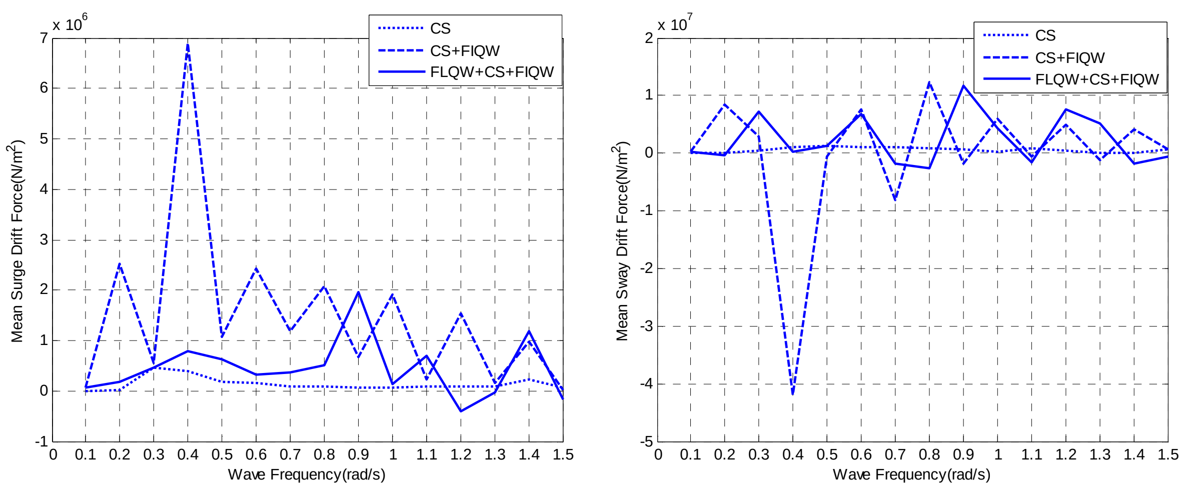

(i) (ii)

Figure 2-15(b). Mean drift force on container ship for 45 degrees wave heading

2.6.2.1 Incident wave heading = 45 degrees with dolphin connection and hawser connection

This is the realistic condition in which two dolphins, one on the forward and the other on the aft portion of the floating quay has been attached to restrict surge and sway motion of the floating quay. The hawser connection to the container ship has the same effect though some surge and sway motion of the container ship is allowed. The motion response of the floating quay and container ship has been illustrated in figure 2-16(a), 2-16(b) and 2-16(c) with dolphin and hawser connections respectively in the presence of fixed quay wall.

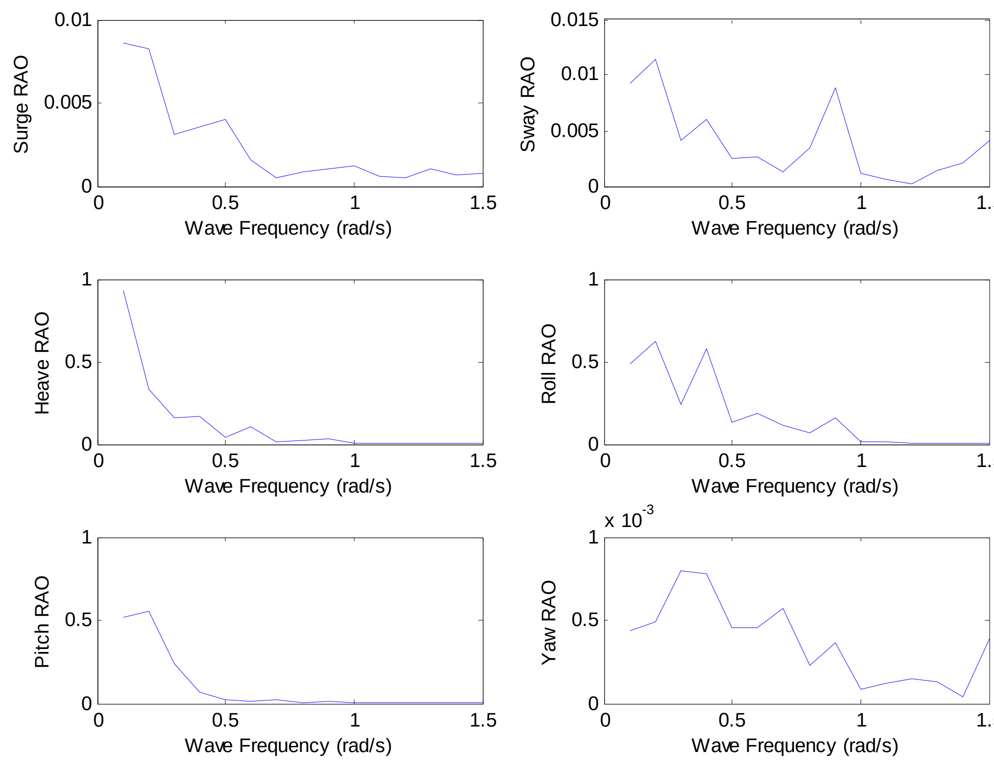

Figure 2-16(a) Motion response of floating quay for 45 degrees wave heading

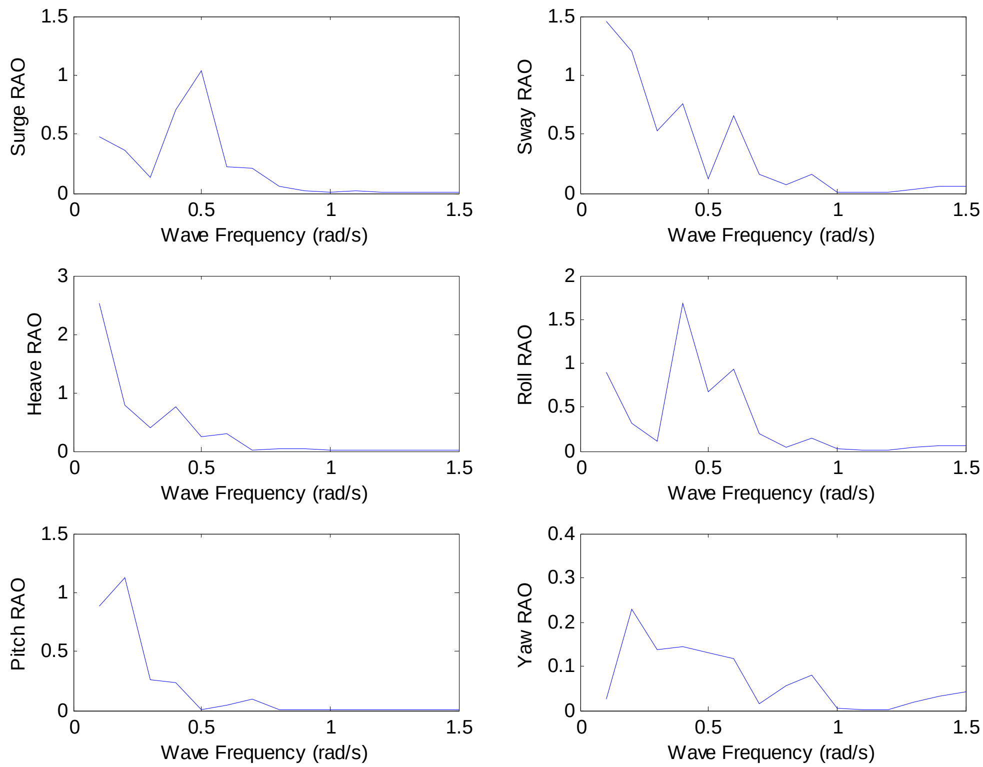

Figure 2-16(b). Motion response of container ship for 45 degrees wave heading

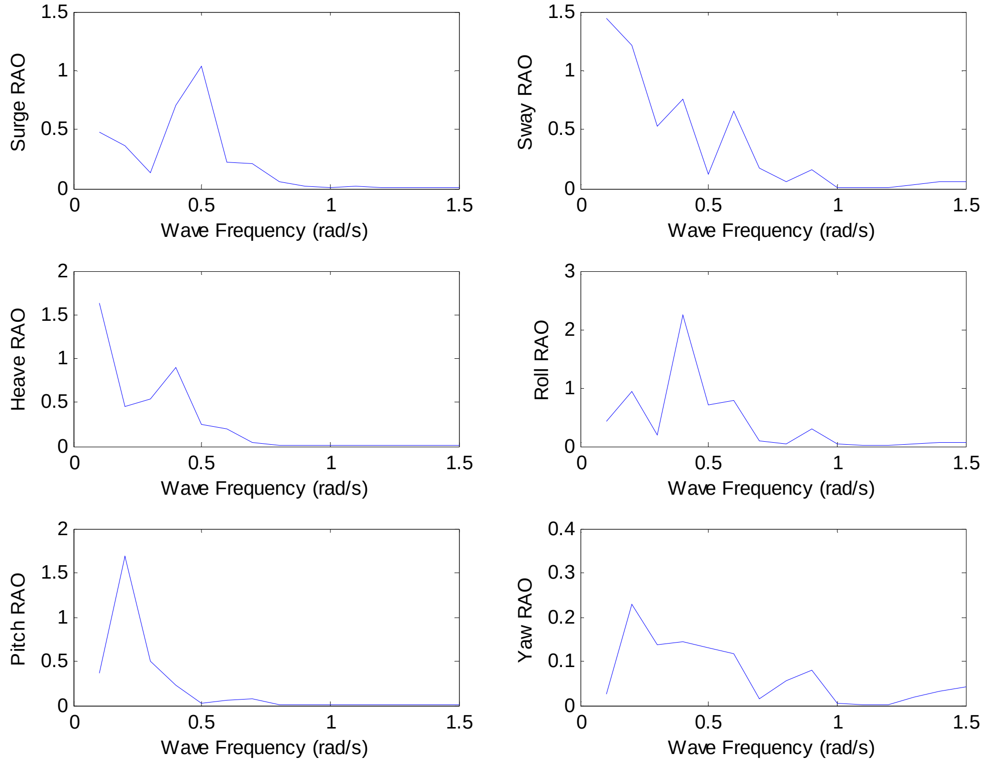

Figure 2-16(c). Relative motion response of floating quay and container ship with dolphin and hawser connections respectively for 45 degrees wave heading

2.6.3 Case 3. Wave Heading = 0 Degrees for "Freely Floating" Container Ship and Floating Quay Wall

Figure 2-17 and Figure 2-18 illustrate the motion response of floating quay and container ship respectively. Due to symmetric structure of the floating quay and container ship, there is no sideways motion of the single body floating structure so the sway response is negligibly small in Figure 2-17(ii) and Figure 2-18(ii). Due to the interaction effect in the multi-body case the motion is significantly greater than that in the single body case and there is sway motion in the multi-body case due to the interaction effect. Container ship roll response shows two sharp peaks at 0.4 rad/s and 0.6 rad/s respectively in Figure 2-18(iv).

Figure 2-19, Figure 2-20 and Figure 2-21 show the relative motion response between the floating quay and the container ship, the wave exciting force on floating quay and container ship respectively for 0 degrees wave heading.

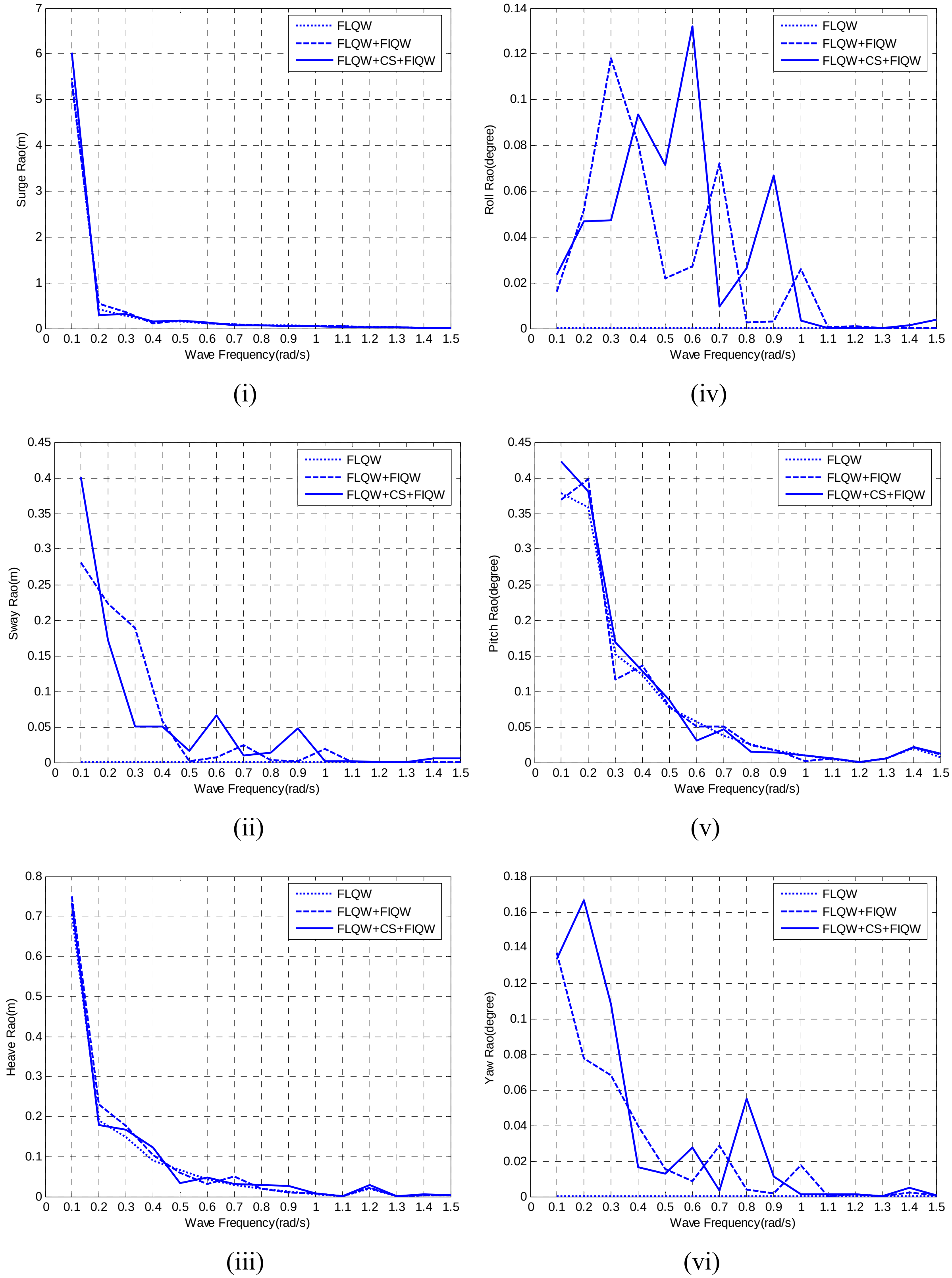

Figure 2-17. Motion response of floating quay for 0 degrees wave heading

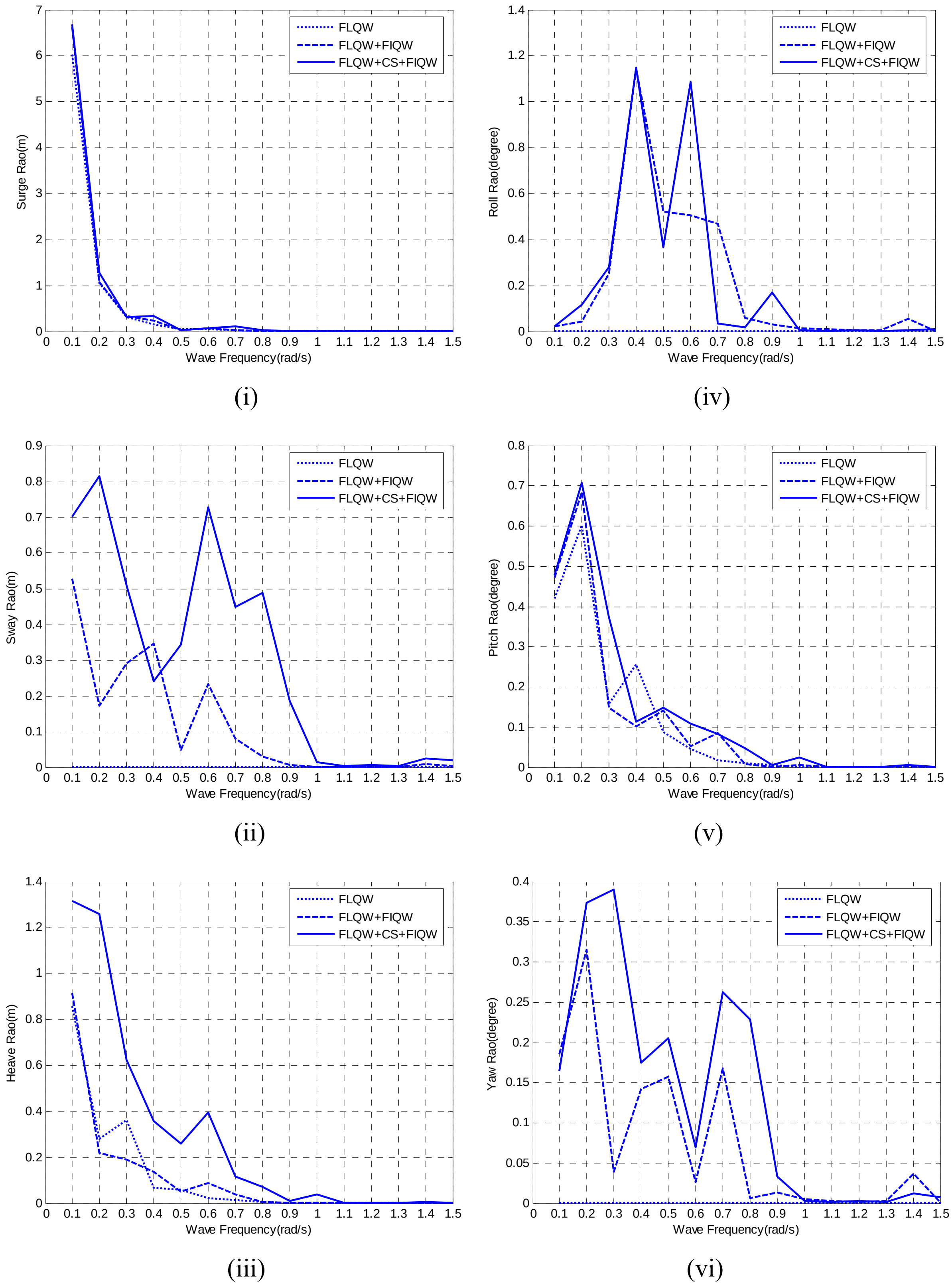

Figure 2-18. Motion response of container ship for 0 degrees wave heading

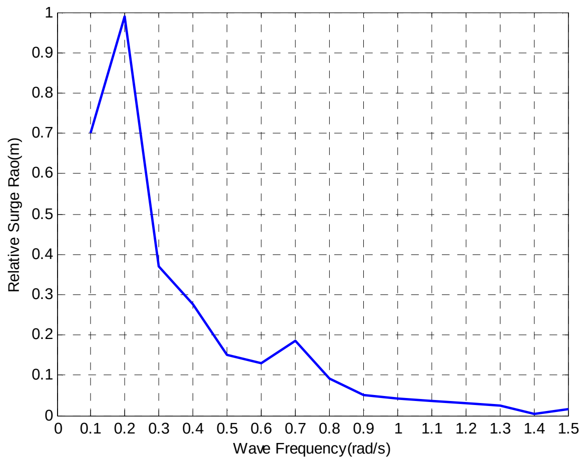

(i)

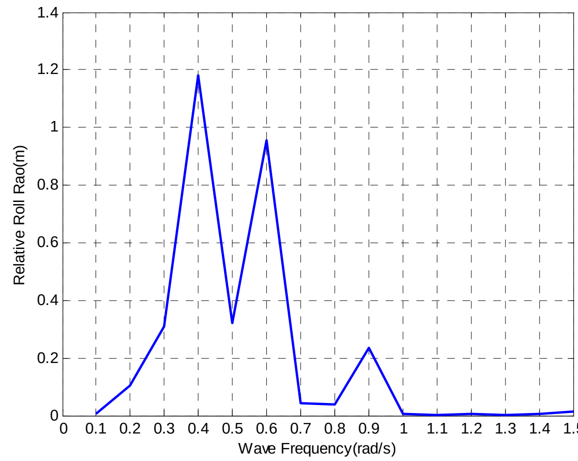

(iv)

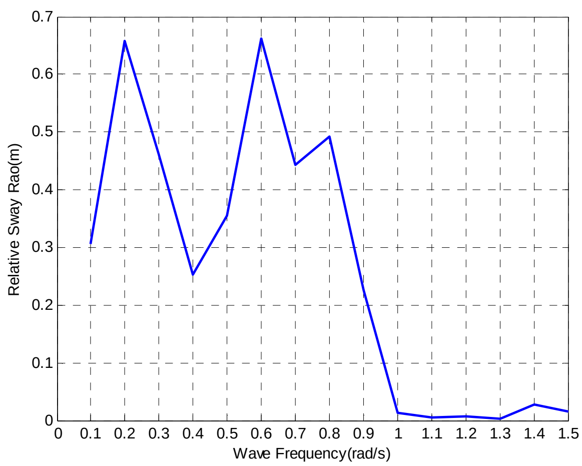

(ii)

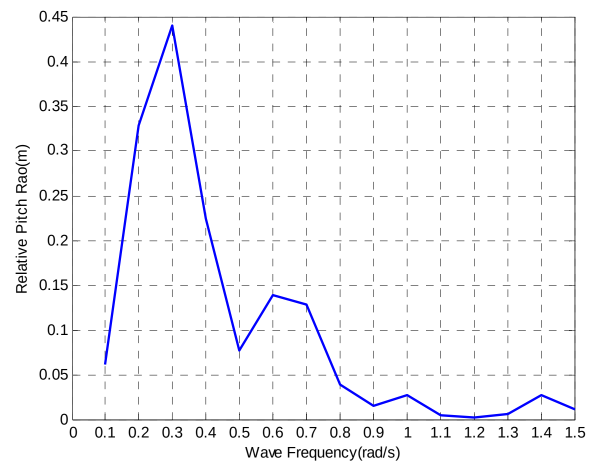

(v)

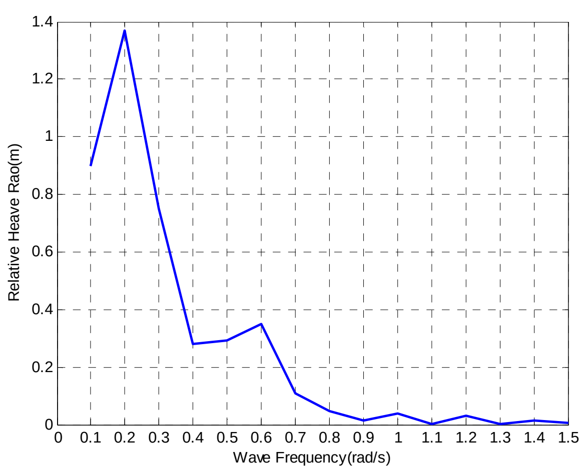

(iii)

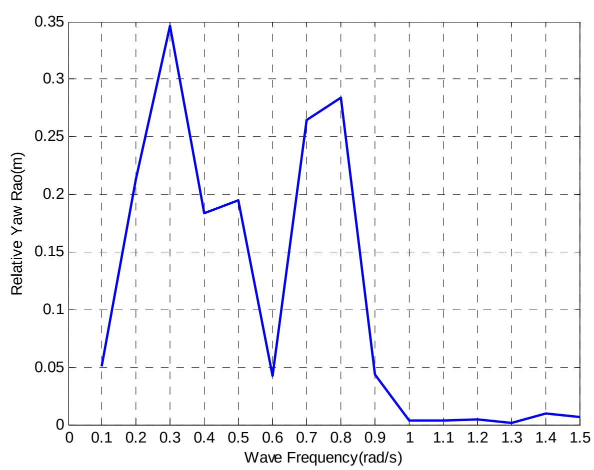

(vi)

Figure 2-19. Relative motion response for 0 degrees wave heading

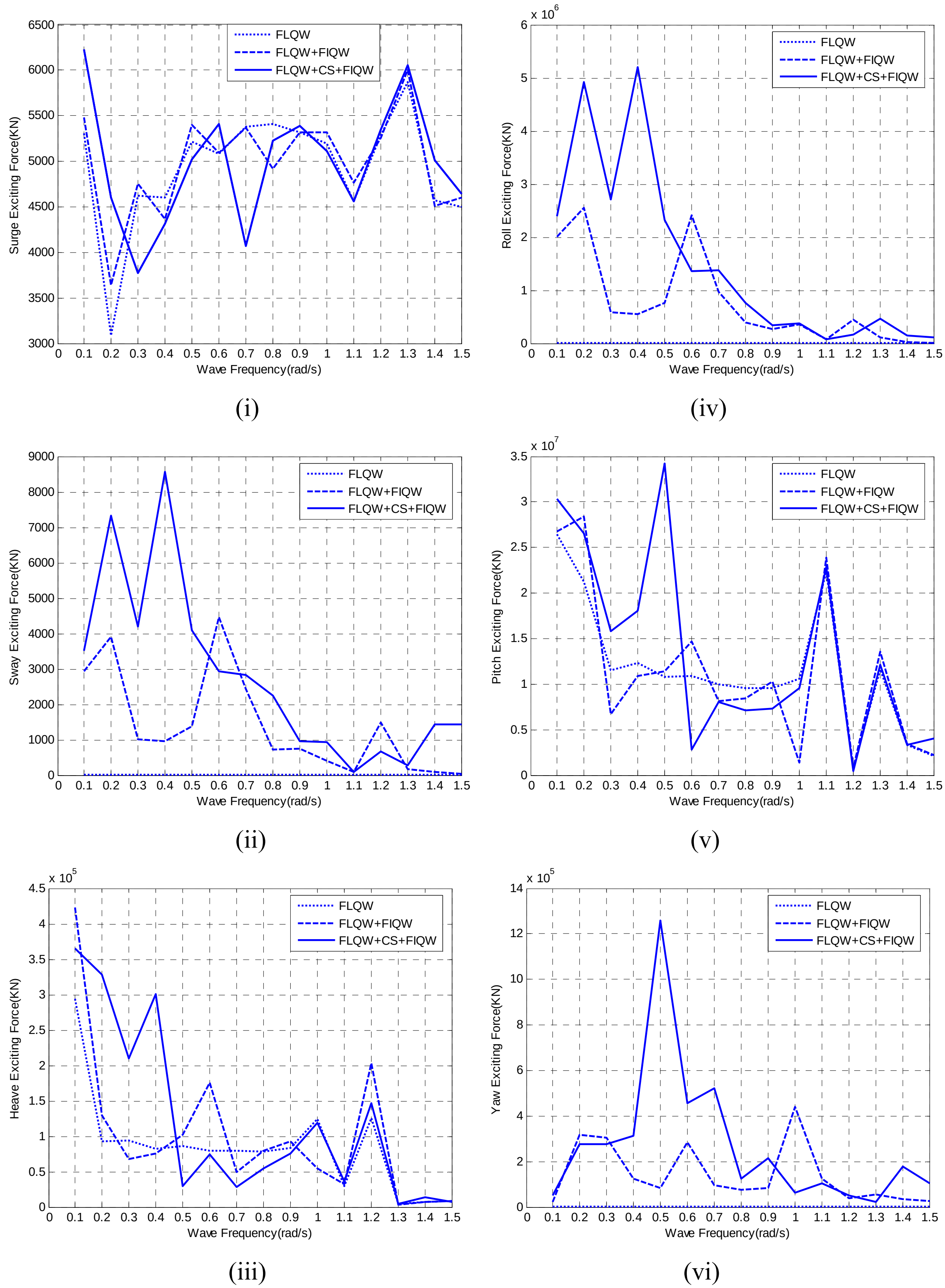

Figure 2-20. Wave exciting force on floating quay for 0 degrees wave heading

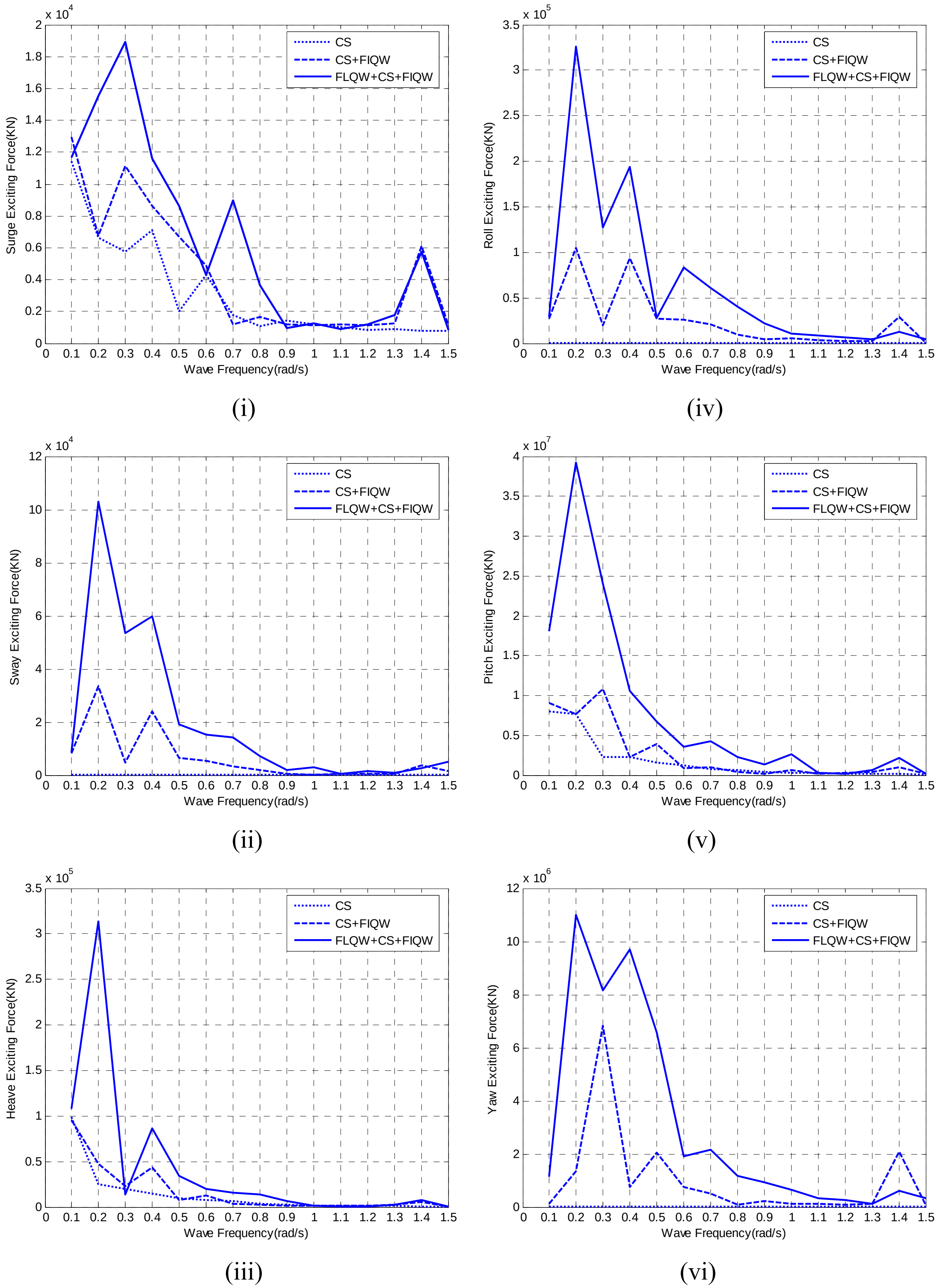

Figure 2-21. Wave exciting force on container ship for 0 degrees wave heading

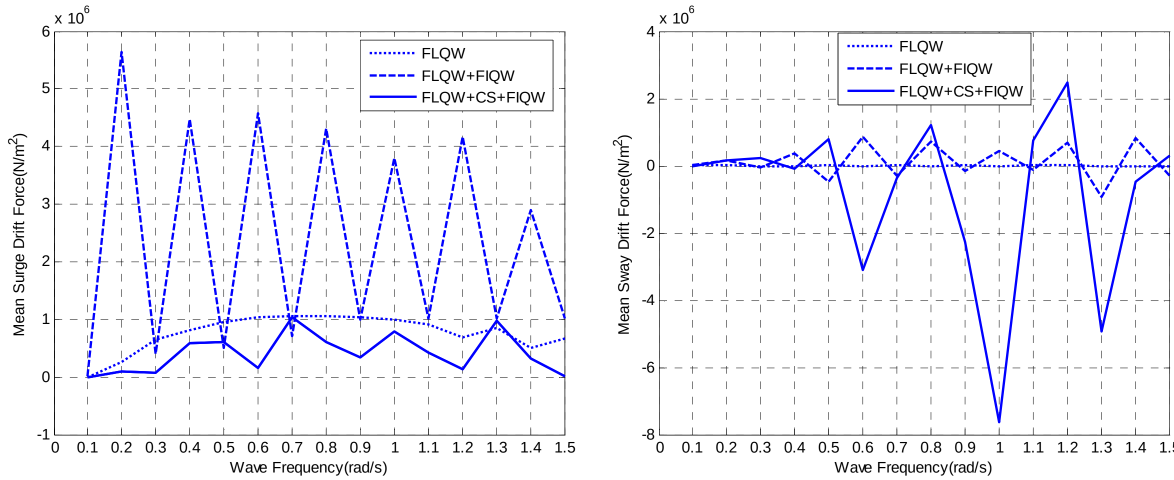

(i) (ii)

Figure 2-22(a). Mean drift force on floating quay for 0 degrees wave heading

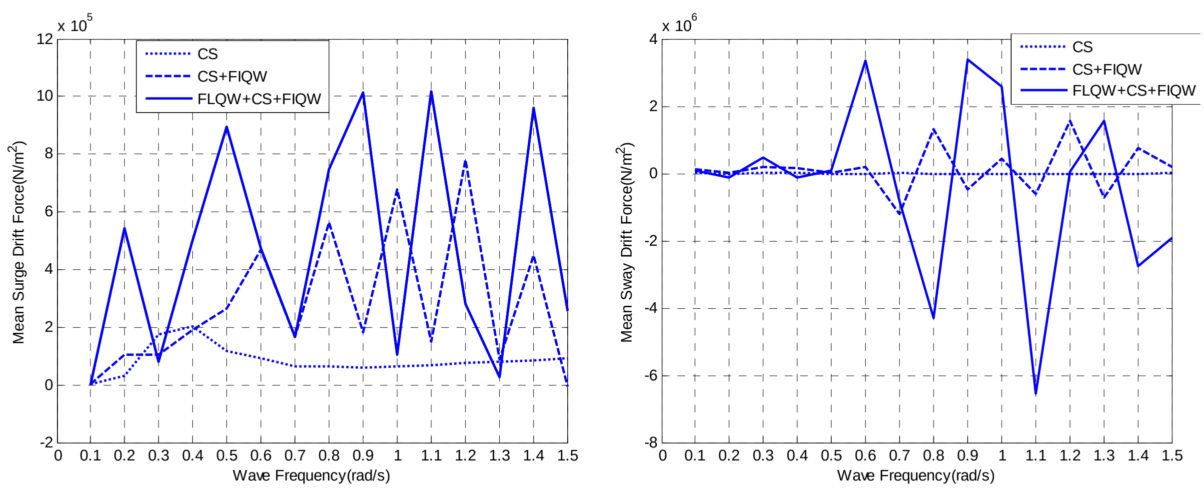

(i) (ii)

Figure 2-22(b). Mean drift force on container ship for 0 degrees wave heading

As mentioned in the beam sea and quadrant sea conditions, the mean drift force in the above figures show large drift force at 1.1 rad/s. This will facilitate the motion of the floating quay and the container ship towards each other.

2.6.3.1 Incident wave heading = 0 degrees with dolphin connection and hawser connection

This is the realistic condition in which two dolphins, one on the forward and the other on the aft portion of the floating quay has been attached to restrict surge and sway motion of the floating quay. The hawser connection to the container ship has the same effect though some surge and sway motion of the container ship is allowed. The motion response of the floating quay and container ship has been illustrated in Figure 2-23(a), Figure 2-23(b) and Figure 2-23(c) with dolphin and hawser connections respectively in the presence of fixed quay wall.

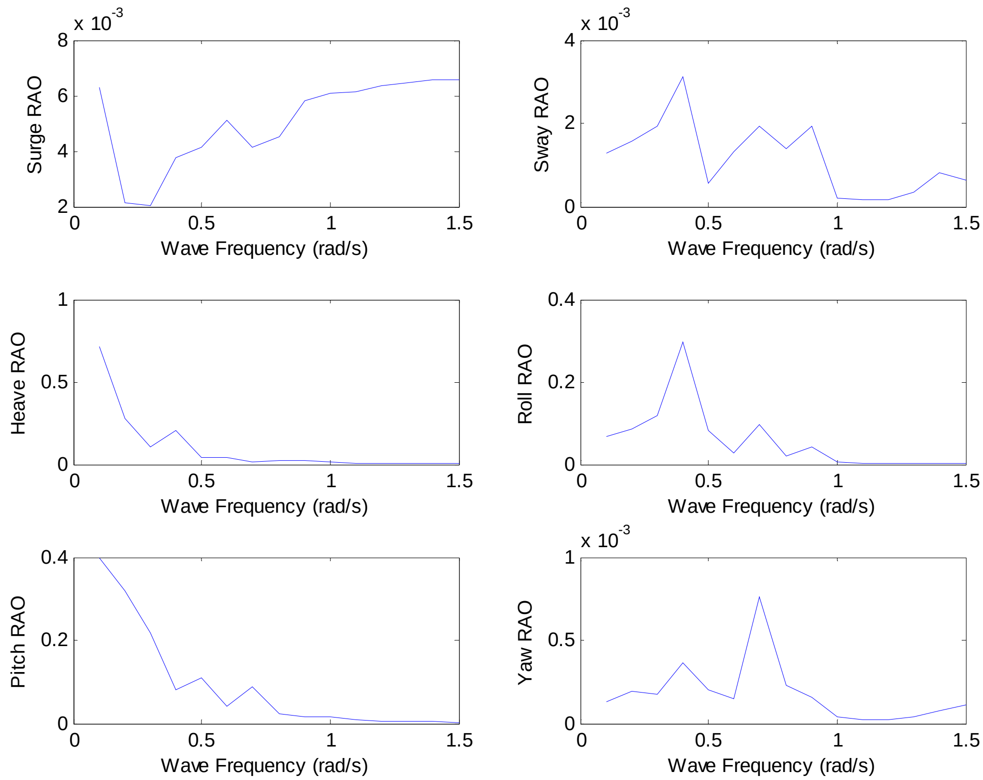

Figure 2-23(a). Motion response of floating quay for 0 degrees wave heading

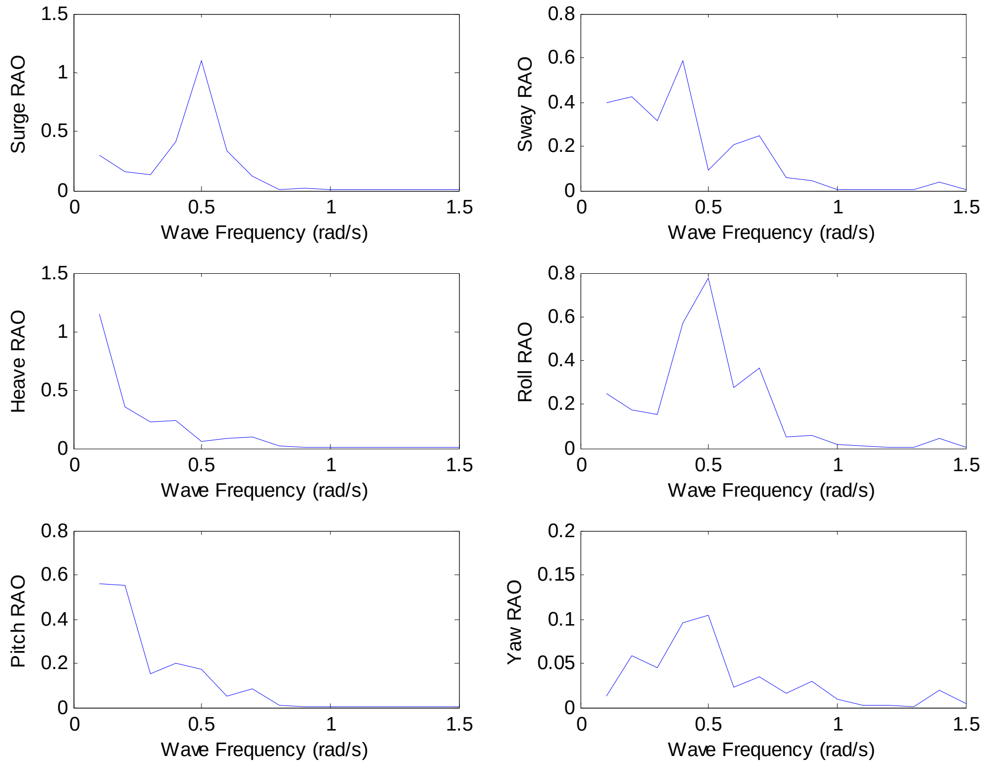

Figure 2-23(b). Motion response of container ship for 0 degrees wave heading

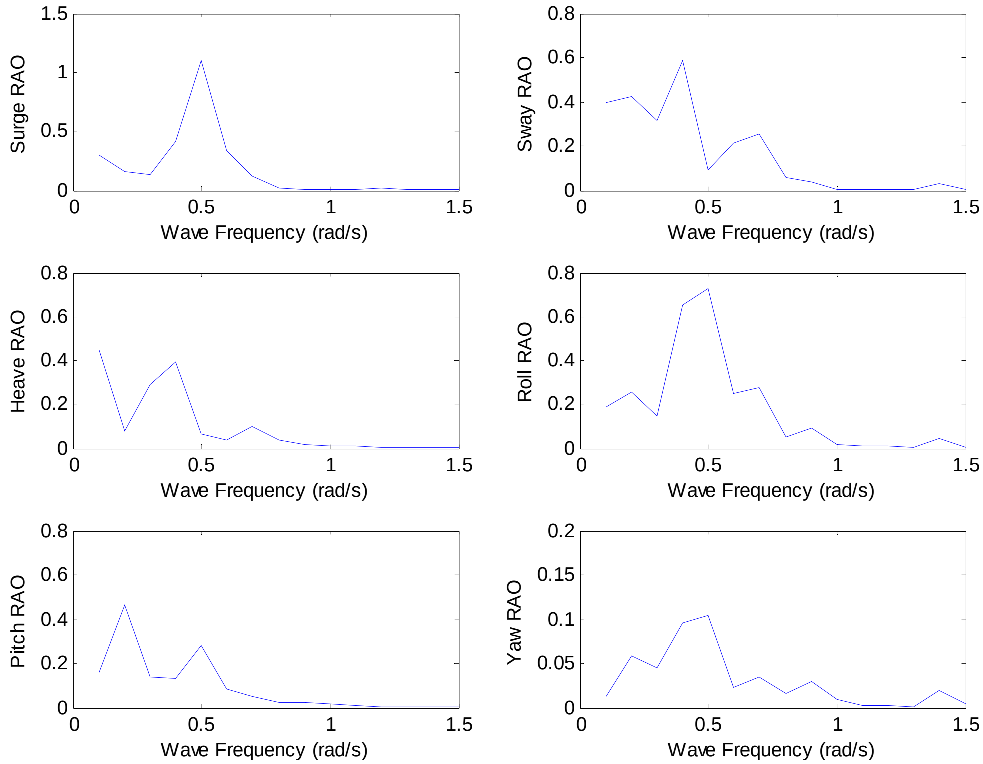

Figure 2-23(c). Relative motion response of floating quay and container ship with dolphin and hawser connections respectively for 0 degrees wave heading

2.7 Coupled Dynamic Analysis in Time Domain Using WINPOST

WINPOST is used for the coupled dynamic analysis of moored offshore structures in time domain. The resulting time domain result is compared with the frequency domain result obtained using WAMIT. Hydrodynamic coefficients and forces from WAMIT output are converted to WINPOST input through the interface program, WAMPOST. The WINPOST program was understood from Kim, M. H., 1997. WINTCOL/WINPOST user's manual. In this WINPOST simulation, the container ship is connected with four hawsers, the floating quay is attached with two dolphin moorings as shown in the layout and fenders are placed between interacting bodies to avoid collision due to the drift forces mentioned earlier in the WAMIT output. The hawsers and dolphin moorings restrict the surge, sway and yaw motion of the container ship and the floating quay. In this case, the dolphin moorings and hawsers have been modeled using external linear spring. The stiffness of spring has been adjusted in such a way that the hawsers do provide small surge, sway and yaw motion in the case of container ship but dolphin moorings greatly restrict surge, sway and yaw motion in the case of the floating quay. After getting the result for the surge, sway and yaw motion RAO, the following are the hawser and the mooring stiffness for restricting the surge, sway and yaw motion RAO.

The floating quay dolphin mooring and container ship hawser stiffness is shown in Table 2-2 and Table 2-3 respectively.

Table 2-2. Floating quay dolphin mooring stiffness

Surge	1.00E+09 N/m
Sway	1.00E+09 N/m
Yaw	6.13E+13 Nm/rad

Table 2-3. Container ship hawser stiffness

Surge	5.00E+07 N/m
Sway	5.00E+07 N/m
Yaw	3.01E+12 Nm/rad

2.7.1 WINPOST Motion Analysis for 90 Minutes Simulation

Time domain WINPOST analysis for 90 minutes simulation time done for 45 degrees wave heading is explained below. The following data in Table 2-4 and Table 2-5 was provided by KORDI. The peak period and significant wave height in the simulation is 14 seconds and 1.8 meters respectively.

Table 2-4. Environmental wave characteristics

Wave Direction	Significant Wave Height(m)	Peak Period(s)
S10W	1.8	15.0
S	1.8	14.0

Table 2-5. Current profile

Tidal Current velocity at free surface (m/s)	0.23
Current velocity profile: $1/7^{th}$ power rule	Current velocity = $VC(1+z/Depth)^{1/7}$
Current incident angle	Same as wave incident angle

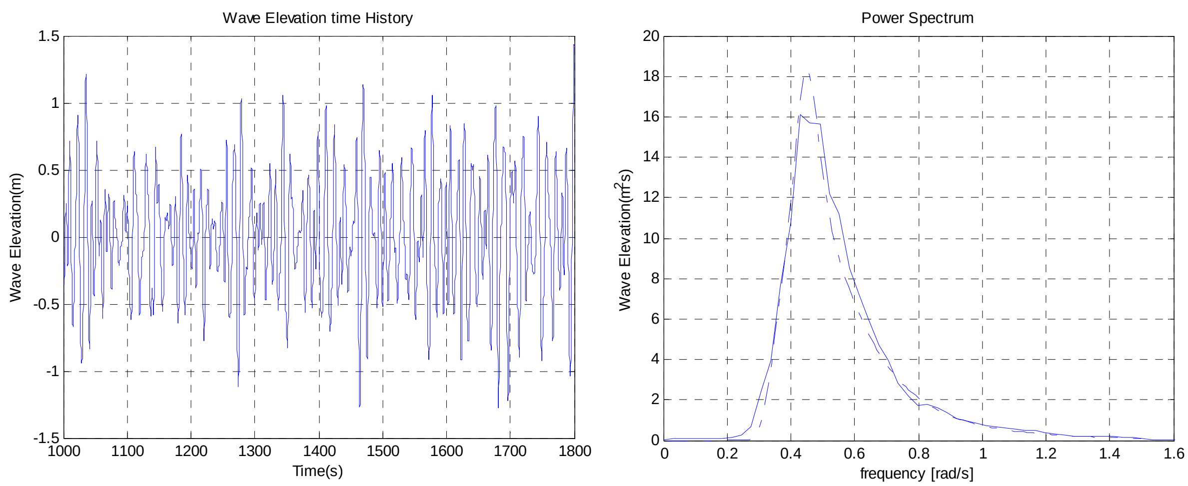

(i) (ii)

Figure 2-24. Wave elevation time history and wave spectrum

WINPOST analysis is done for the data given above with simulation time of 90 minutes. The peak parameter, $\gamma = 1.5$ for JONSWAP spectrum has been assumed for the simulation for the above wave conditions.

2.7.1.1 Container ship motion in the three body case for wave heading = 45 degrees

The following plots show container ship motion time history in three body case and container ship motion response spectrum comparison for two body case and three body case. Three body (FLQW+CS+FIQW) means container ship motion in the presence of floating quay as well as fixed quay whereas two body (CS+FIQW) means container ship motion in the presence of fixed quay i.e. without floating quay.

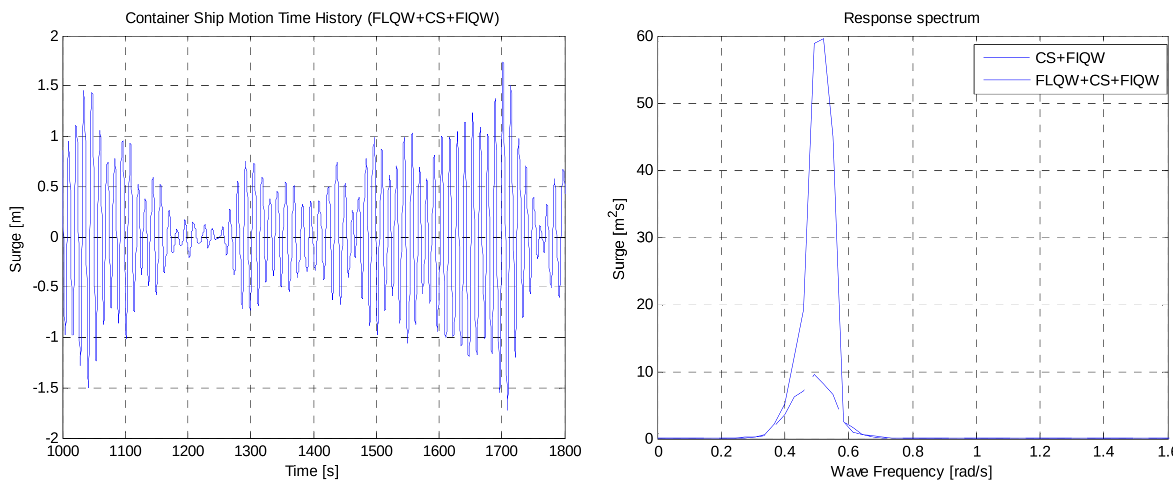

(i) (ii)

Figure 2-25. Container ship surge motion for 45 degrees wave heading

Figure 2-25 shows the container ship surge motion time history in three body case and container ship surge motion response spectrum comparison for two body case and three body case. The motion in the three body case is higher due to the interaction with the reflected waves from both sides of the container ship.

Figure 2-26 shows the container ship sway motion time history and sway motion response spectrum comparison for two body and three body cases. The reflected wave effect boosts the motion response in the three body case. There are two peaks in the motion response spectrum in the three body case due to the interaction effect.

Figure 2-27 shows the container ship heave motion time history and heave motion response spectrum comparison for two body and three body cases. There is some notably higher two body response in the 0.35 rad/s to 0.55 rad/s frequency range.

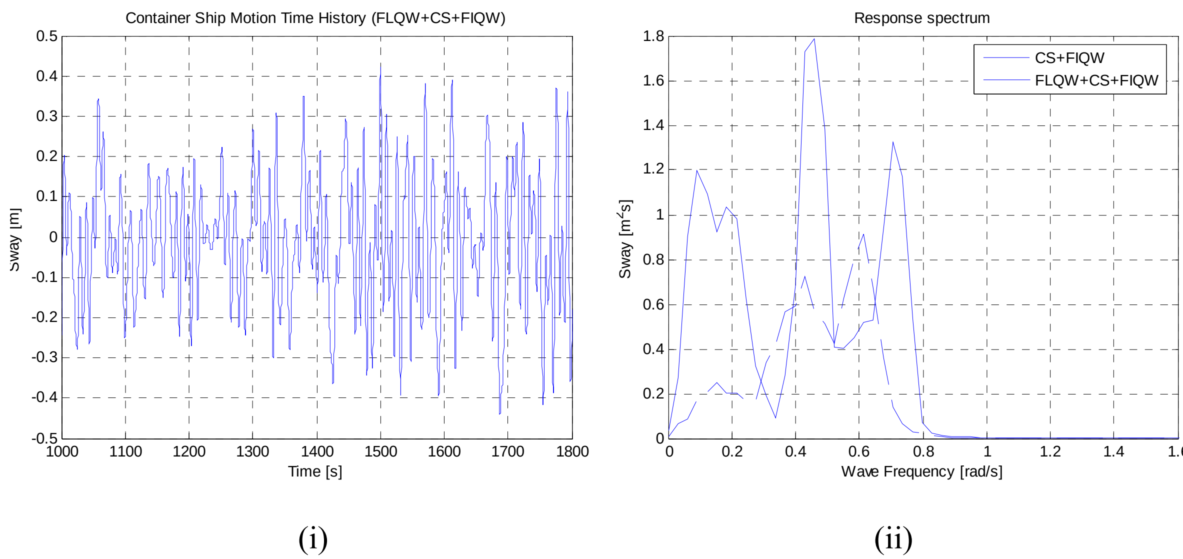

Figure 2-26. Container ship sway motion for 45 degrees wave heading

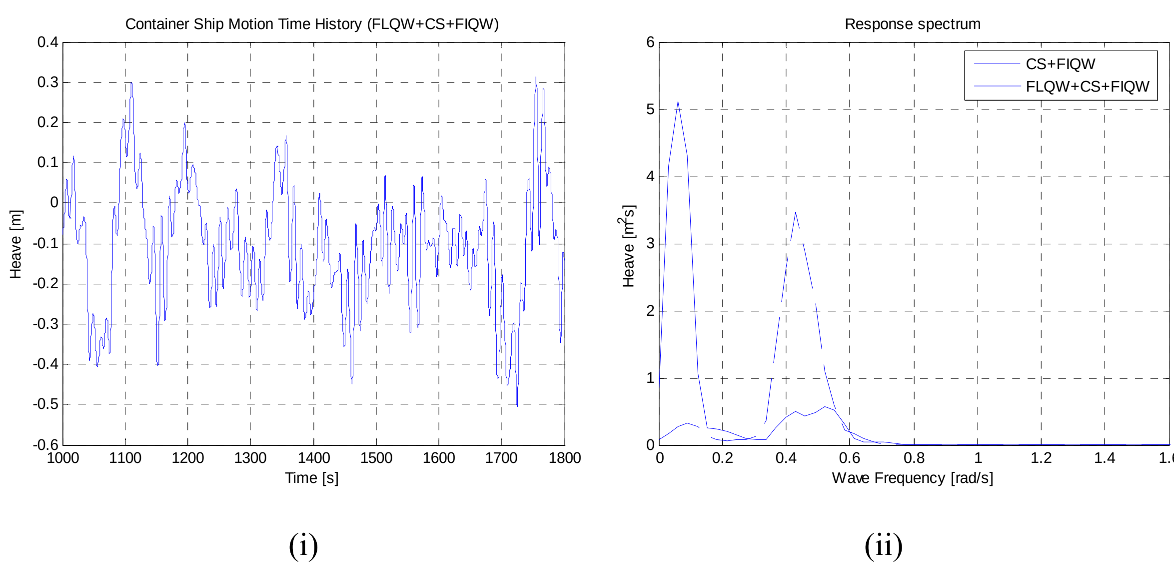

Figure 2-27. Container ship heave motion for 45 degrees wave heading

Figure 2-28 shows the container ship roll motion time history and roll motion response spectrum comparison for two body and three body cases. The three body roll response is higher than the two body roll response in this case.

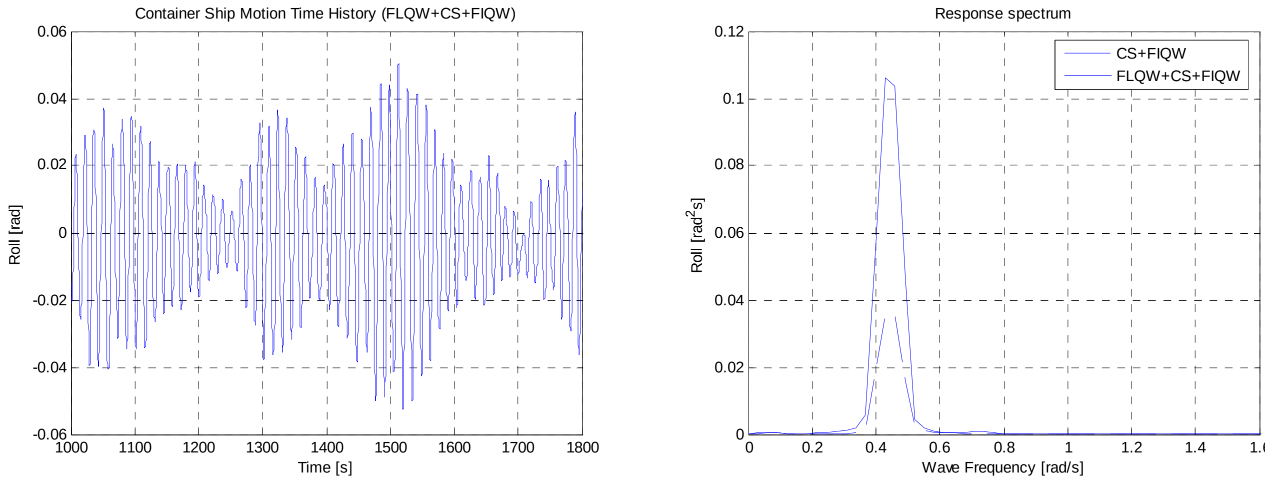

(i) (ii)

Figure 2-28. Container ship roll motion for 45 degrees wave heading

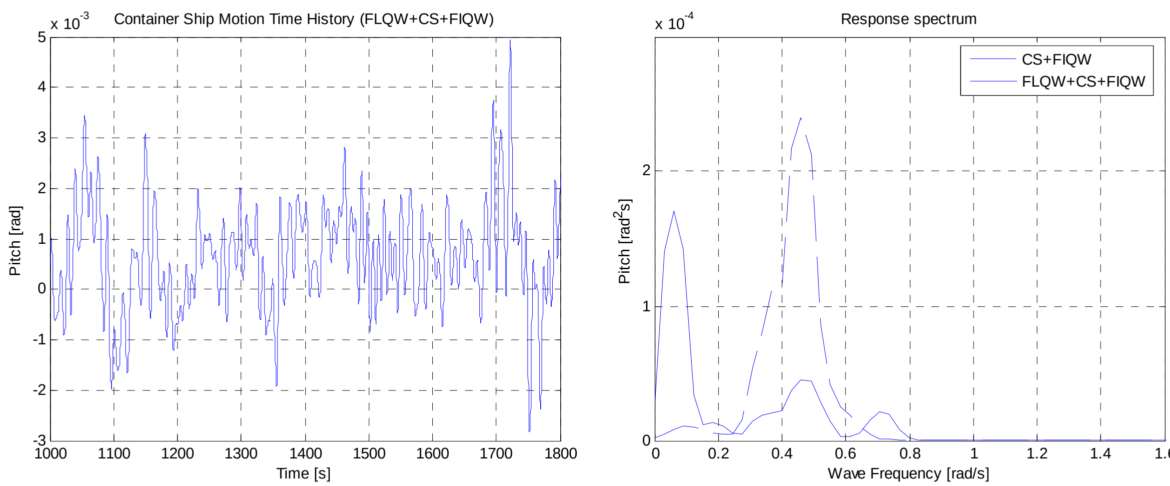

(i) (ii)

Figure 2-29. Container ship pitch motion for 45 degrees wave heading

Figure 2-29 shows the container ship pitch motion time history and pitch motion response spectrum comparison for two body and three body cases. It can be noticed that the two body motion response is greater than that of three body response though the magnitude of the response is very small.

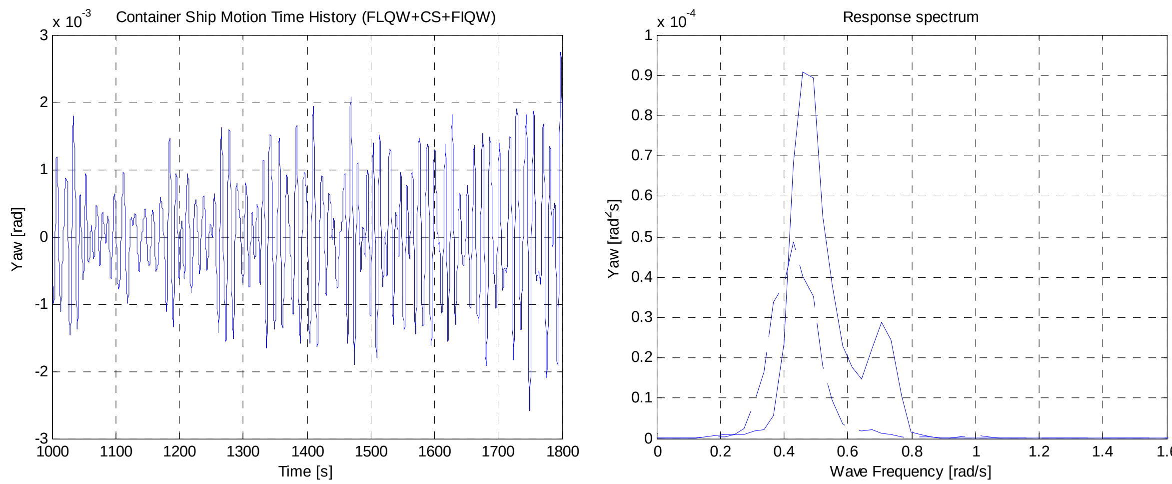

(i) (ii)

Figure 2-30. Container ship yaw motion for 45 degrees wave heading

Figure 2-30 shows the container ship yaw motion time history and yaw motion response spectrum comparison for two body and three body cases. The presence of third body stimulates higher yaw motion response in this case.

Table 2-6 shows WINPOST result for relative motion of floating quay (with dolphin) with respect to container ship (with hawser) in the presence of fixed quay wall wherwas Table 2-7 shows WINPOST result for relative motion of container ship (with hawser) with respect to fixed quay in the absence of floating quay for 45 degrees wave heading.

Table 2-6. WINPOST result for relative motion of floating quay (with dolphin) with respect to container ship (with hawser) in the presence of fixed quay wall

	Wave heading = 0	Wave heading =45	Wave heading =90
Surge(m)	Max = -1.163	Max = -1.8648	Max = -1.2625
	Mean = -0.00206	Mean = -0.002042	Mean = .001008
	Std. Dev. = 0.33784	Std. Dev. = 0.59363	Std. Dev. = 0.42648
Sway(m)	Max = -0.41246	Max = 0.78684	Max = 0.91149
	Mean = 0.00067	Mean = 0.011653	Mean = 0.002857
	Std. Dev. = 0.10203	Std. Dev. = 0.18544	Std. Dev. = 0.18968
Heave(m)	Max = 0.86077	Max = 0.79985	Max = 1.5071
	Mean = 0.06121	Mean = 0.10646	Mean = 0.15737
	Std. Dev. = 0.17102	Std. Dev. = 0.189	Std. Dev. = 0.3198
Roll(deg)	Max = 3.0971	Max = 4.419	Max = 5.2315
	Mean = 0.046667	Mean = 0.10429	Mean = 0.22686
	Std. Dev. = 1.0287	Std. Dev. = 1.2816	Std. Dev. =1.2642
Pitch(deg)	Max = -0.40542	Max = -0.38895	Max = -0.52485
	Mean = -0.022732	Mean = -0.037154	Mean = -0.050191
	Std. Dev. =0.088611	Std. Dev. =0.084831	Std. Dev. =0.10651
Yaw(deg)	Max = 0.19573	Max = 0.23225	Max = 0.11078
	Mean = 0.000302	Mean =-0.000036	Mean = 0.000107
	Std. Dev.= 0.05773	Std. Dev. =0.055032	Std. Dev.= 0.030483

Table 2-7. WINPOST result for relative motion of container ship (with hawser) with respect to fixed quay in the absence of floating quay for wave heading =45 degrees

	Wave heading =45
Surge(m)	Max = 0.8126 Mean = 0.0052 Std. Dev. = 0.2662
Sway(m)	Max = -0.3812 Mean = -0.0160 Std. Dev. = 0.1135
Heave(m)	Max = -0.5884 Mean = -0.0388 Std. Dev. = 0.1523
Roll(deg)	Max = -2.2894 Mean = -0.0775 Std. Dev. = 0.7149
Pitch(deg)	Max = 0.2751 Mean = 0.0084 Std. Dev. = 0.0783
Yaw(deg)	Max = 0.1173 Mean = -0.8337 Std. Dev. = 0.0354

2.7.1.2 Floating quay motion in the three body case for wave heading = 45 degrees

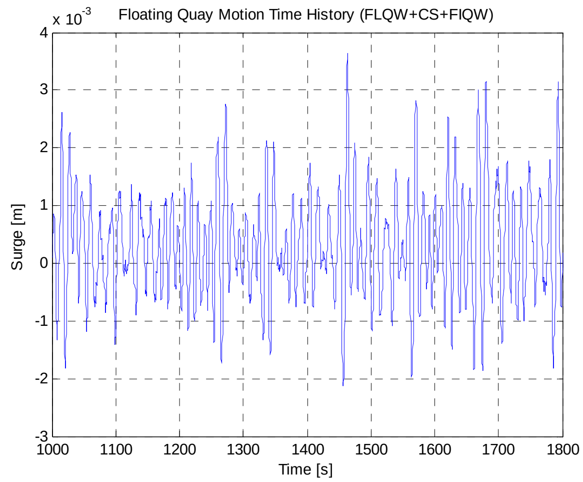

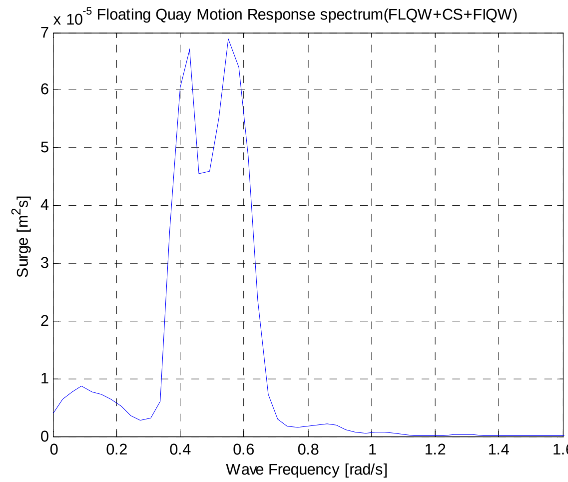

(i) (ii)

Figure 2-31. Floating quay surge motion for 45 degrees wave heading

Figure 2-31(ii) shows two peaks in the motion response spectrum but the magnitude is extremely small due to the use of high external spring stiffness for dolphin mooring.

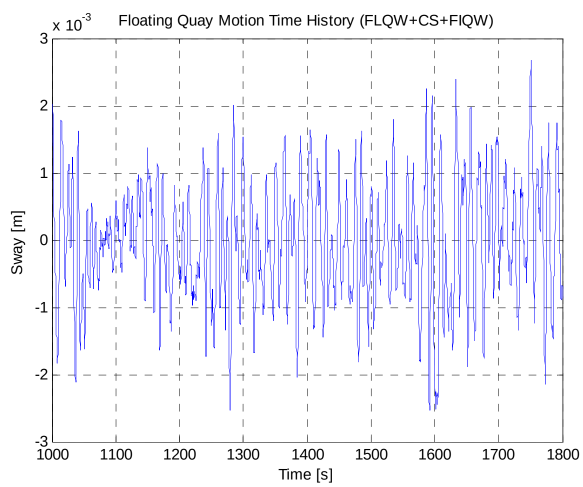

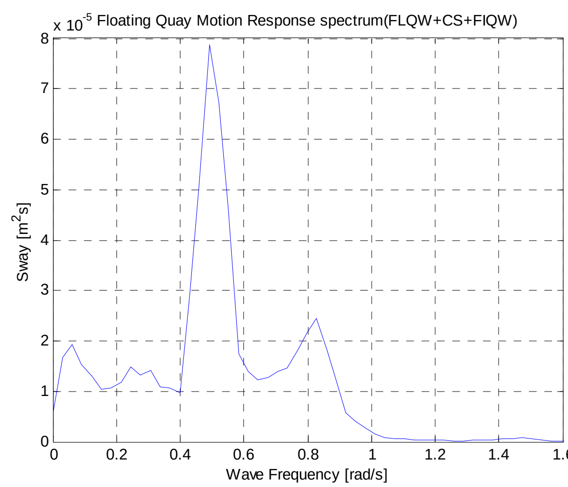

(i) (ii)

Figure 2-32. Floating quay sway motion for 45 degrees wave heading

Figure 2-32(ii) shows a peak at 0.5 rad/s in the motion response spectrum. As in the case of surge, the magnitude of values in the motion response spectrum is very low in sway direction due to the use of high external spring stiffness for dolphin mooring.

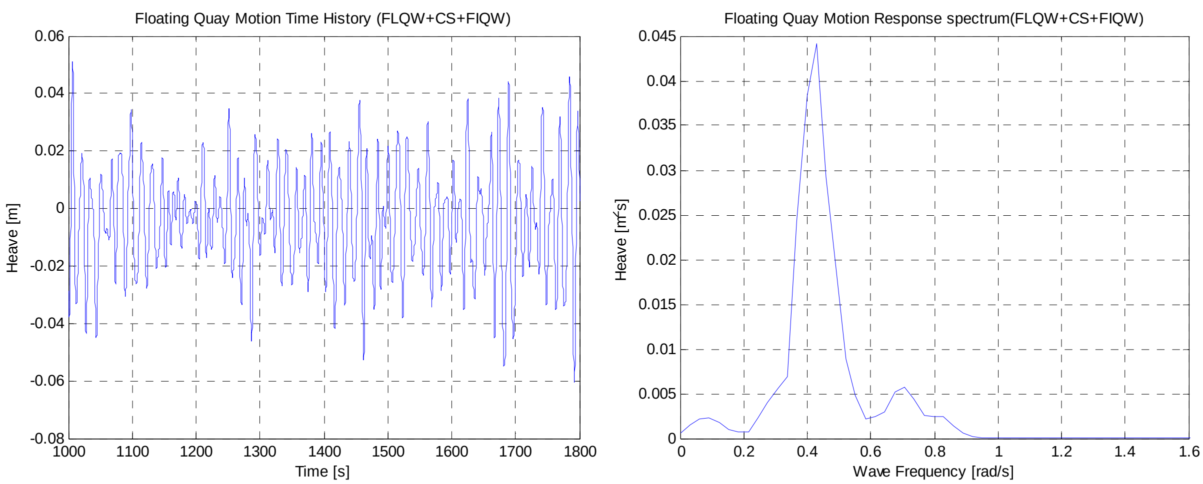

(i) (ii)

Figure 2-33. Floating quay heave motion for 45 degrees wave heading

Figure 2-33 shows floating quay heave motion time history and motion response spectrum. The response spectrum plot shows a peak at the frequency corresponding to peak period of the environmental wave condition.

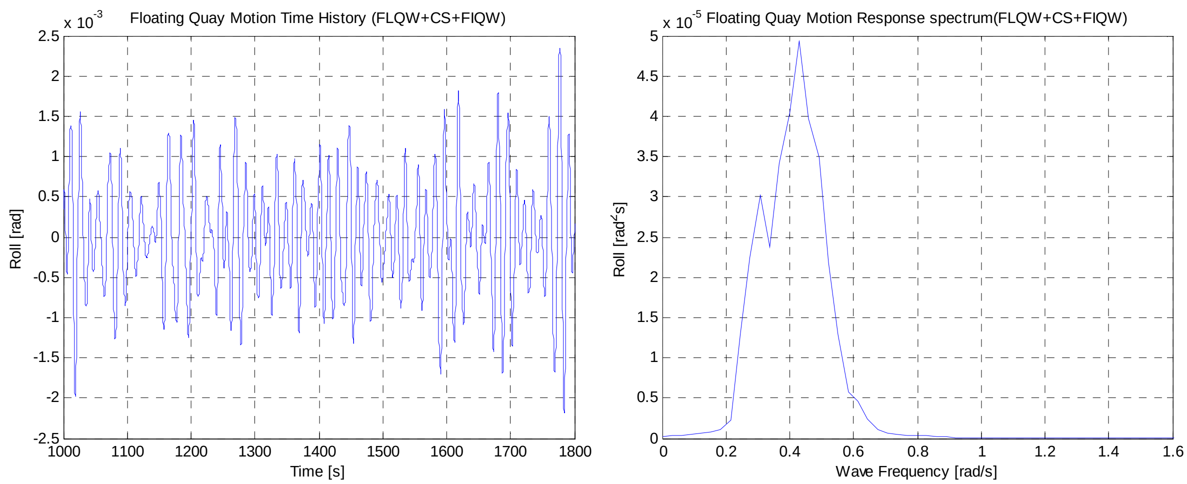

(i) (ii)

Figure 2-34. Floating quay roll motion for 45 degrees wave heading

Figure 2-34 shows floating quay roll motion time history and motion response spectrum. The response spectrum plot shows two peaks, the second one at the frequency corresponding to the peak period of the incoming wave.

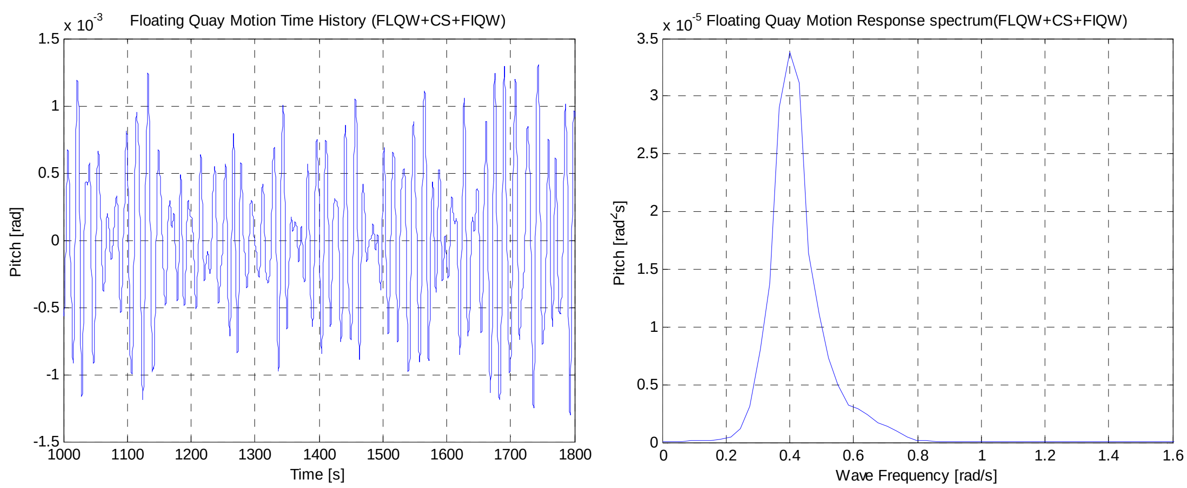

(i) (ii)

Figure 2-35. Floating quay pitch motion for 45 degrees wave heading

Figure 2-35 shows floating quay pitch motion time history and motion response spectrum. The response spectrum plot shows the peak at 0.4 rad/s which is slightly lower than the frequency corresponding to the peak period of the incoming wave.

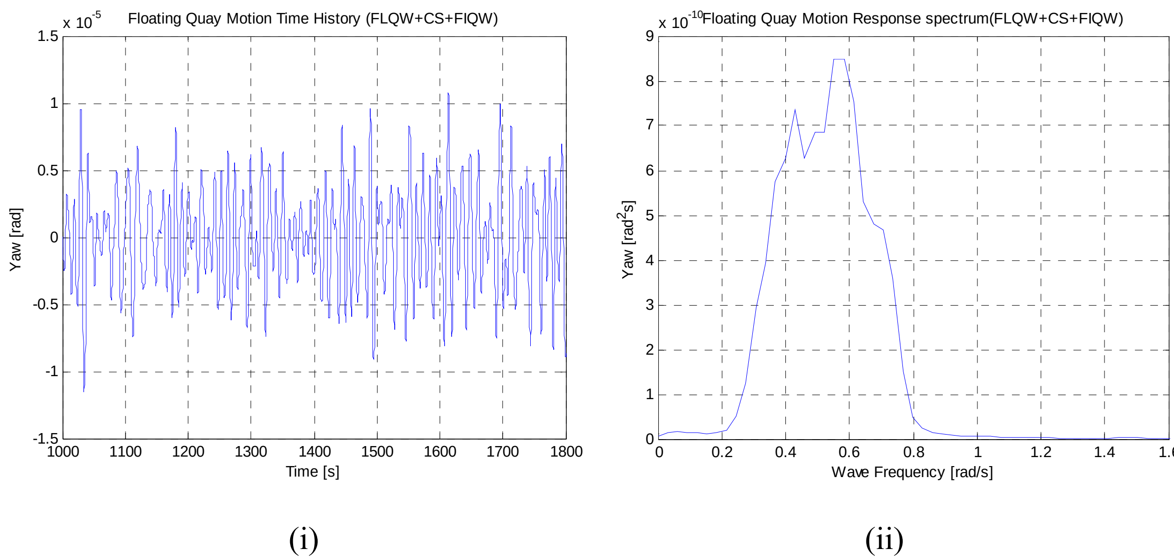

Figure 2-36. Floating quay yaw motion for 45 degrees wave heading

Figure 2-36 shows floating quay yaw motion time history and motion response spectrum. The response spectrum plot shows two peaks, the first one at the frequency corresponding to the peak period of the incoming wave. The magnitude of values in the response spectrum is very low due to the use of high external spring stiffness for dolphin mooring to restrict the motion in the surge, sway and yaw directions.

2.7.1.3 Relative motion time history and spectrum for wave heading = 45 degrees

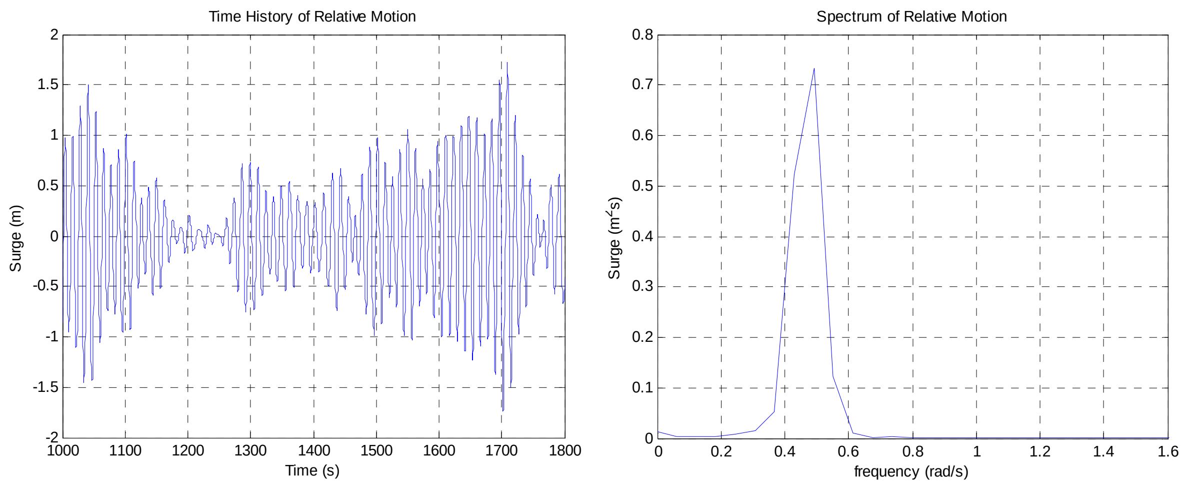

(i) (ii)

Figure 2-37. Relative surge response for 45 degrees wave heading

Figure 2-37(ii) and figure 2-38(ii) show the surge and sway response spectrums respectively. The low values in these plots are due to very high external stiffness used to suppress the surge and sway motion of the container ship and the floating quay.

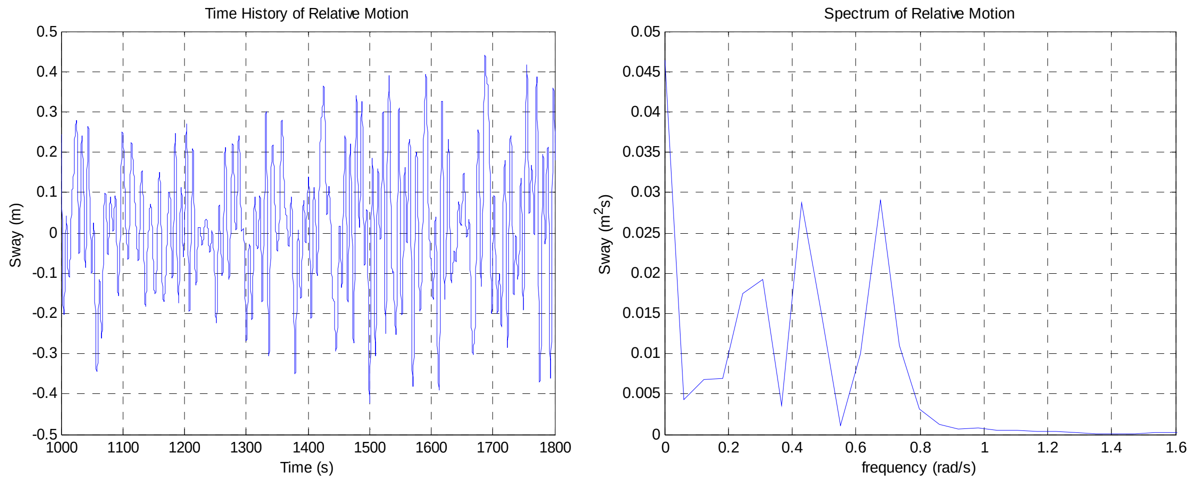

(i) (ii)

Figure 2-38. Relative sway response for 45 degrees wave heading

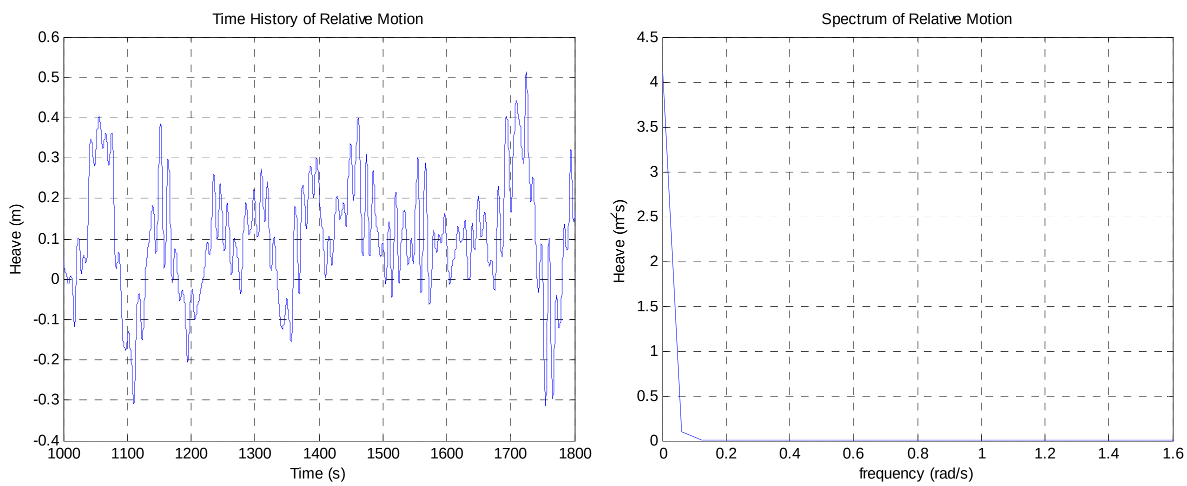

(i) (ii)

Figure 2-39. Relative heave response for 45 degrees wave heading

Figure 2-39 shows the heave time history and response spectrum. Figure 2-40 shows the roll time history and response spectrum. The response spectrum has a peak at the frequency corresponding the peak period of the wave. Figure 2-41 shows the pitch time history and response spectrum. Figure 2-42 shows the pitch time history and response spectrum.

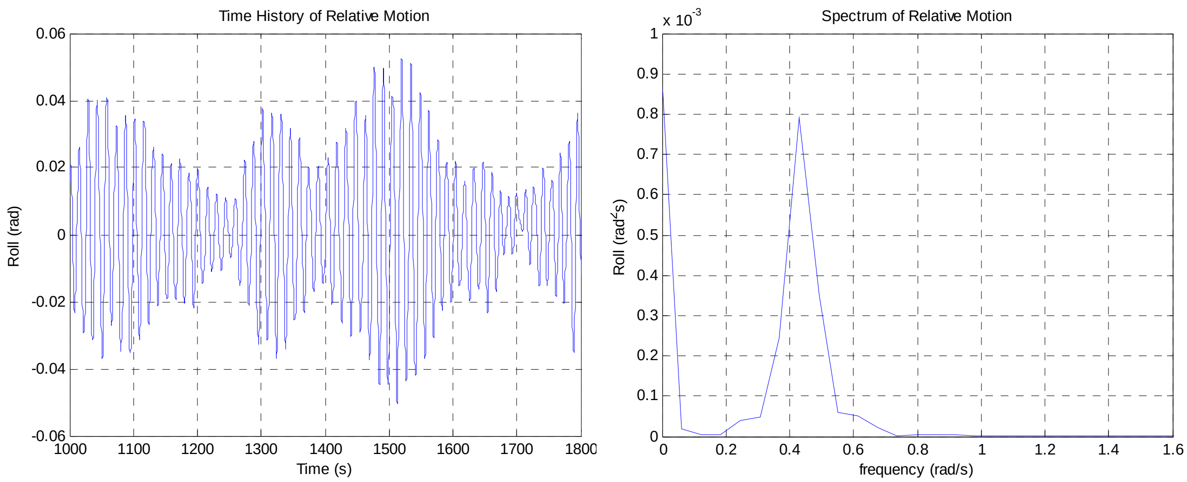

Figure 2-40. Relative roll response for 45 degrees wave heading

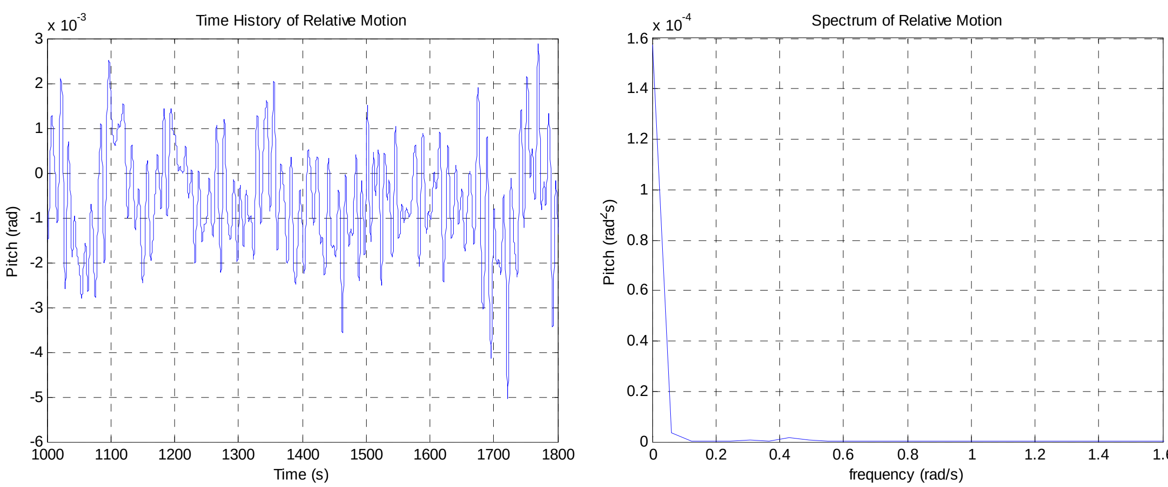

Figure 2-41. Relative pitch response for 45 degrees wave heading

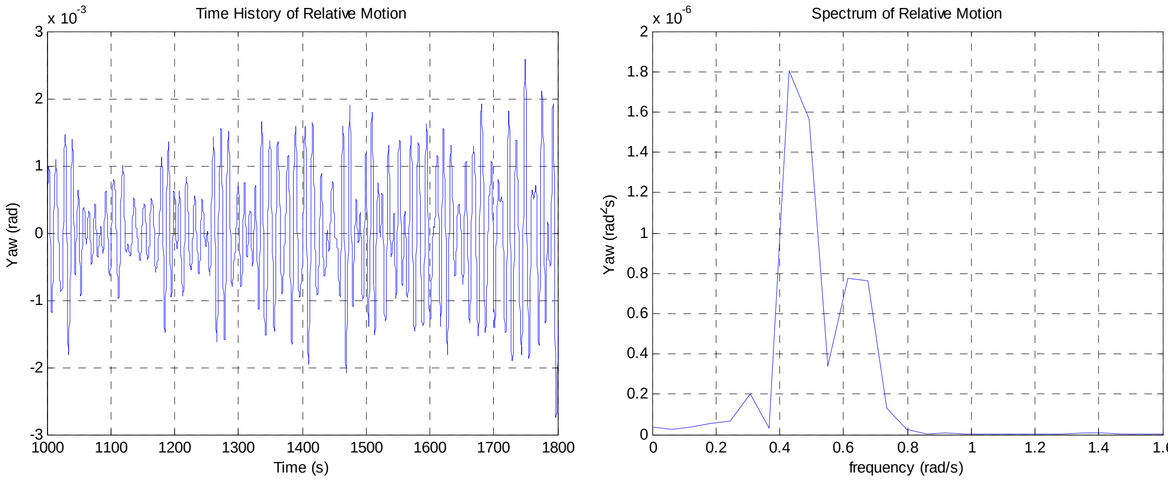

Figure 2-42. Relative yaw response for 45 degrees wave heading

The response spectrum at very low (upto 0.3 rad/s) and very high frequencies (from 0.8 rad/s to 1.5 rad/s) have been omitted for clear understanding of the results.

2.7.2 WINPOST Motion Analysis for 180 Minutes Simulation

Time domain WINPOST analysis for 180 minutes simulation time done for 0, 45 and degrees wave headings is explained below. Time domain WINPOST analysis for 90 minutes simulation time done for 45 degrees wave heading is explained in section 2.7.1.

2.7.2.1 Floating quay motion in the three body case for wave heading = 45 degrees

Figure 2-43 and Figure 2-44 show the floating quay motion time history and response spectrum respectively for 45 degrees wave heading. Three body (FLQW+CS+FIQW) means floating quay motion in the presence of container ship as well as fixed quay.

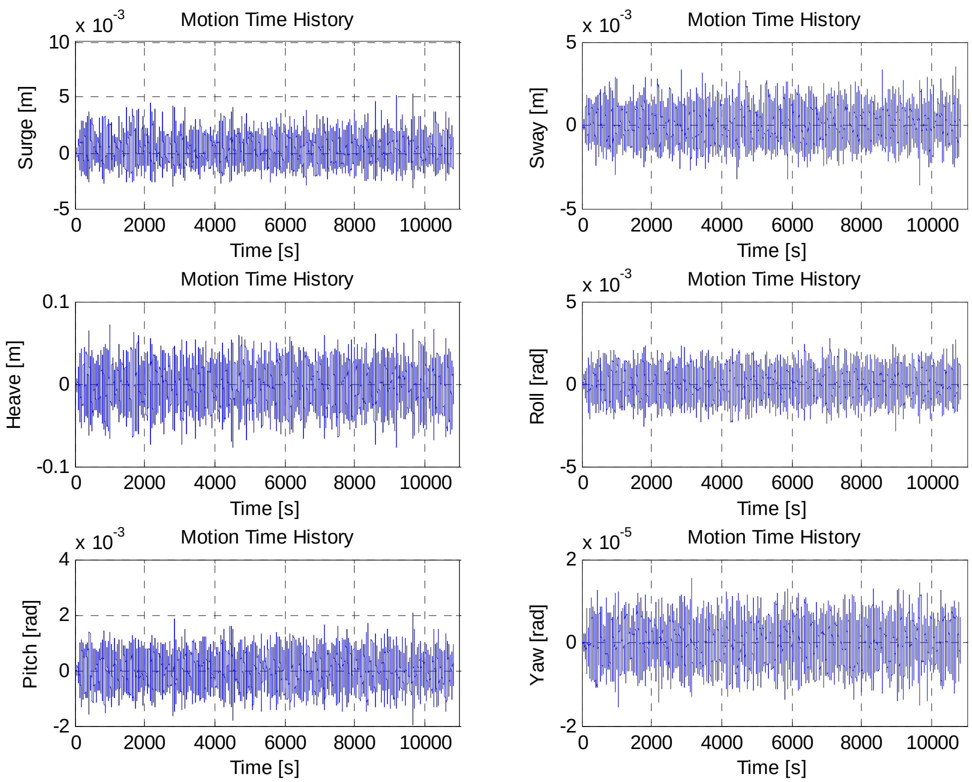

Figure 2-43. Floating quay motion time history for 45 degrees wave heading

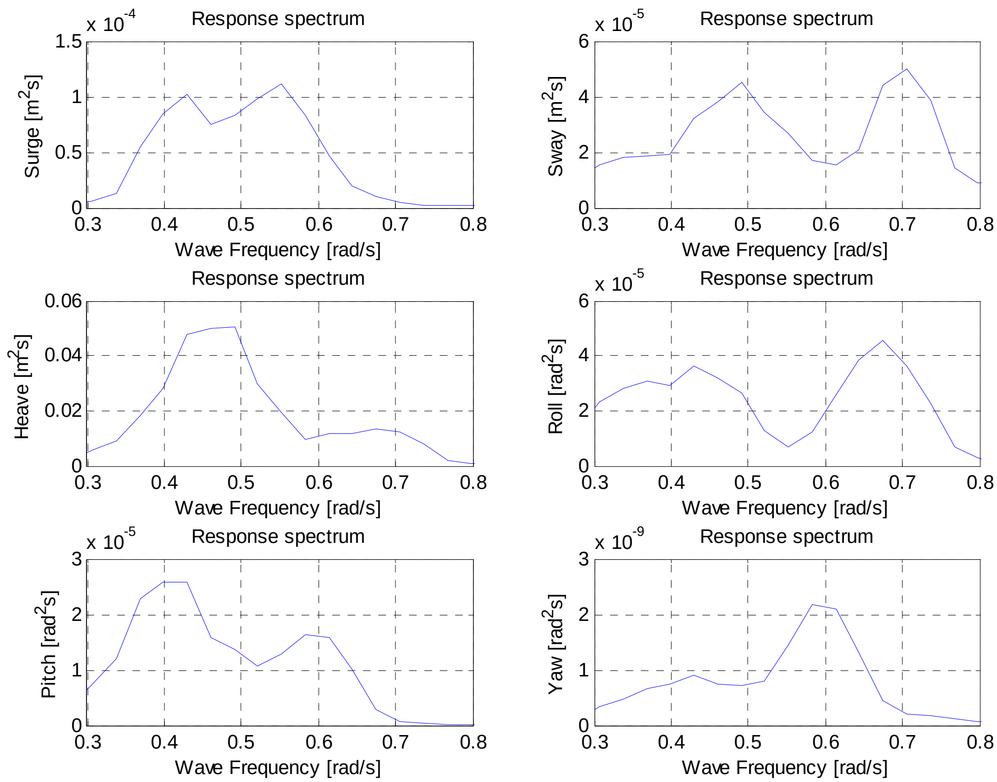

Figure 2-44. Floating quay Response Spectrum for 45 degrees wave heading

2.7.2.2 Container ship motion in the three body case for wave heading = 45 degrees

Figure 2-45 and Figure 2-46 show the container ship motion time history and response spectrum respectively for 45 degrees wave heading. Three body (FLQW+CS+FIQW) means container ship motion in the presence of floating quay as well as fixed quay.

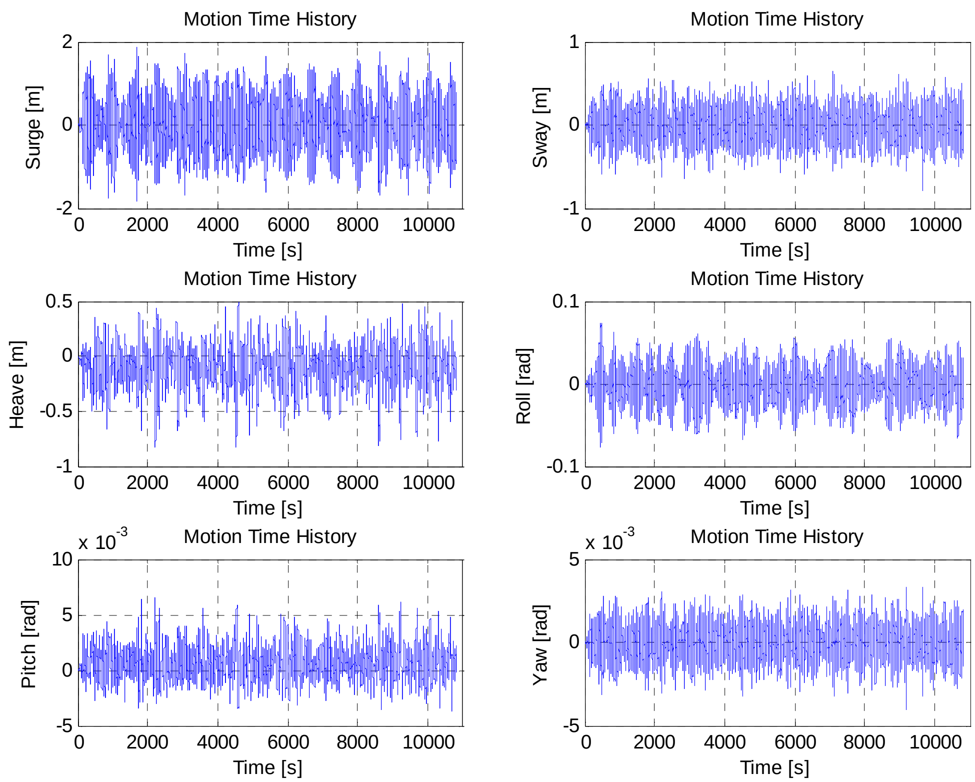

Figure 2-45. Container ship motion time history for 45 degrees wave heading

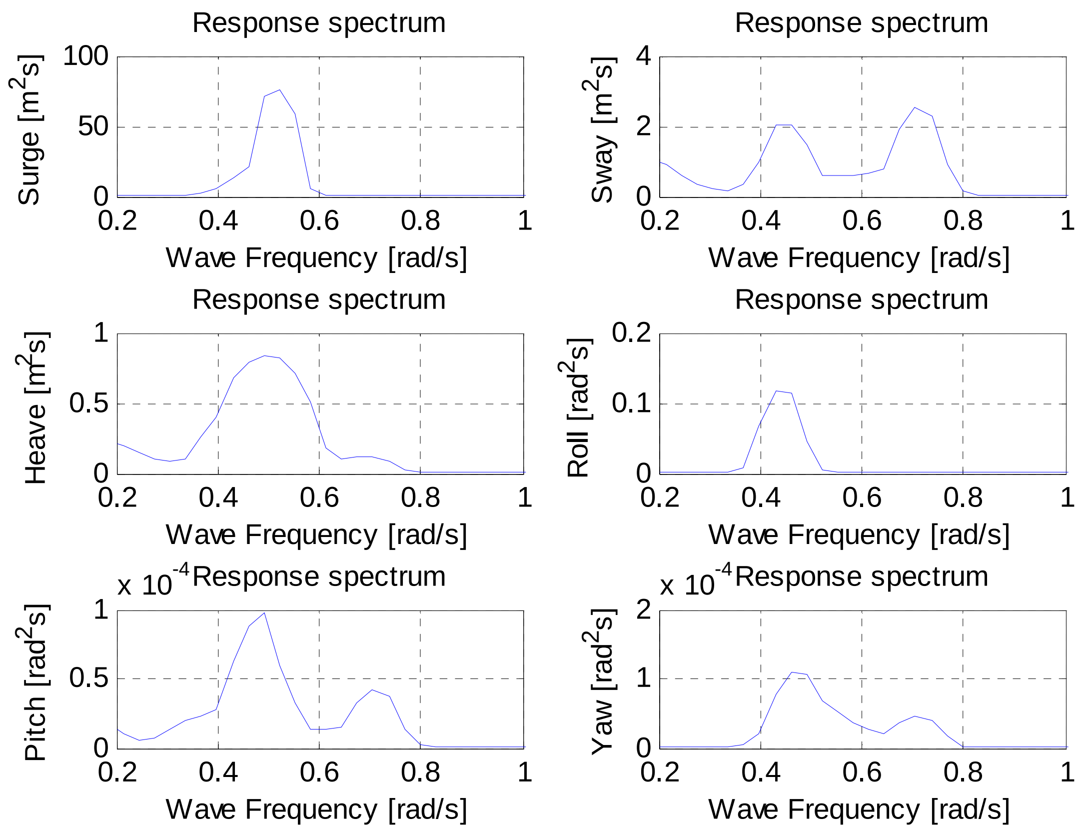

Figure 2-46. Container ship response spectrum for 45 degrees wave heading

2.7.2.3 Relative motion time history and spectrum for wave heading = 45 degrees

Figure 2-47 and Figure 2-48 show the relative motion time history and response spectrum respectively for 45 degrees wave heading. Three body (FLQW+CS+FIQW) means container ship motion in the presence of floating quay as well as fixed quay. The relative motion time history for 45 degrees wave heading shows that container loading and unloading operation can be can be carried out smoothly in the given wave conditions.

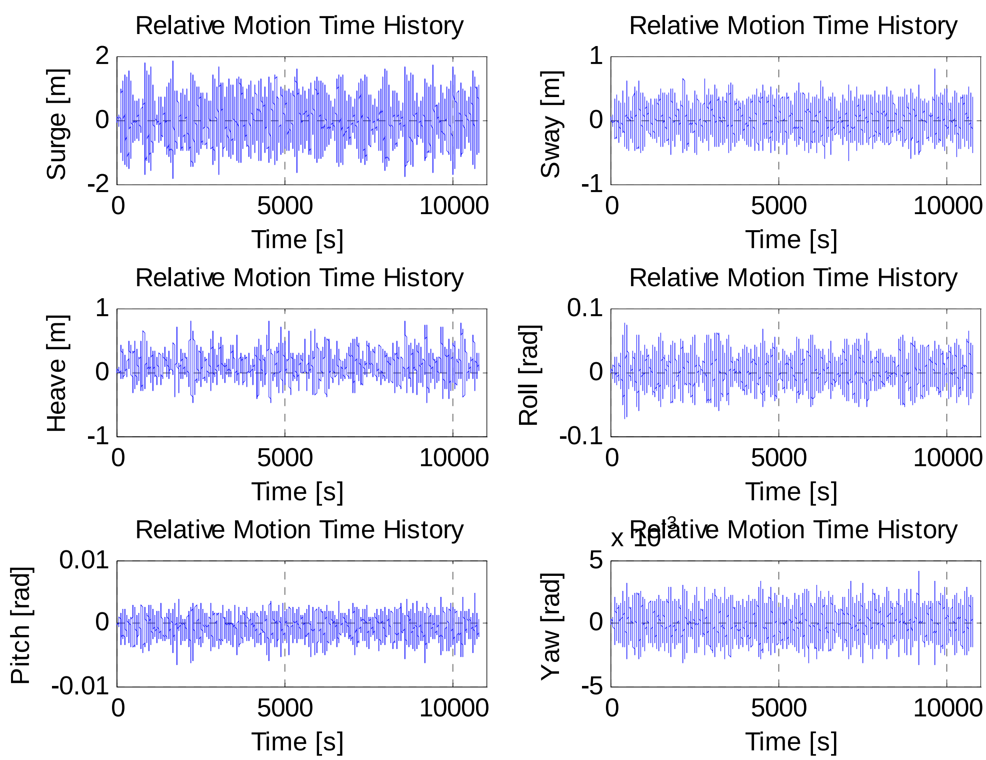

Figure 2-47. Relative motion time history between container ship and floating quay

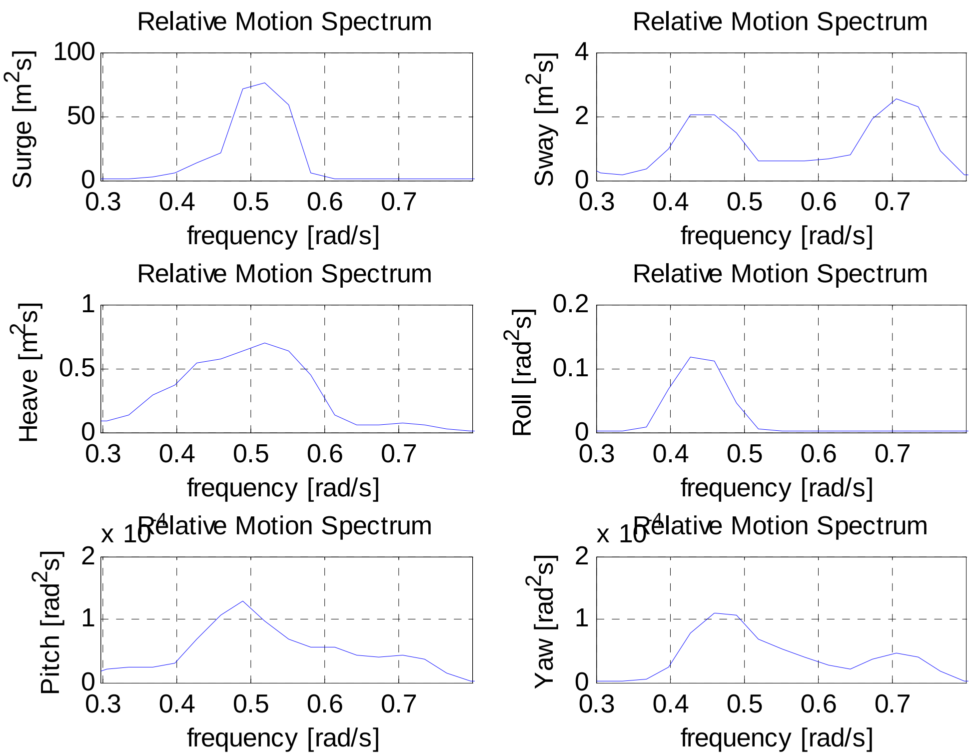

Figure 2-48. Relative motion response spectrum between container ship and floating quay

2.7.2.4 Floating quay motion in the three body case for wave heading = 0 degrees

Figure 2-49 and Figure 2-50 show the floating quay motion time history and response spectrum respectively for 0 degrees wave heading. Three body (FLQW+CS+FIQW) means floating quay motion in the presence of container ship as well as fixed quay.

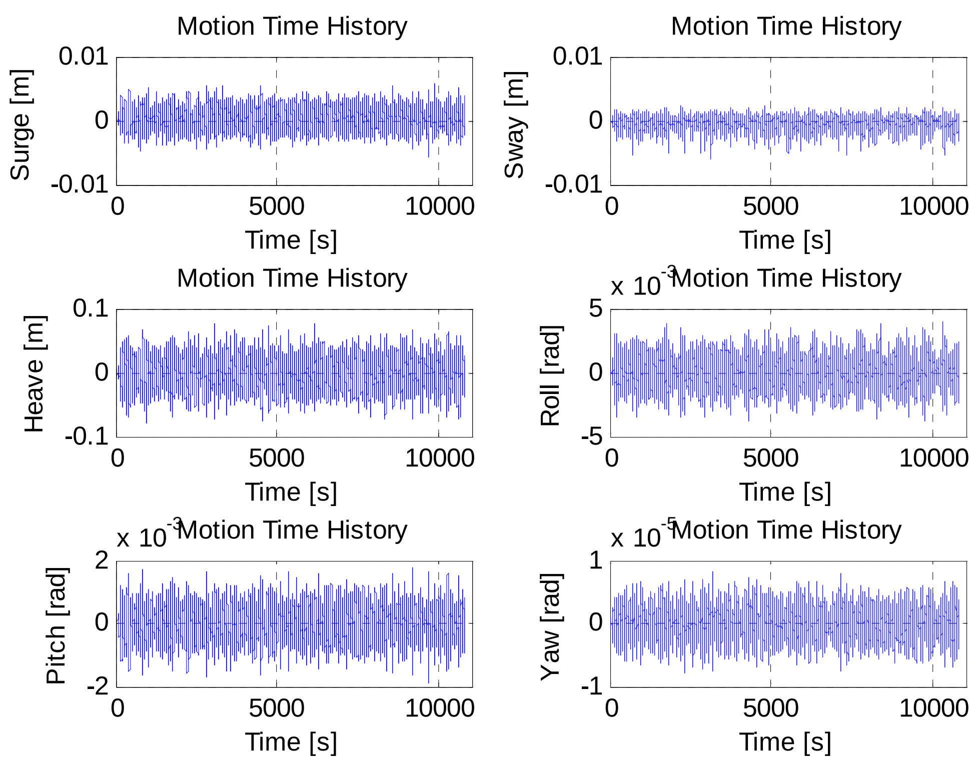

Figure 2-49. Floating quay motion time history for 0 degrees wave heading

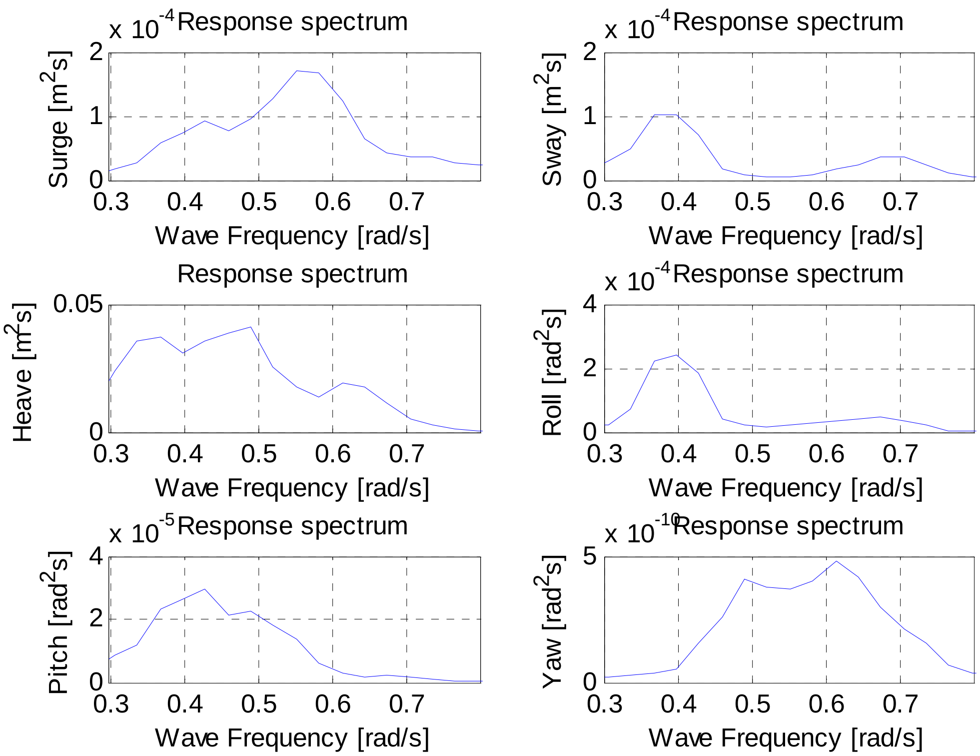

Figure 2-50. Floating quay response spectrum for 0 degrees wave heading

2.7.2.5 Container ship motion in the three body case for wave heading = 0 degrees

Figure 2-51 and Figure 2-52 show the container ship motion time history and response spectrum respectively for 0 degrees wave heading. Three body (FLQW+CS+FIQW) means container ship motion in the presence of floating quay as well as fixed.

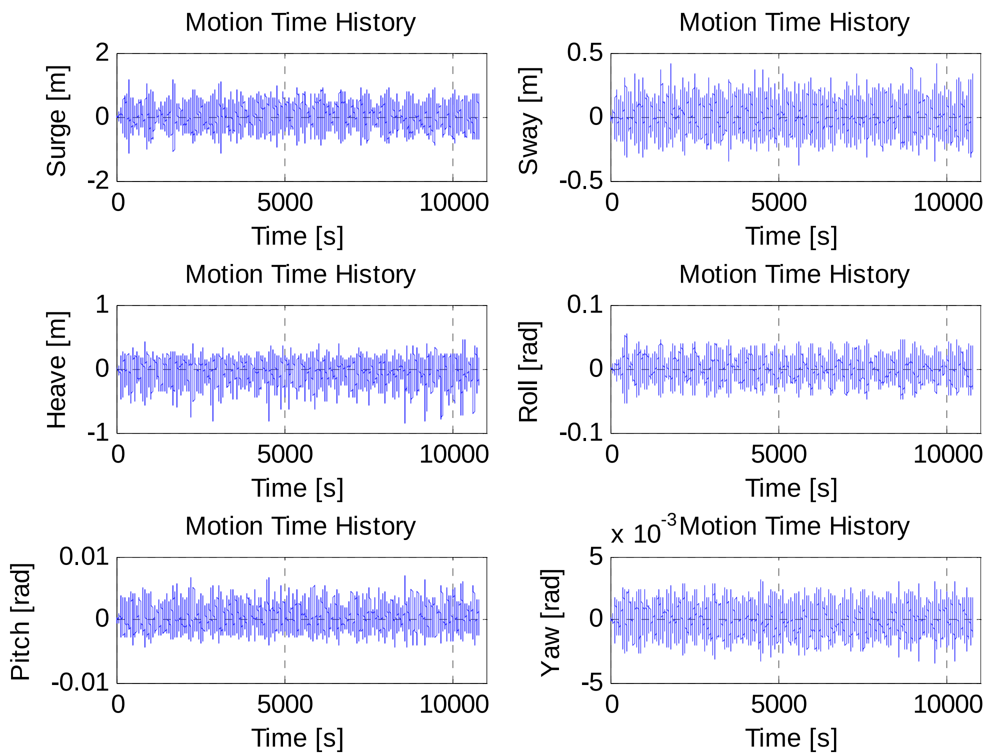

Figure 2-51. Container ship motion time history for 0 degrees wave heading

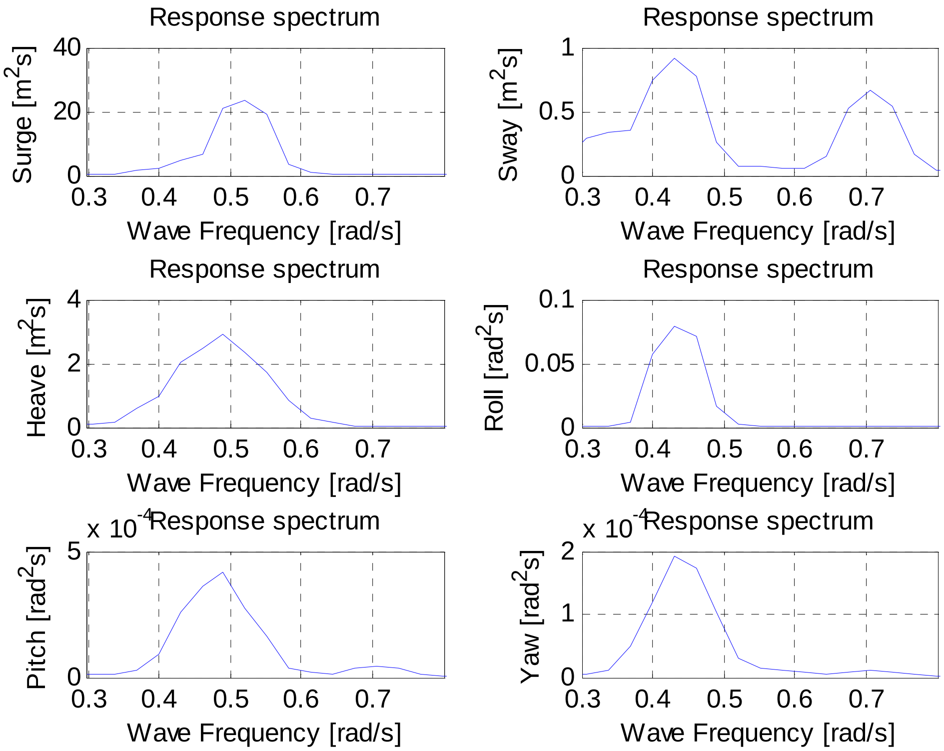

Figure 2-52. Container ship response spectrum for 0 degrees wave heading

2.7.2.6 Relative motion time history for wave heading = 0 degrees

Figure 2-53 shows the relative motion time history for 0 degrees wave heading. Three body (FLQW+CS+FIQW) means container ship motion in the presence of floating quay as well as fixed quay. The relative motion time history for 0 degrees wave heading shows that container loading and unloading operation can be can be carried out smoothly in the given wave conditions.

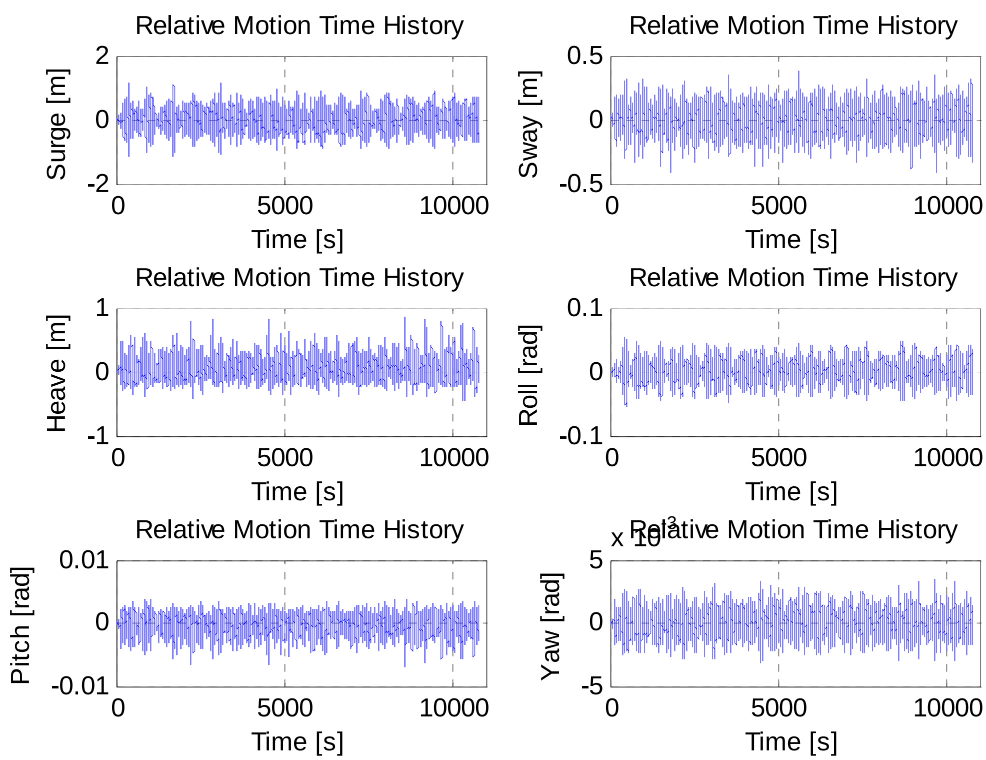

Figure 2-53. Relative motion time history between container ship and floating quay

2.7.2.7 Floating quay motion in the three body case for wave heading = 90 degrees

Figure 2-54 and Figure 2-55 show the floating quay motion time history and response spectrum respectively for 90 degrees wave heading. Three body (FLQW+CS+FIQW) means floating quay motion in the presence of container ship as well as fixed quay.

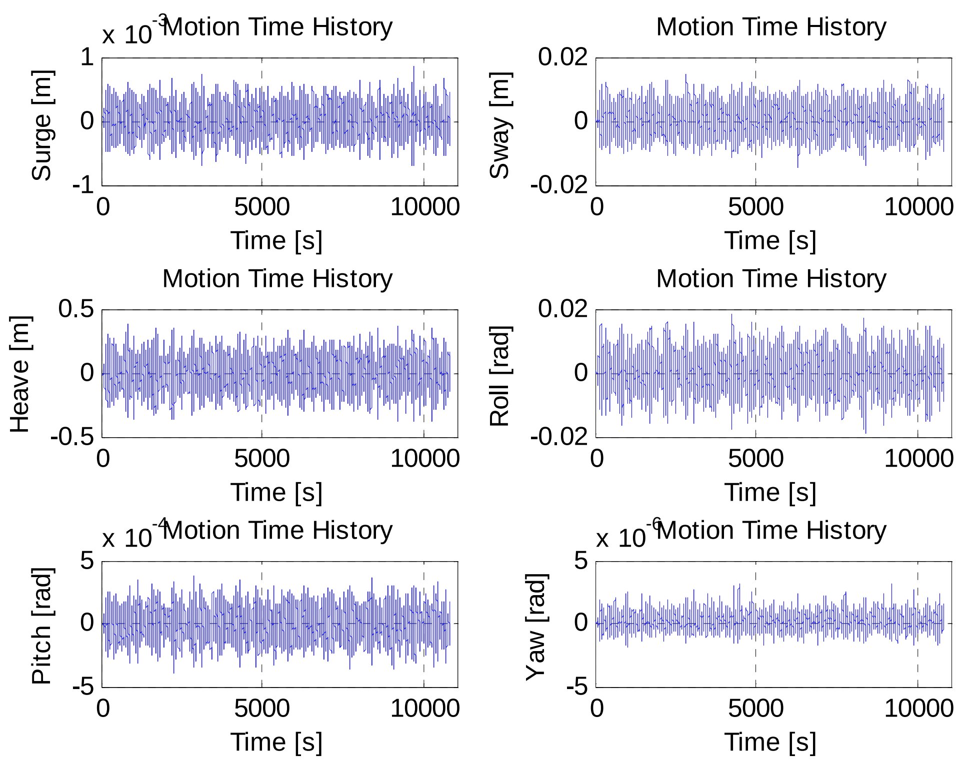

Figure 2-54. Floating quay motion time history for 90 degrees wave heading

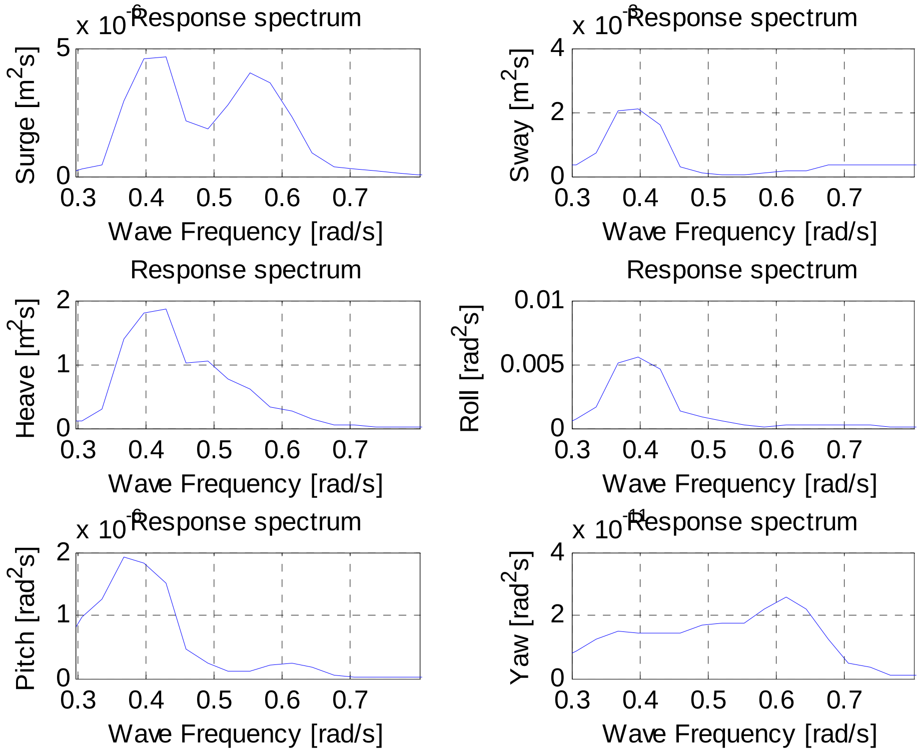

Figure 2-55. Floating quay response spectrum for 90 degrees wave heading

2.7.2.8 Container ship motion in the three body case for wave heading = 90 degrees

Figure 2-56 and Figure 2-57 show the container ship motion time history and response spectrum respectively for 90 degrees wave heading. Three body (FLQW+CS+FIQW) means container ship motion in the presence of container ship as well as fixed quay.

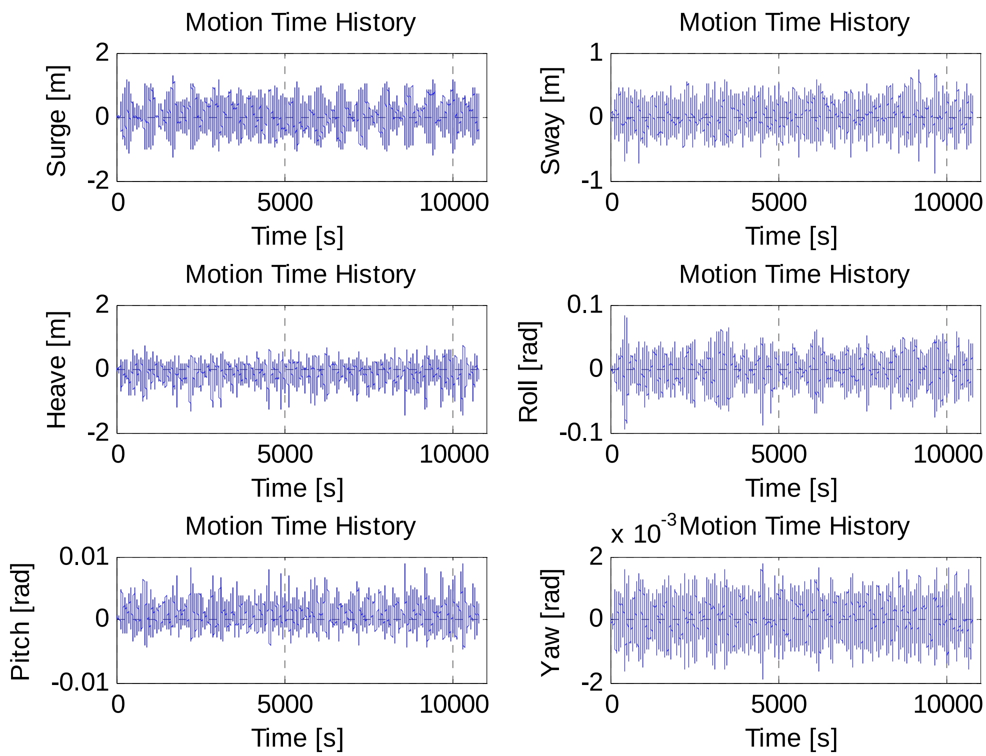

Figure 2-56. Container ship motion time history for 90 degrees wave heading

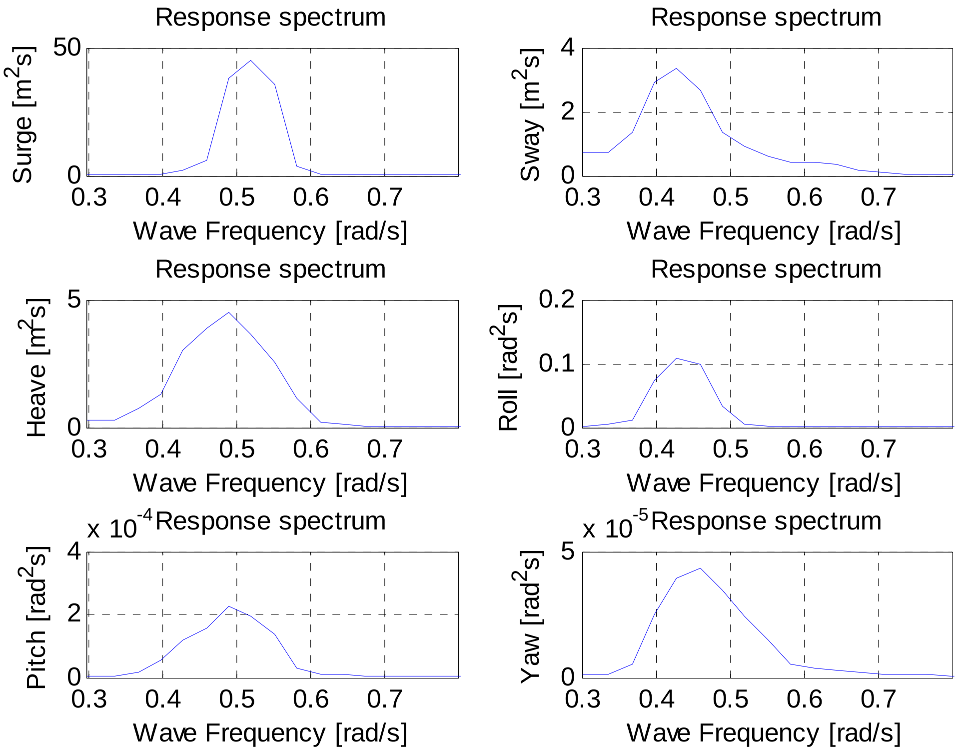

Figure 2-57. Container ship response spectrum for 90 degrees wave heading

2.7.2.9 Relative motion time history and spectrum for wave heading = 90 degrees

Figure 2-58 and Figure 2-59 show the relative motion time history and response spectrum respectively for 90 degrees wave heading. Three body (FLQW+CS+FIQW) means container ship motion in the presence of floating quay as well as fixed quay. The relative motion plots for 90 degrees wave heading shows that container loading and unloading operation can be can be carried out smoothly in the given wave conditions.

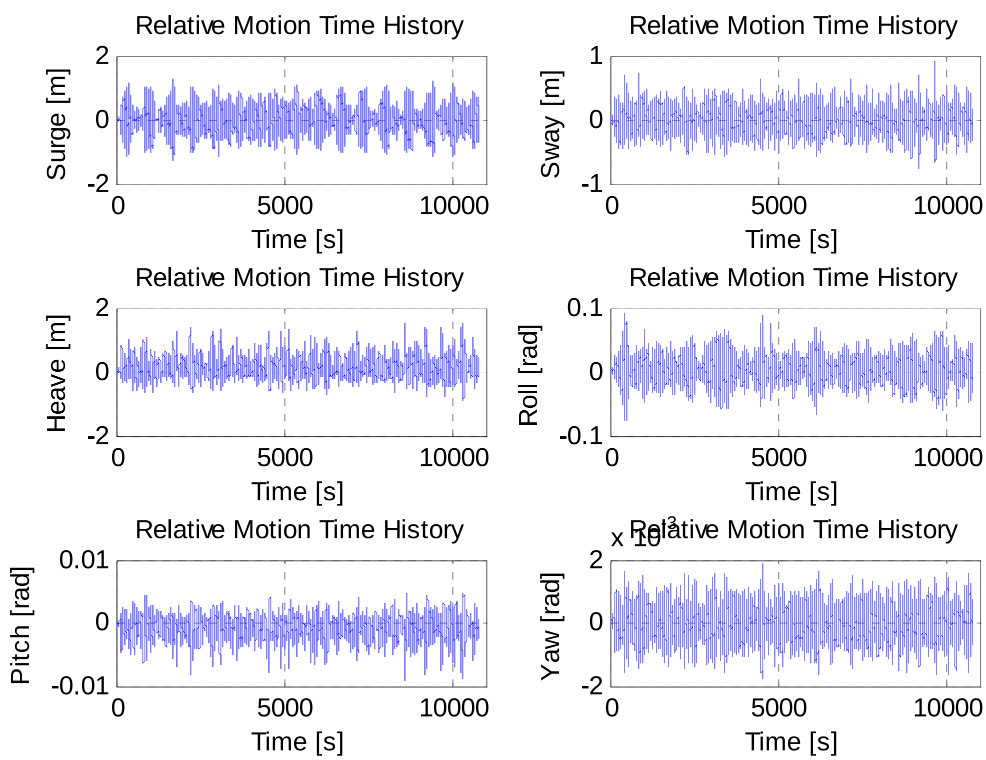

Figure 2-58. Relative motion time history between container ship and floating quay

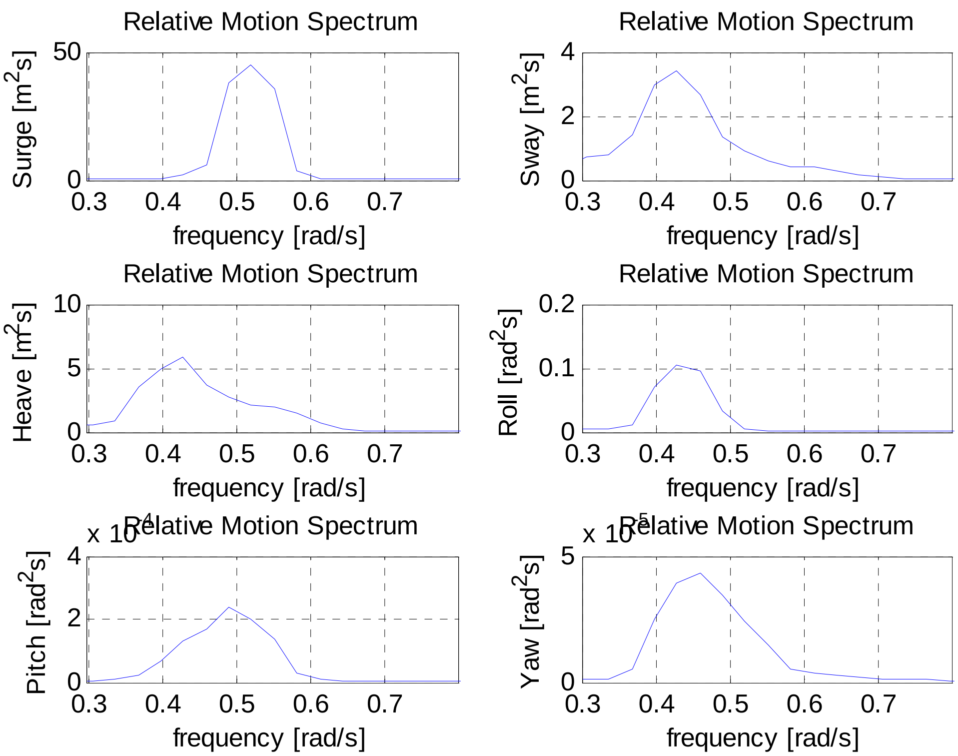

Figure 2-59. Relative response spectrum between container ship and floating quay

2.7.3 RAO Comparison from WAMIT and WINPOST

Very low and very high frequencies have been omitted in 0, 45 and 90 degrees wave headings and so the frequency range for RAO comparison is 0.3 rad/s to 0.8 rad/s to minimize erroneous conclusion.

2.7.3.1 RAO comparison from WAMIT and WINPOST for wave heading = 0 degrees

In this case, dolphin connections to floating quay and hawser connections to container ship with WAMIT simulation has been compared with that of WINPOST simulation without current, drag and drift force. This is done to compare WAMIT and WINPOST output as these results should be nearly the same when WINPOST simulation does not include current, drag and drift force. As shown below, there is slightly higher roll response in the case of floating quay WINPOST simulation. Figure 2-60 and Figure 2-61 show the floating quay and the container ship motion responses respectively for 0 degrees wave heading.

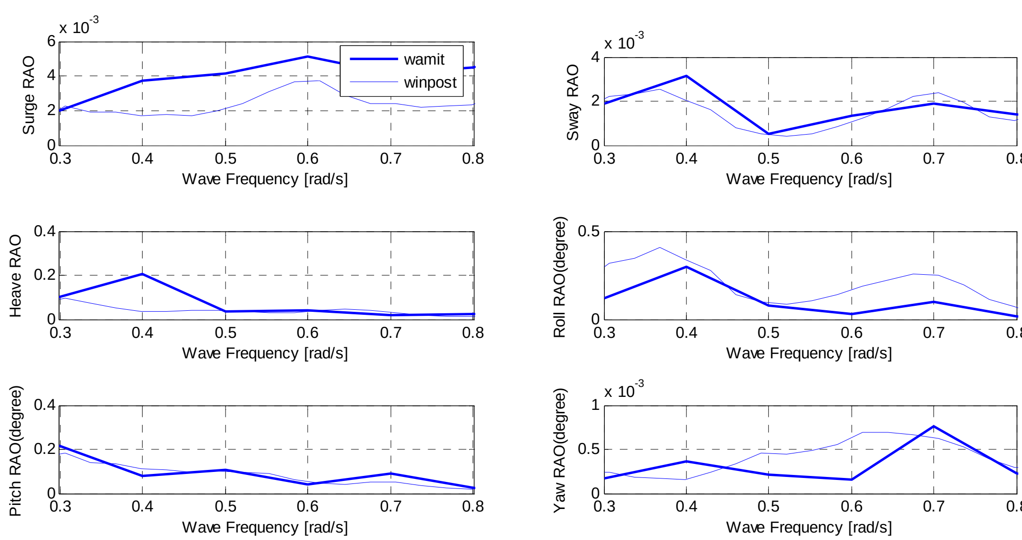

Figure 2-60. Floating quay motion response for 0 degrees wave heading

Container ship roll response in the case of WINPOST simulation is significantly higher than that of the WAMIT due to the presence of roll natural frequency at 0.45 rad/s.

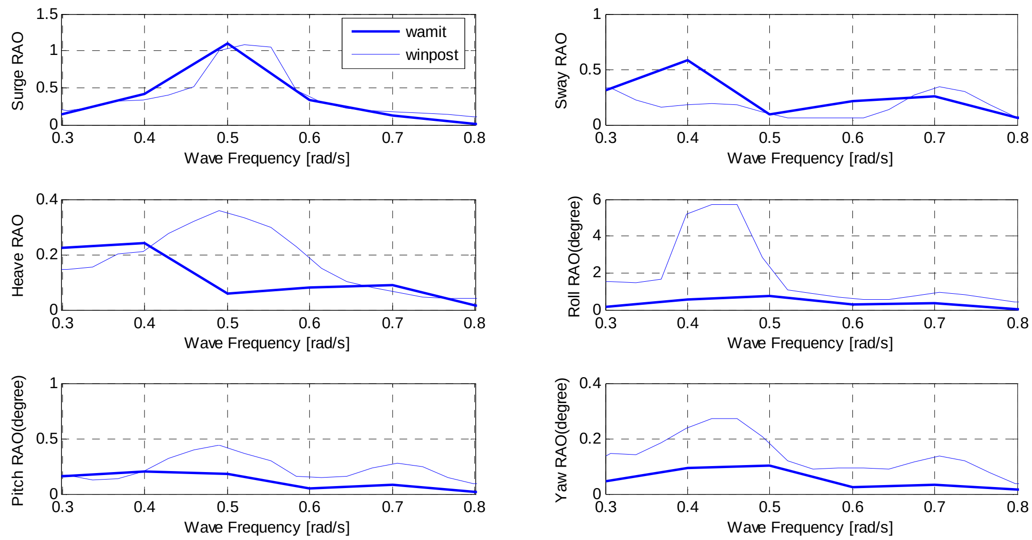

Figure 2-61. Container ship motion response for 0 degrees wave heading

2.7.3.2 RAO comparison from WAMIT and WINPOST for wave heading = 45 degrees

In this case, dolphin connections to floating quay and hawser connections to container ship with WAMIT simulation has been compared with that of WINPOST simulation without current, drag and drift force. This is done to compare WAMIT and WINPOST output as these results should be nearly the same when WINPOST simulation does not include without current, drag and drift force. As shown below, WAMIT and WINPOST simulation for floating quay almost coincides with each other. Figure 2-62 and Figure 2-63 show the floating quay and the container ship motion responses respectively for 45 degrees wave heading.

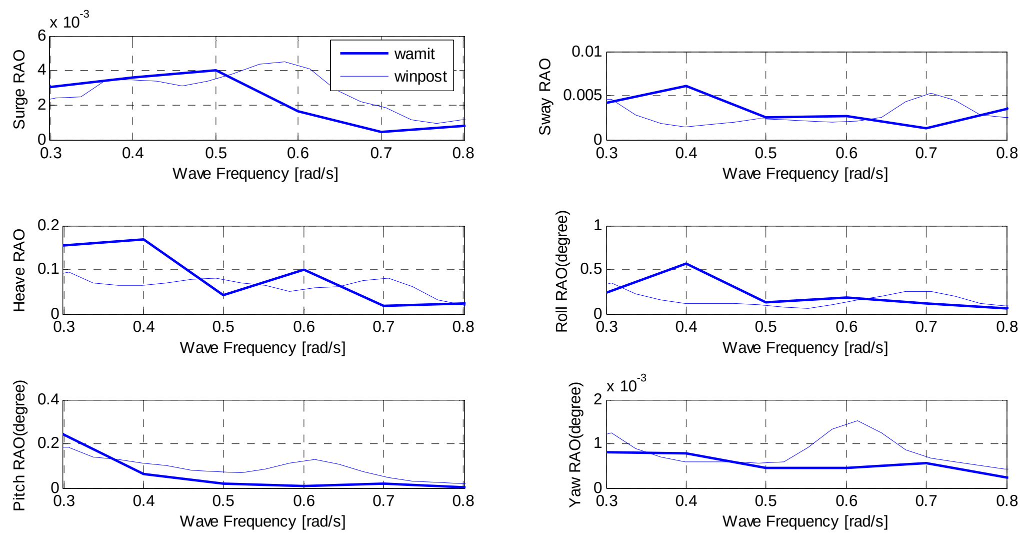

Figure 2-62. Floating quay motion response for 45 degrees wave heading

Container Ship roll response in the case of WINPOST simulation is significantly higher than that of the WAMIT due to the presence of roll natural frequency at 0.45 rad/s.

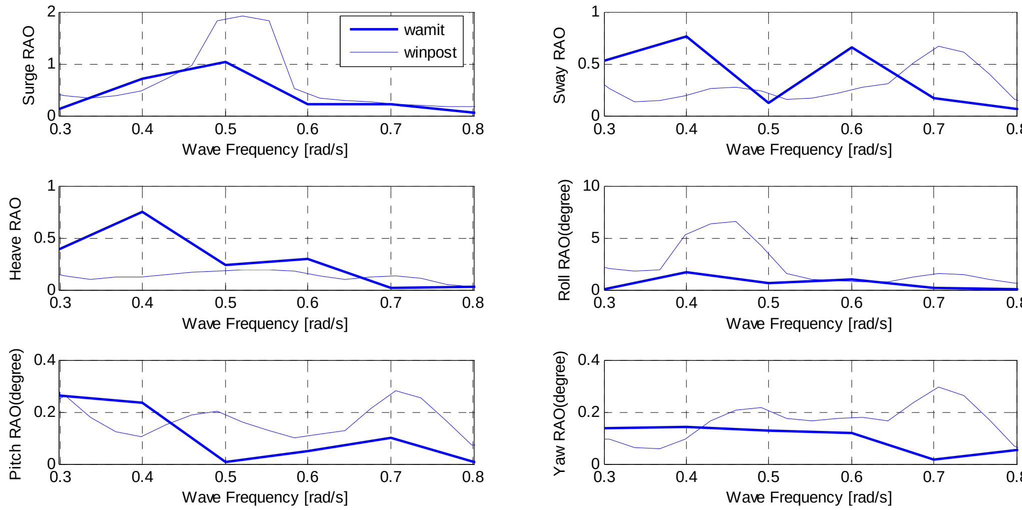

Figure 2-63. Container ship motion response for 45 degrees wave heading

2.7.3.3 RAO comparison from WAMIT and WINPOST for wave heading =90 degrees

In this case, dolphin connections to floating quay and hawser connections to container ship with WAMIT simulation has been compared with that of WINPOST simulation without current, drag and drift force. This is done to compare WAMIT and WINPOST output as these results should be nearly the same when WINPOST simulation does not include without current, drag and drift force. As shown below, WAMIT and WINPOST simulation for floating quay almost coincides with each other. Figure 2-64 and Figure 2-65 show the floating quay and the container ship motion responses respectively for 90 degrees wave heading.

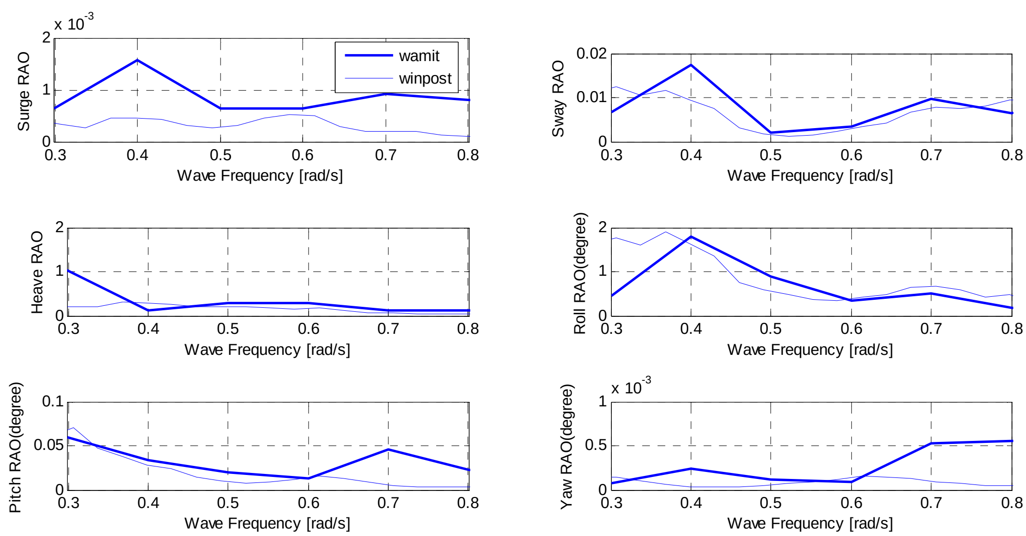

Figure 2-64. Floating quay motion response for 90 degrees wave heading

Container Ship roll response in the case of WINPOST simulation is significantly higher than that of the WAMIT due to the presence of roll natural frequency at 0.45 rad/s and there is an interestingly higher response for surge in the case of WINPOST simulation.

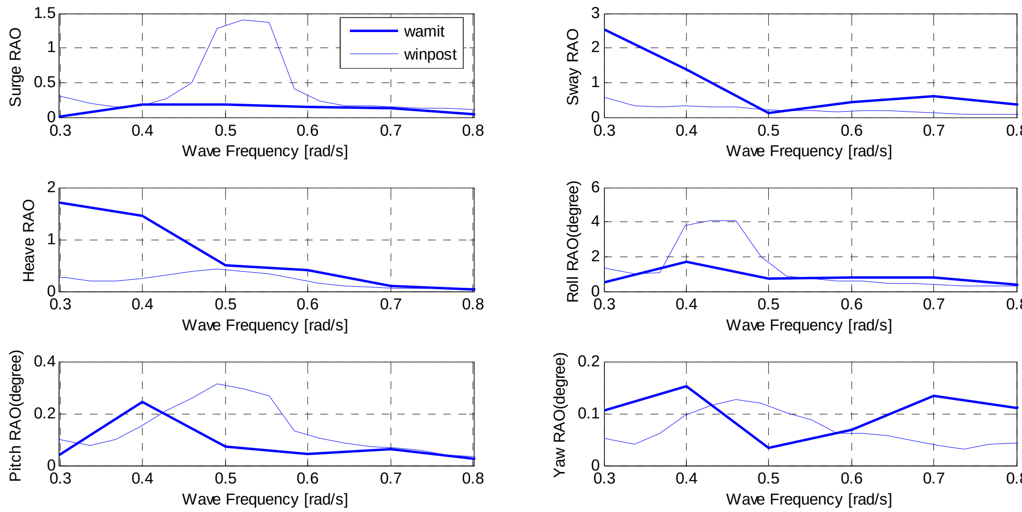

Figure 2-65. Container ship motion response for 90 degrees wave heading

2.7.4 Force on Dolphins

The force time history on forward and aft dolphins of the floating quay for 0, 45 and 90 degrees wave headings is shown below.

2.7.4.1 Force on forward and aft dolphins for 0, 45 and 90 degrees heading

As shown in Figure 2-66, Figure 2-67, Figure 2-68, Figure 2-69, Figure 2-70 and Figure 2-71, the force time history on the dolphins has been calculated by multiplying the dolphin stiffness with the motion time history at the location of the forward and aft dolphins.

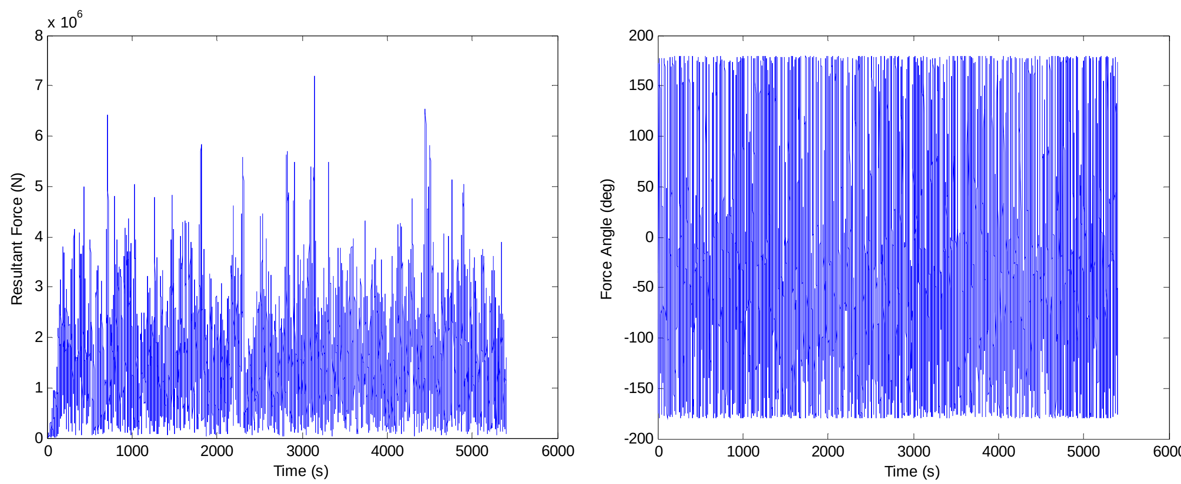

Figure 2-66. Force on forward dolphin: incident wave = 0 degrees

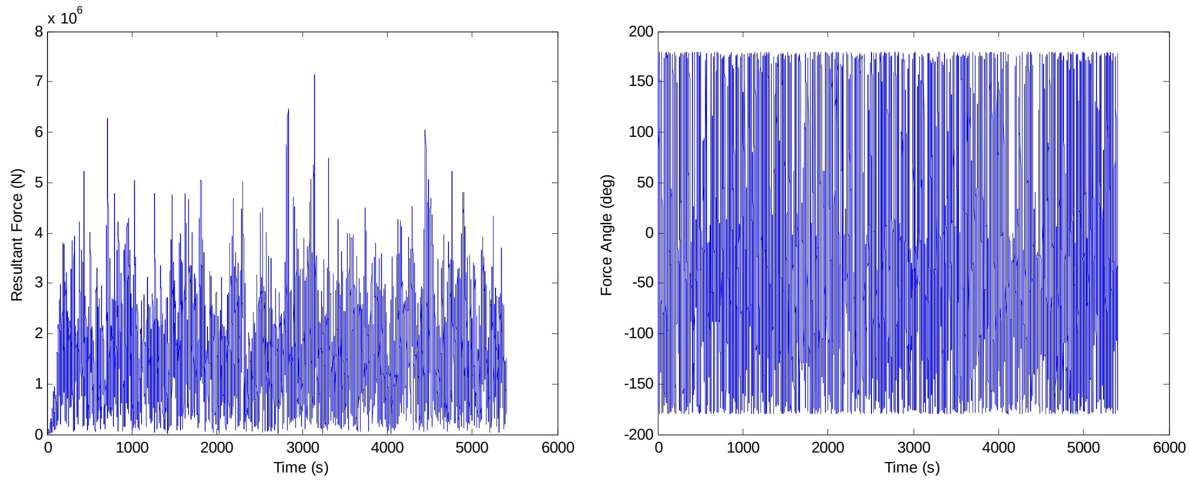

Figure 2-67. Force on aft dolphin: incident wave = 0 degrees

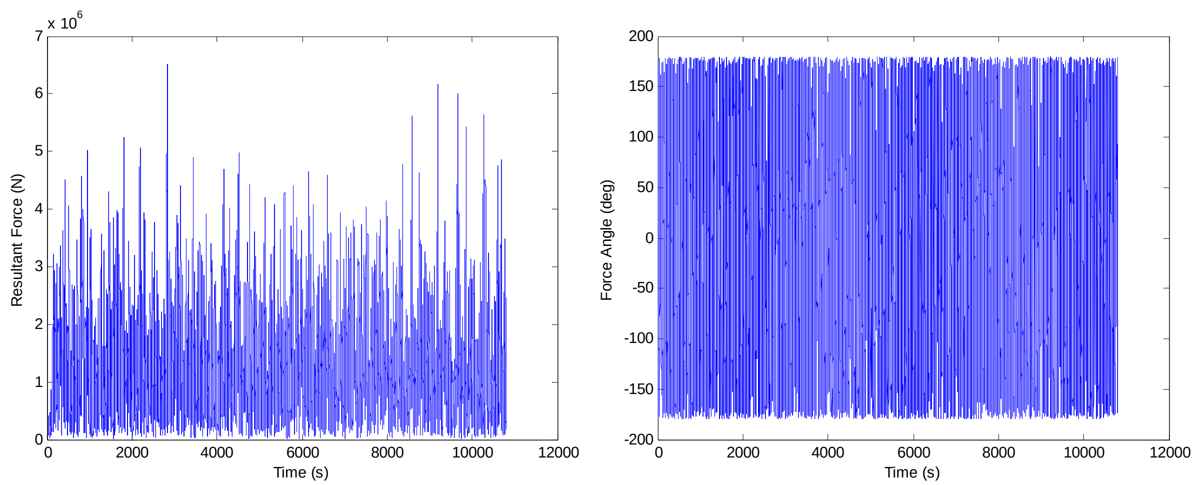

Figure 2-68. Force on forward dolphin: incident wave = 45 degrees

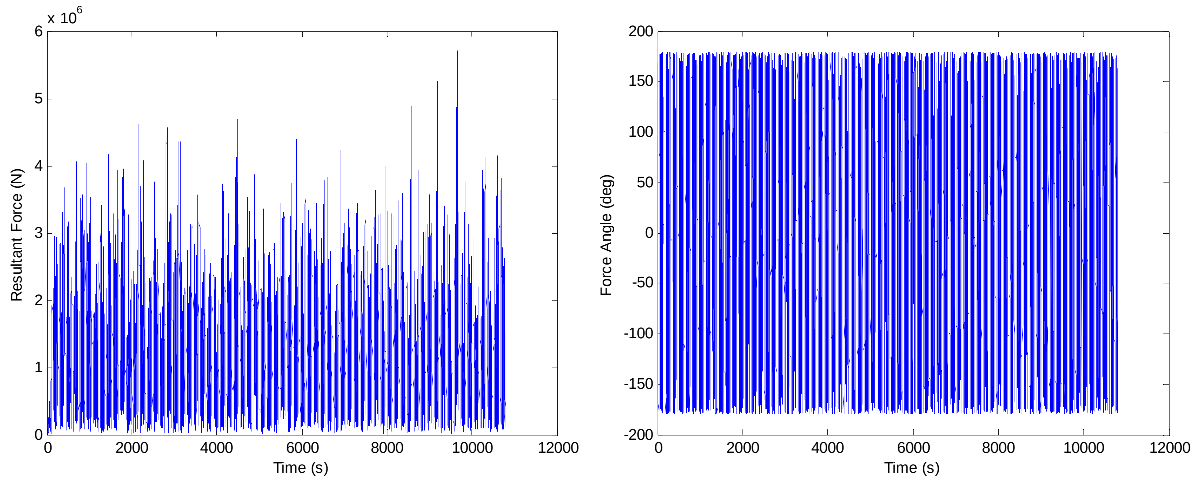

Figure 2-69. Force on aft dolphin: incident wave = 45 degrees

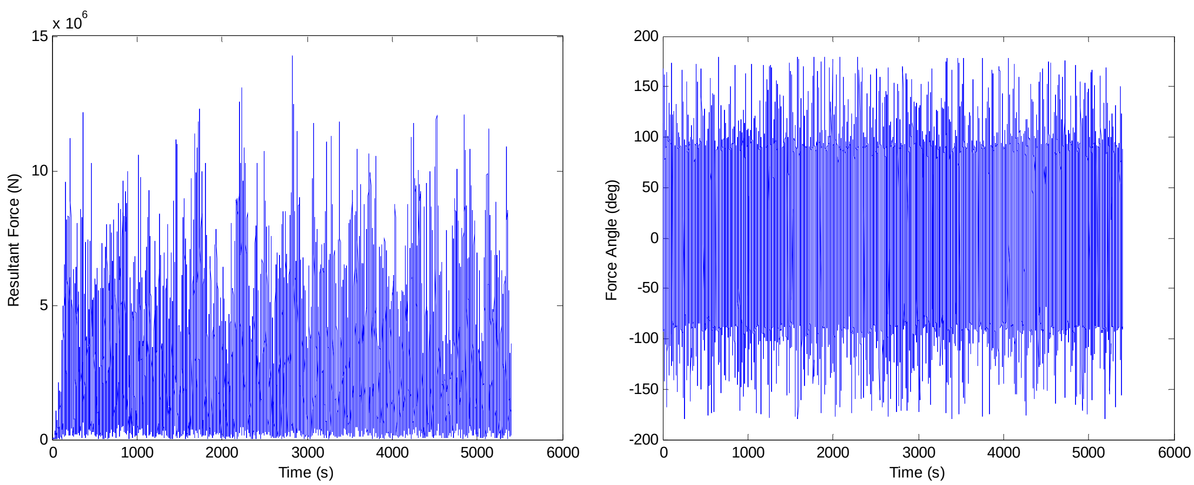

Figure 2-70. Force on forward dolphin: incident wave = 90 degrees

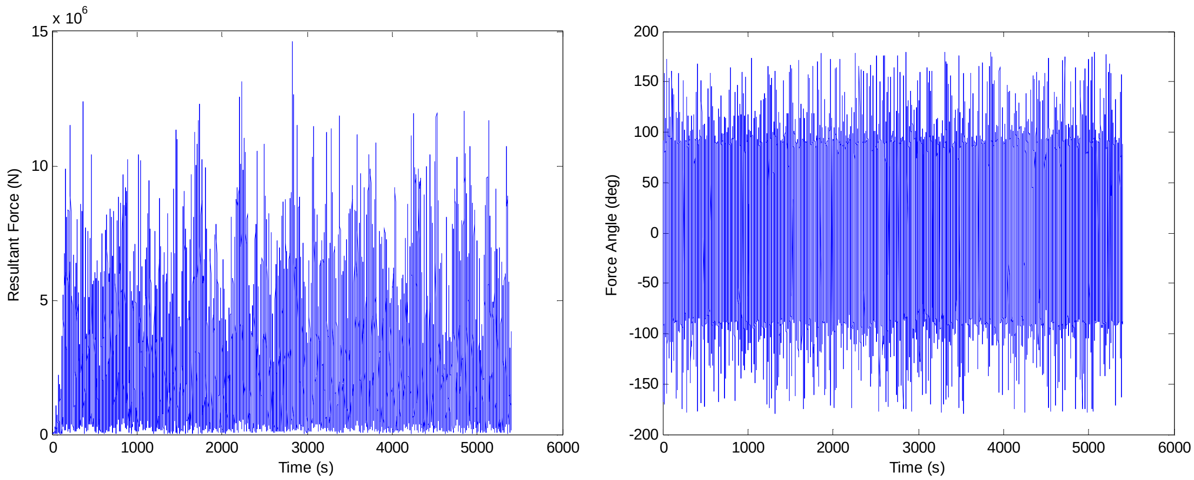

Figure 2-71. Force on aft dolphin: incident wave = 90 degrees

Table 2-8. Statistics table for forces (in Newton) on forward and aft dolphins

Incident wave = 0 degrees

	Maximum force	Mean force	Std deviation
Forward dolphin	7.1910e+006	1.6291e+006	9.7059e+005
Aft dolphin	7.1374e+006	1.6834e+006	9.5070e+005

Incident wave = 45 degrees

	Maximum force	Mean force	Std deviation
Forward dolphin	6.5140e+006	1.4487e+006	8.3897e+005
Aft dolphin	5.7054e+006	1.3454e+006	7.4950e+005

Incident wave = 90 degrees

	Maximum force	Mean force	Std deviation
Forward dolphin	1.4261e+007	3.1364e+006	2.3790e+006
Aft dolphin	1.4261e+007	3.1364e+006	2.3790e+006

Table 2-8 shows the statistics table for forces (in Newton) on forward and aft dolphins for 0, 45 and 90 degrees wave headings respectively.

2.7.5 Drag Force and Wave Excitation Force

The drag force and wave excitation force time history on the floating quay is shown below.

2.7.5.1 Drag force on floating quay for 0, 45 and 90 degrees headings

As shown in Figure 2-72, Figure 2-73 and Figure 2-74, the drag force time history acting on the floating quay wall for the wave headings 0, 45 and 90 degrees has been shown below.

Drag force (in Newton)

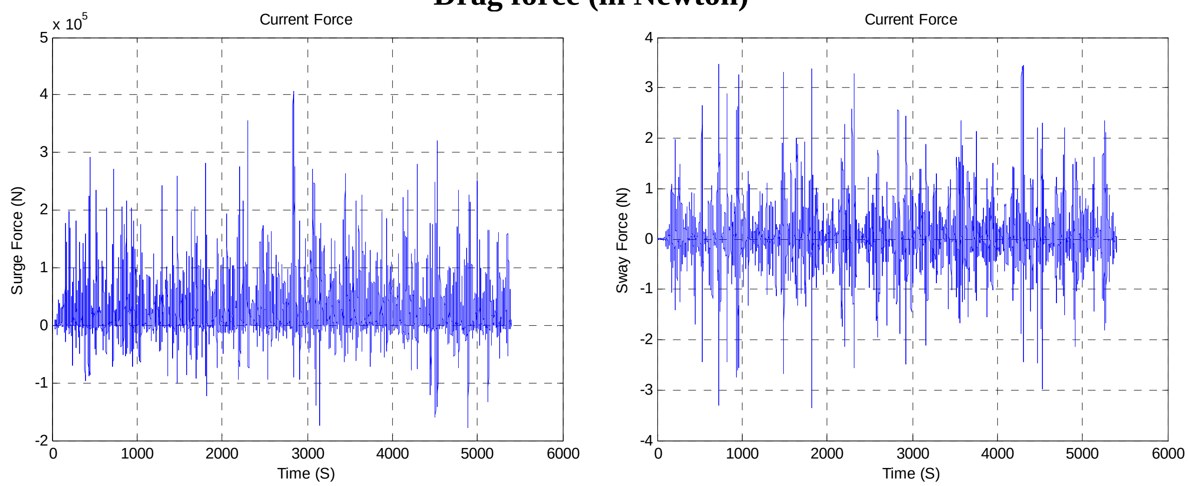

Figure 2-72. Drag force for wave heading = 0 degrees

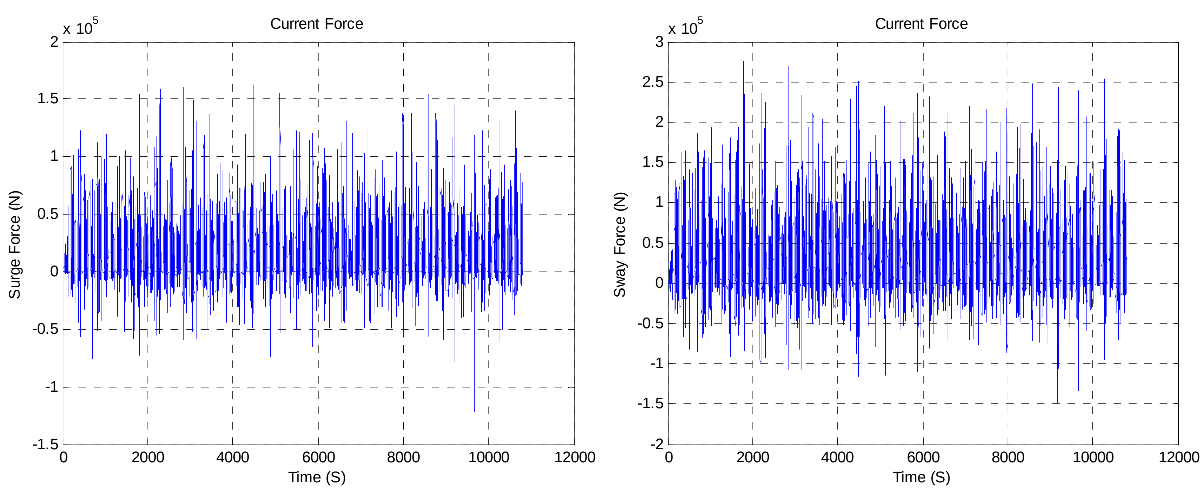

Figure 2-73. Drag force for wave heading = 45 degrees

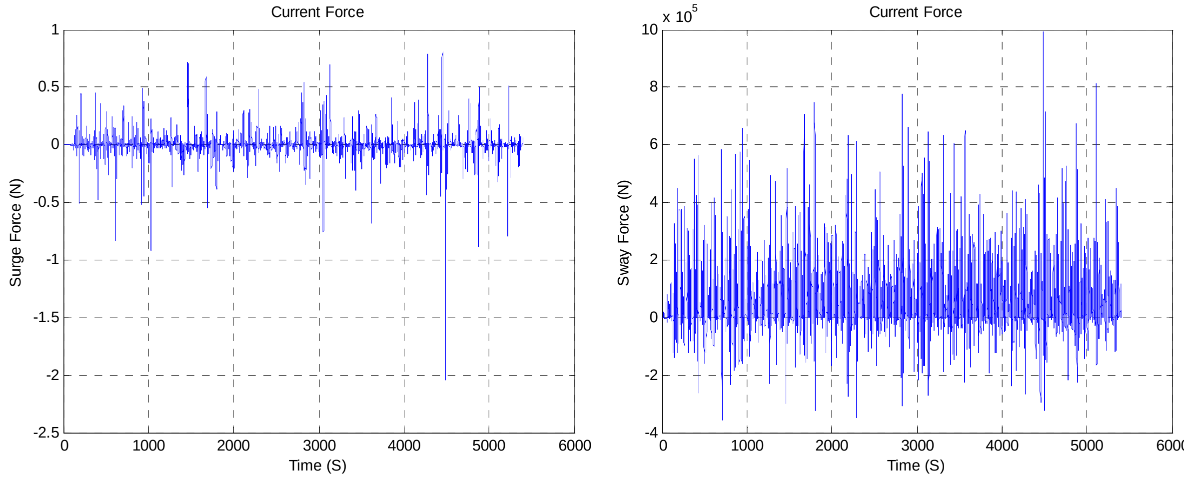

Figure 2-74. Drag force for wave heading = 90 degrees

Table 2-9. Statistics table for drag force (in Newton)

Wave heading = 0 degrees

	Maximum force	Mean force	Standard deviation
Surge force	4.0762e+005	2.2211e+004	4.5196e+004
Sway force	3.4785	0.0432	0.5130

Wave heading = 45 degrees

	Maximum force	Mean force	Standard deviation
Surge force	1.6255e+005	1.1105e+004	2.2278e+004
Sway force	2.7561e+005	2.7809e+004	4.1530e+004

Wave heading = 90 degrees

	Maximum force	Mean force	Standard deviation
Surge force	-2.0436	0.0055	0.0916
Sway force	9.9577e+005	5.4949e+004	1.1100e+005

Table 2-9 shows the statistics table for drag force (in Newton) for 0, 45 and 90 degrees wave headings respectively.

2.7.5.2 Wave excitation force on floating quay for 0, 45 and 90 degrees headings

Wave excitation force time history acting on the floating quay wall for the wave headings 0, 45 and 90 degrees is shown below in Figure 2-75, Figure 2-76 and Figure 2-77 respectively.

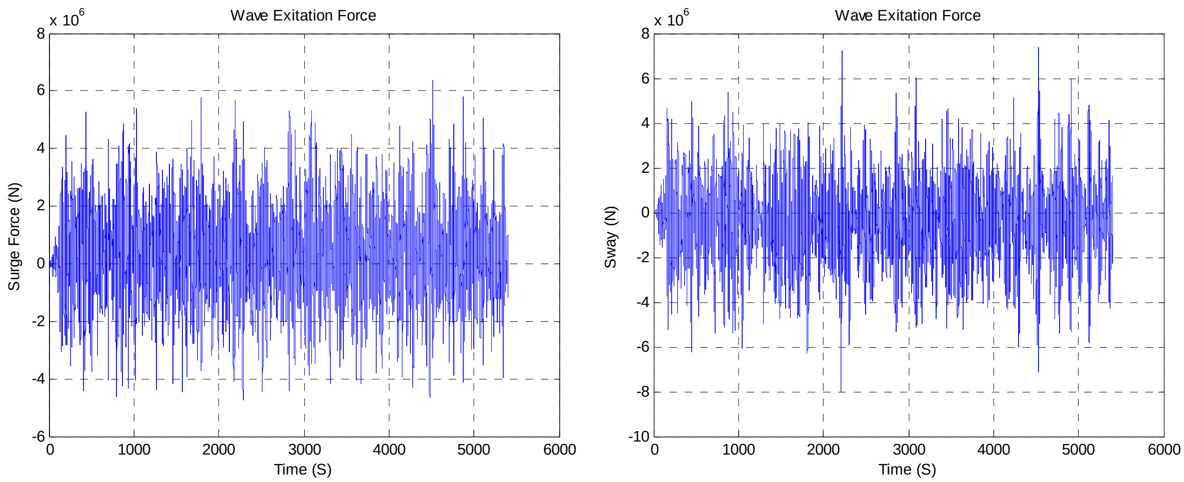

Figure 2-75. Wave excitation force for incident wave = 0 degrees

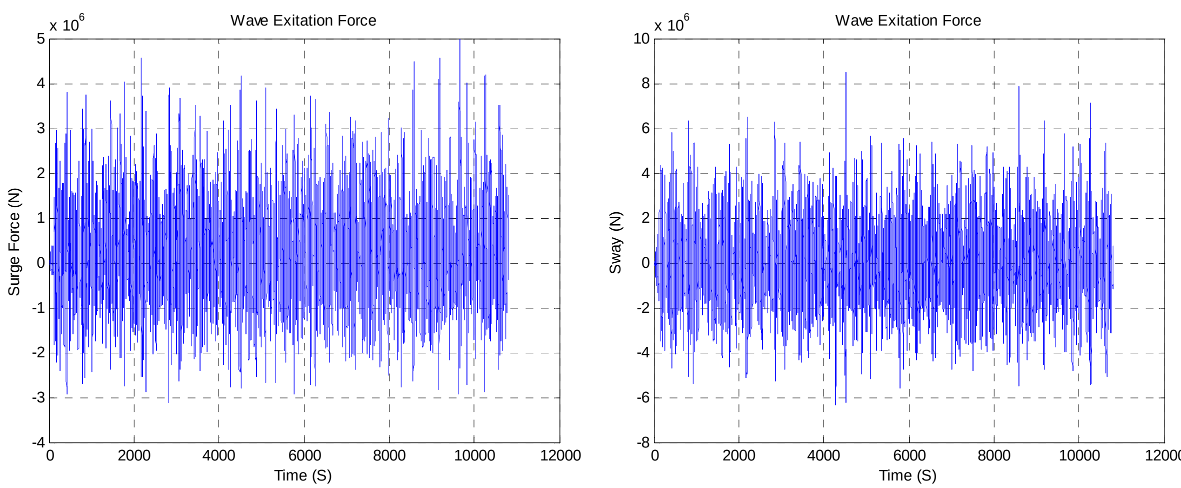

Figure 2-76 Wave excitation force for incident wave = 45 degrees

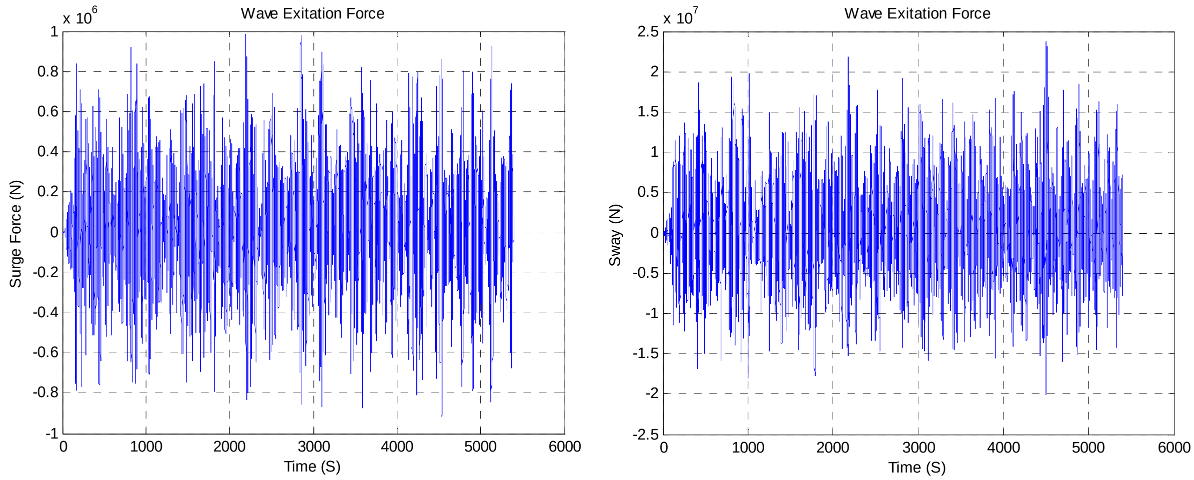

Figure 2-77. Wave excitation force for incident wave = 90 degrees

Table 2-10. Statistics table for wave excitation force (in Newton)

Wave heading = 0 degrees

	Maximum force	Mean force	Standard deviation
Surge force	6.3697e+006	3.3483e+005	1.6490e+006
Sway force	-8.0039e+006	-4.8456e+005	1.9584e+006

Wave heading = 45 degrees

	Maximum force	Mean force	Standard deviation
Surge force	4.9947e+006	2.9500e+005	1.1199e+006
Sway force	8.4885e+006	2.8134e+004	1.8932e+006

Wave heading = 90 degrees

	Maximum force	Mean force	Standard deviation
Surge force	9.8387e+005	1.8328e+004	2.9728e+005
Sway force	2.3777e+007	4.4670e+005	6.2487e+006

Table 2-10 shows the statistics table for wave excitation force (in Newton) for 0, 45 and 90 degrees wave headings respectively.

3. SUMMARY AND CONCLUSION

The hydrodynamic interaction of the multi bodies in close proximity is different from that of the single body. The motion response of the interacting bodies in the case of multi body interaction sometimes doubles the motion response of the single body.

The purpose of this project was to find out the effect of the floating mobile container terminal on the motion response of the container ship for smooth container loading/unloading operation in rough weather condition. It can be concluded from the results that the presence of floating mobile container terminal does give rise to elevated motion response due to interaction effects but the relative motion response between container ship and the floating quay in the presence of the floating quay is within the acceptable limits. The interaction effects are particularly pronounced in the 90 degrees (beam sea) wave incident angle compared to the other wave incident angles.

REFERENCES

Buchner, B., Dijk, A., Wilde, J., 2001. Numerical Multiple-body Simulations of Side-by-side Mooring to an FPSO. In Proceedings of the Eleventh International Offshore and Polar Engineering Conference, Stavanger, Norway, 343-353.

Buchner, B., Gerrit, B., Jaap, W., 2004. The Interaction Effects of Mooring in Close Proximity of Other Structures, In Proceedings of 14th ISOPE Conference, Toulon, France, 297-306.

Choi, Y.R., Hong, S.Y., 2002. An Analysis of Hydrodynamic Interaction of Floating Multi-body Using Higher-order Boundary Element Method. In Proceedings of the Twelfth International Offshore and Polar Engineering Conference, Kitakyushu, Japan, 303-308.

Chen, H.C., Huang E. T., 2004. Time-domain Simulation of Floating Pier/Ship Interactions and Harbor Resonance. In Proceedings of the Fourteenth International Offshore and Polar Engineering Conference, Toulon, France, Volume I, 772-774.

Huijsmans, R.H.M., Pinkster, J.A., Wilde, J.J., 2001. Diffraction and Radiation of Waves Around Side-by-side Moored Vessels. In Proceedings of the Eleventh International Offshore and Polar Engineering Conference, Stavanger, Norway, 406-412.

Inoue, Y., Islam, M.R., 1999. Comparative Study of Numerical Simulation and Experimental Results for a Parallely Connected FPSO and LNG in Waves. In Proceedings of the Ninth International Offshore and Polar Engineering Conference, Brest, France, 360-367.

Kim, M. H., 1997. WINTCOL/WINPOST user's manual. Ocean Engineering Program, Civil Engineering Department, Texas A&M University, College Station, TX.

Kodan, N., 1984. The Motions of Adjacent Floating Structures in Oblique Waves. In Proceedings of the Third International Conference on Offshore Mechanics & Arctic Engineering, 1, 206-213.

Lee, C.H., 1995. WAMIT theory manual. Department of Ocean Engineering, Massachusetts Institute of Technology, Cambridge, MA.

Mercier, R., 2004. Dynamics of offshore structures, class notes, OCEN-676-600, Texas A&M University, College Station, TX.

Ran, Z., 2000. Coupled Dynamic Analysis of Floating Structures in Waves and Currents. Ph.D. Dissertation. Texas A&M University, College Station, TX.

Sannasiraj, S.A., Sundaravadivelu, R., Sundar, V., 2000. Diffraction-radiation of multiple floating structures in directional waves. Ocean Engineering, 28, 201-234.

Watanabe, E., Wang, C.M., Utsunomiya, T. and Moan, T., Very large floating structures: applications, analysis and design, Centre for Offshore Research and Engineering, National University of Singapore, core report no. 2004-02.

VITA

Brajesh Kumar
14504 Briar Forest Drive, Apt #417,
Houston, TX 77077
Ph: (832)474-6674
Email: brajeshmarine@yahoo.com

EDUCATION

• Master of Science December 2005
  Major: Ocean Engineering
  Texas A&M University
  GPA: 3.6

• Bachelor of Engineering: October 1996
  Major: Marine Engineering
  Marine Engineering & Research Institute, Calcutta, India.

EXPERIENCE

• Houston Offshore Engineering, Houston, Texas (September 2005 – Present)

• Texas A&M University, College Station, Texas (Jan. 2005 – August 2005)
  Graduate Research Assistant, Civil Engineering Department

• Texas A&M University, College Station, Texas (Sept. 2003 – Dec. 2004)
  Graduate Teaching Assistant, Civil Engineering Department

• Marine Engineer (On Board Ship)

1) World Tankers Pvt. Ltd (Mar 02 - Dec 02)
   Third Assistant Engineer on Product Tanker

2) Essar Shipping Ltd. (Nov 99 - Jan 02)
   Third Assistant Engineer on Oil Tanker & Oil-Bulk-Ore

3) United Ship Management (April 99 - Aug 99)
   Junior Engineer on Bulk Carrier

4) Barber Ship Management (Jan 97 - Mar 99)
   Junior Engineer on Self Unloader